

**AES/ RE/10-32 Viability of Storage Options of CO<sub>2</sub> in Ca Silicates**

**A.E. Peksa**

Title : Investigation of Viability of Storage Options  
of CO<sub>2</sub> in Ca Silicates

Author(s) : A.E. Peksa

Date : 8 October 2010

Professor(s) : Prof. Dr. J.Bruining

Supervisor(s) : Prof. Dr. J.Bruining

TA Report number : AES/RE/10-32

Postal Address : Section for GeoEngineering  
Department of Applied Earth Sciences  
Delft University of Technology  
P.O. Box 5028  
The Netherlands

Telephone : (31) 15 2781328 (secretary)

Telefax : (31) 15 2781189

Copyright ©2008 Section for GeoEngineering

*All rights reserved.  
No parts of this publication may be reproduced,  
Stored in a retrieval system, or transmitted,  
In any form or by any means, electronic,  
Mechanical, photocopying, recording, or otherwise,  
Without the prior written permission of the  
Section for GeoEngineering*

## ABSTRACT

Satisfying continuously growing world energy demand by use of fossil fuels has increased carbon dioxide (CO<sub>2</sub>) concentration in the atmosphere. Dramatically higher concentration of the CO<sub>2</sub> has a negative environmental impact, for that reason a need for analyzing possible mitigation options has arisen. The research framework on the mitigation options includes conducting studies on capturing the CO<sub>2</sub> and its permanent and safe disposal via mineral carbonation. Mineral carbonation of wollastonite (CaSiO<sub>3</sub>) appears to be the most promising sequestration option for CO<sub>2</sub> fixation on silicate minerals: its reaction rate is considered faster than for the other minerals such as magnesium silicates or basalts.

This report investigates a direct aqueous route of mineral carbonation of wollastonite under elevated pressure and temperature. Choice of the wollastonite was made based on its high reactivity rate and the method was determined by a catalytic effect of water on the adsorption kinetics. To improve the process and limit duration of the step where CO<sub>2</sub> diffuses in solution before attaining the solid surface, most of the experiments were dedicated to carry in a moistened sample. As a result it could benefit from the catalytic effect of water and transport of CO<sub>2</sub> was fast enough due to pressure equilibration. To investigate the influence of the water content of the sample, the experiments for this research were carried out with different water fractions.

The idea of the direct aqueous wollastonite carbonation was studied experimentally. For this purpose a set-up was designed and built. It comprised of a closed system with a reference cell, a sample cell and tubing. The whole set-up was placed in a thermal reactor to achieve elevated temperature conditions. Sample represented by mixture of water and CaSiO<sub>3</sub> was stirred until obtaining homogeneous slurry. The slurry contained 50 v/v% of water for the samples with the highest saturation. The unsaturated sample contained 20% of water. After introducing of CO<sub>2</sub> to the reference cell and opening a valve connecting with sample cell, pressure started to decrease until reaching an equilibrium pressure. The pressure decrease in the set-up was monitored by a pressure device.

In addition a dedicated reactive diffusion model was built to interpret the experimental results. The reaction rate for the adsorbed phase and the free phase is proportional to the deviation from equilibrium, which is given by the Langmuir isotherm. A comparison between the experiment and the model leads to the determination of the reaction rate parameters.

The research on the direct aqueous mineral carbonation led to the following results: the maximum adsorption is 493 kg/m<sup>3</sup>; amount of water and particle sizes have the strongest influence on the carbonation process; water behaves as a catalyst, however it may limit the conversion rate in time; the direct aqueous carbonation is a complex heterogeneous reaction that involves dissolution, nucleation, interface reaction and mass transfer.

## Table of Contents

<b>CHAPTER 1 .....</b>	<b>6</b>
<b>INTRODUCTION.....</b>	<b>6</b>
<b>CHAPTER 2 .....</b>	<b>8</b>
<b>MINERAL CARBONATION .....</b>	<b>8</b>
2.1 ROUTES OF MINERAL CARBONATION PROCESS.....	9
2.2 PROCESS ANALYSIS.....	12
2.2.1 ECONOMIC ANALYSIS .....	12
2.2.2 ENVIRIOMENTAL ANALYSIS .....	14
<b>CHAPTER 3 .....</b>	<b>15</b>
<b>EVALUATION OF THE MOST FAVOURABLE SOURCE AND METHOD FOR MINERAL CARBONATION OF CARBON DIOXIDE.....</b>	<b>15</b>
3.1 CHOICE OF SOURCES FOR MINERAL CARBONATION.....	15
3.2 CHOICE OF THE EXPERIMENTALA METHOD BASED ON THE.....	17
CURRENTLY STATE OF AFFAIRS .....	17
3.3.1 DIRECT CARBONATION OF WOLLASTONITE .....	21
3.3.2 INDIRECT CARBONATION .....	22
<b>CHAPTER 4 .....</b>	<b>24</b>
<b>EXPERIMENTAL SECTION .....</b>	<b>24</b>
4.1 THEORETICAL BACKGROUND OF EXPERIMENT.....	24
4.1.1 THE MAIN RATE LAWS GOVERING MINERAL CARBONATION.....	24
4.1.2 KINETICS OF MINERAL CARBONATION OF CALCIUM META SILICATE .....	25
4.2 EXPERIMENTAL SETUP .....	34
4.3 SAMPLE DESCRIPTION .....	37
4.4 EXPERIMENTAL METHODS .....	43
4.5 MODEL OF MASS TRANSPORT IN MINERAL CARBONATION PROCESS .....	45
4.2.1 MODEL.....	45
<b>CHAPTER 5 .....</b>	<b>49</b>
<b>RESULTS AND DISCUSSION .....</b>	<b>49</b>
5.1 SEM AND CT SCANNER EXAMINATION OF THE SAMPLES.....	56
5.2 THE CONVERSION OF WOLLASTONITE TO CALCIUM CARBONATE.....	58
5.3 THE EFFECT OF PRESSURE ON THE CARBONATION OF WOLLASTONITE	

REACTED AT 334K DURING 3 DAYS.....	59
5.4 THE EFFECT OF WATER ON THE CARBONATION OF WOLLASTONITE	
REACTED AT 334K .....	60
5.5 MASS OF CARBON DIOXIDE CAPTURED IN THE EXPERIMENT .....	63
5.6 FIRST (FAST) STAGE OF CARBONATION .....	65
5.6 ADSORPTION ISOTHERM TEST RESULTS .....	67
5.7 MAJOR LIMITATIONS OF THE MINERAL CARBONATION PROCESS	
CONDUCTED IN THE EXPERIMENTAL SETUP .....	68
<b>CHAPTER 6 .....</b>	<b>69</b>
<b>MODEL SIMULATIONS.....</b>	<b>69</b>
<b>CHAPTER 7.....</b>	<b>71</b>
<b>CONCLUSIONS.....</b>	<b>71</b>
<b>TABLE OF FIGURES .....</b>	<b>72</b>
<b>TABLE OF TABLES .....</b>	<b>74</b>
<b>REFERENCES.....</b>	<b>75</b>
<b>ANNEX 1.....</b>	<b>80</b>
<b>ANNEX 2.....</b>	<b>81</b>
<b>ANNEX 3.....</b>	<b>82</b>
<b>ANNEX 4.....</b>	<b>83</b>

# CHAPTER 1

## INTRODUCTION

For over a decade, there is continuous discussion about global warming problem, caused by emission of greenhouses gases – mainly carbon dioxide and methane. Those negotiations culminated last year at the Copenhagen conference but failed so far to propose a follow up of the Kyoto protocol, the international framework for climate change.

Since the beginning of the Industrial Age, rise of 30% of atmospheric CO<sub>2</sub> concentration has been observed (IPCC, 2001). It is commonly thought that change in the composition of atmosphere is a result of anthropogenic activities, like fossil fuel combustion (burning of coal, oil, and natural gas), deforestation and agricultural and industrial practices. There is no doubt, that human actions are strongly impacting the level of CO<sub>2</sub> concentration, but natural sources of carbon dioxide cannot be ignored. An enormous amount of CO<sub>2</sub> is released each year into the atmosphere by volcanic eruption, forests and steppes fires, the decomposition of plants and as a product of gas exchange of plants, animals, fungi and microorganisms.

Mitigation of CO<sub>2</sub> can be achieved in different ways; for instance by the deployment of renewable energy technologies, like wind power, hydropower, solar energy, biomass, biofuel and geothermal energy. Also clean coal technologies have been mentioned as one of the options to reduce greenhouse gas emissions. However, the need of innovative and radical solutions appears with increasing demand for energy and the consistently large percentages of energy production from fossil fuels. A promising option that may lead to a significant reduction of the CO<sub>2</sub> concentrations level in the atmosphere is sequestration.

Carbon dioxide sequestration can be categorized into terrestrial sequestration, geological sequestration, ocean storage and mineral carbonation (NYSERDA, 2006; IEA, 2008).

Geological Sequestration refers to CO<sub>2</sub> trapping techniques from industrial processes, subsequent transportation and long term underground storage. Numerous methods for underground deposition of CO<sub>2</sub> and several types of potential geological reservoirs can be considered (Dahowski, 2004). The main one includes deep saline aquifers, depleted gas and oil fields, CO<sub>2</sub> enhanced oil recovery (EOR), CO<sub>2</sub> enhanced gas recovery, CO<sub>2</sub> enhanced coal-bed methane.

Ocean storage involves enhancing the natural capacity of oceans to fixation and store carbon dioxide (SCOR, 2007). Two types of this process can be considered: (1) a long term process of keeping injected CO<sub>2</sub> at the oceans floor or depression site (lake type scenario); (2) a process of accelerating dispersion of dissolved CO<sub>2</sub> by injecting it into deep water (Ohsumi, 2002).

Mineral carbonation represents the conversion of gaseous CO<sub>2</sub> into solid carbonates. Two main types of process routes may be distinguished: (1) direct carbonation represent by a single step and (2) indirect carbonation characterized as a multi step process, involving metal extraction from the matrix and subsequent precipitation in the form of carbonates.

The aim of this work was investigation of the viability of storage options of CO<sub>2</sub> in Ca silicates. Two parts are distinguished: theoretical (chapters 1-3) and experimental (chapter 4-6).

The report starts with a description of the sequestration problem (Chapter 1). Chapter 2 gives the extensive introduction to the mineral CO<sub>2</sub> sequestration, its origin, advantages and disadvantages. The first Section (2.1) presents the general information about possible process routes, both direct and indirect, additionally describing the pretreatment methods. The second part (Section 2.2) consists of an evaluation of a process analysis (considers economical and environmental aspects of mineral carbonation).

In Chapter 3 the discussion on the most suitable feedstock (Section 3.1) and process route (Section 3.2) for conducting a mineral carbonation experiment is presented. It is based on the current state of art of mineral sequestration, found in the available literature (books, journals, conference contribution, and reports).

The experimental part starts with Chapter 4, where first the theoretical analyses with governing laws and detailed description of kinetics of the process are presented (Section 4.1). It is followed by a description of the experimental set up (Section 4.2), used minerals (Section 4.3) and experimental methods with process conditions (Section 4.4). The last section (Section 4.4) copes with modeling of mass transport that is accompanied with reversible, complex chemical reactions inclusive the derivation of the adsorption constants.

A summary of achieved results and a discussion of the process, with influence of different water fraction and initial pressure are presented in Chapter 5. Chapter 6 presents results of model simulation using the COMSOL Multiphysic software.

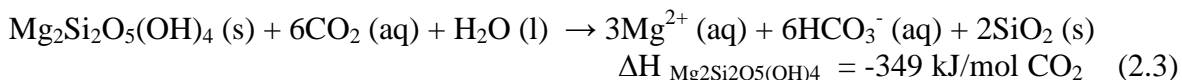
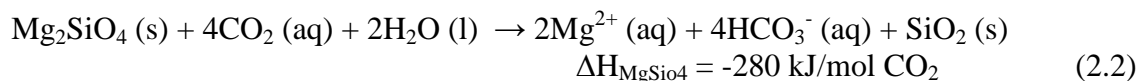
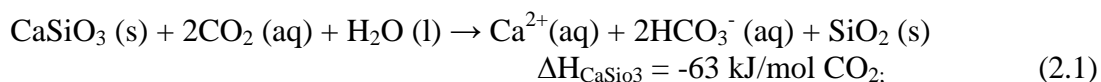
An extensive bibliography of the literature used in this work is given at the end of the report. Annex 1 contains specification of the mineral CaSiO<sub>3</sub>, Annex 2 presents the calculations of specific surface area and Annex 3 describes the procedure of determination the amount of CO<sub>2</sub> adsorbed during the carbonation process.

## CHAPTER 2

### MINERAL CARBONATION

Mineral carbonation mimics a natural phenomenon, viz. the natural silicate weathering process. It belongs to the reactions that evoke the ageing of rocks under atmospheric conditions (Kojima *et al.* 1997). The theory of implementation mineral carbonation for industrial purposes was first outlined by Seifritz (Seifritz, 1990) and discussed further by Dumsmore (1992). The theories were extended by Lackner and coworkers (Lackner *et al.*, 1995) who showed that the economics of the process are favorable (Lackner *et al.*, 1995).

In natural silicate weathering, atmospheric carbon dioxide dissolves in rainwater, forming weak carbonic acid. Next, the slightly acid rainwater with dissolved CO<sub>2</sub> leaches calcium (magnesium) from continental calcium silicate deposits (Brownlow, 1996). Subsequently the calcium ions are transported with rainwater to river and oceans to form solid calcium (magnesium) carbonates (typical reactions are showed below).



The method observed in nature, which was further developed by Seifritz, seems to offer numerous benefits, like stable fixation of atmospheric CO<sub>2</sub> and limitation of negative environmental effects consequential to high carbon dioxide concentration. The most convincing advantage is the long term permanent storage, which makes considering the mineral carbonation as a promising option of carbon dioxide binding (Zevenhoven *et al.*, 2002). As a result of mineral trapping, CO<sub>2</sub> is locked away. Furthermore, it is environmentally safe, leakage - free and once fixed, does not require any post-storage treatment and monitoring.

Teir *et al.* performed many experiments and analysis concerning stability of carbonates in rain water and nitric acid solution. As a result of his experiments, he demonstrated that calcium and magnesium silicates are compounds stable enough over geological time frames to avoid any negative environmental impacts (Tier *et al.*, 2006).

Another noteworthy benefit is the large potential capacity of mineral sequestration that derives from abundant occurrence of naturally available reactants – silicates- in the earth's crust (Brownlow, 1979; Herzog, 2002; Yegulalp *et al.*, 2000). The quantum of readily available deposits highly exceeds the sequestration capacity of coal (Vision 21, 1998).

Moreover, the reaction of forming carbonates is exothermic and have negative free energies of formation; hence, the formed products are thermodynamically stable (Herzog, 2002; Huijgen, Comans, 2003). It is a result of lower energy state of carbonates than carbon dioxide. Theoretically the process of mineral carbonation does not require energy inputs. There is no firm

proof of this statement; because all of the processes conducted up to date are energy demanding. The method used presents disadvantages, the most distinctive one being the rate of the process. As the process of conversion to stable carbonates is slow, there is a need of acceleration; this is done by increasing pressure and temperature and/or chemical additives, heat treatment, mechanical activation etc.

The mineral carbonation process can be conducted both in situ and ex situ. In situ means underground and is combined with geological sequestration of carbon dioxide. Carbon dioxide is injected into silica rich formations or into alkaline aquifers. This process is related to mineral trapping, in which dissolved CO<sub>2</sub> reacts with reservoir rock, forming stable minerals (IPPC, 2007). Ex situ is carried out above the ground with a use of industrial facilities, after mining, crushing and grounding up the source of mineral carbonation. It can be performed as “end of a pipe” testing or technologically integrated process. Carbon dioxide may be introduced to the minerals in the processing plant to form solid carbonates (Lackner, Worzel, 2010).

## 2.1 ROUTES OF MINERAL CARBONATION PROCESS

Reductions of atmospheric concentration of carbon dioxide through mineral carbonation can occur in numerous different ways, ranging from the basic weathering of rocks to advanced multistep processes. The main mineral carbonation processes may be distinguished into:

- direct carbonation (e.g. gas phase, aqueous – one, two or three steps, or additive-enhanced aqueous);
- indirect carbonation (e.g. multi step gas phase, acetic acid route, ph swinging process, three steps base enhance process).

Some of the processes have been already abandoned due to different reasons – for instance too slow reaction rates, too costly and energy demanding, or causing negative environmental impacts (IEA GHG, 2000). Literature postulated that the simplest one is direct carbonation - the minerals are carbonated in a single process step. Direct process means that extraction of metal from mineral and following nucleation reactions are conducted in the same reactor. This process can occur in two different ways (1) direct dry gas-solid and (2) wet carbonation (Zevenhoven *et al.*, 2008). In dry gas-solid process, metal oxides are introduced to gaseous carbon dioxide at a specified temperature and pressure. In the case of wet carbonation, water is used for improving the reaction rate.

Another type of mineral sequestration is indirect carbonation. Compared to direct mineral carbonation, it includes additional step(s) during which the reactive compound is separate from the mineral matrix. (Huijgen and Comans, 2003). It can occur through multistage gas-solid carbonate route, acid route, two step aqueous carbonation, or application of different enhancing additives.

An additional option of mineral carbonation can be found in literature – “enhanced weathering”. This option can be defined as the introduction of a reactive compound (e.g. silicate mineral) that reacts with atmospheric carbon dioxide with help of acid rain (Schuiling, 2002). Minerals are

spread on woodlands or farmlands. It may be one of the cheapest ways of carbon dioxide fixation, but unfortunately, the investigations show slow reaction kinetics.

Mineral carbonation, which could be a promising option for carbon dioxide fixation still required improved methods for accelerating carbonation rate. Several of above mentioned mineral carbonation routes utilize various pre-treatment methods for increasing the kinetics of the process. The most significant ones are size reduction, magnetic separation, heat activation and thermal treatment. Those methods are presented below.

## **MECHANICAL ACTIVATION – SIZE REDUCTION**

Mechanical activation uses very intensive grinding that change the character of the mineral. As a result a more reactive product is received. It may be achieved by particle size reduction and increase of surface area of the feedstock material (Tkáčová, 1989). Those treatments may significantly affect the rate of carbonation.

The rate of chemical reaction strongly depends upon the surface area of solid reactant. Based on the chemical kinetics it is well known that the greater the surface area of reactant is, the higher the rate of reaction. In order to obtain a desirable reaction rate, the size of minerals grains should be significantly decreased by grinding. Laboratories studies were conducted inter alia by O'Connor *et al.* in Albany Research Center who studied the influence of the particle size on the activation of the minerals. Results obtained in these investigations point to the acceleration of the rate of mineral dissolution by enlarged surface area. They show that the reduction in particle size from 106-150 $\mu\text{m}$  to <37  $\mu\text{m}$  increases conversion rate from involving 10% of the sample to 90% of the sample (O'Connor *et al.*, 2002).

This research has been extended by Gerdemann *et al.* work (Gerdemann *et al.*, 2007); it covers the importance of the attrition grinding, i.e., the process of grinding material in a stirring chamber containing balls. Achieved results were much better than with utilization of conventional grinding methods. However, the option of attrition grinding proposed by Gerdemann *et al.* demands higher energy than the O'Connor option and can encounter difficulties in large scale application. Generally, the higher reactivity of minerals gained by implementing pretreatment methods requires more energy (Penner *et al.*, 2004).

Moreover, it is worth to emphasize, that all grinding and milling techniques involve not only adjuvant energy demand, but as well as are a source of additional carbon dioxide emission. Good illustration of the statement is work of Kojima and coworkers. They evaluated that pulverization of approximately one ton of wollastonite ore (grain size 0,2 m - 75  $\mu\text{m}$ ) would result in emission of an extra 18,7 kg of CO<sub>2</sub>. It means that 18,7kg more of carbon dioxide needs to be sequestrated, which would cause significant cost increment of the whole process (Kojima *et al.*, 1997).

## **MAGNETIC SEPARATION**

Magnetic separation is another route proposed by researchers to accelerate the carbonation reaction efficiency and rate. It is a process of removal of magnetic contamination from a mixture of compounds using a magnetic force.

This method seems to be applicable in the case of ore containing iron, for instance olivine, because iron may be attracted by a magnet. Utilization of this technique is favorable in case of an ore that contains iron. Presence of Fe may result in undesirable effects, like lowering the rate of carbonation. The presence of iron causes oxidation process. Such a phenomenon precedes hematite layer formation on the surface of mineral (Fauth *et al.*, 2000). There are several other ways of avoiding such a situation, like conducting carbonation in non-oxidizing atmosphere, but it would make the process sophisticated and notably increase the overall costs. Thus, a promising option can be a magnetic separation integrated mineral carbonation process (NETL, 2001). Moreover additional benefits can be achieved, because formed iron ore by-product is marketable (O'Connor *et al.*, 2001a).

## HEAT ACTIVATION

Another pretreatment method already used in mineral carbonation process is heat activation. Thermal treatment is a technique that involves high temperatures in the processing of the mineral feedstock.

The main aim of thermal treatment is removal of hydroxyl groups from the compound to promote carbonation. O'Connor and coworkers conducted investigation on heating serpentine ( $\text{Mg}_3\text{Si}_2\text{O}_5(\text{OH})_4$ ), which contains up to 15 % of  $\text{H}_2\text{O}$  by weight chemically bounded water (Boslough *et al.*, 1980). Heating up to temperatures 600 – 650 °C can result in the creation of open structures (O'Connor *et al.*, 2000b). The National Energy Technology Laboratory (NETL) showed that heat treatment of antigorite ( $(\text{Mg},\text{Fe}^{2+})_3\text{Si}_2\text{O}_5(\text{OH})_4$ ) – polymorph of serpentine, increased its specific surface area from 8,5 to 18,7  $\text{m}^2/\text{g}$  (NETL, 2001). This process might be advanced in removing MgO from the matrix by application of higher temperatures (from range above 900 °C) (Zevenhoven *et al.*, 2002).

Just like the size reduction method, the heat activation is integrated with the energy demand. According to the recent knowledge (Zevenhoven *et al.*, 2002; O'Connor *et al.*, 2000b), the thermal treatment is impractical from an energetic point of view.

## SURFACE ACTIVATION TECHNIQUES

Surface activation techniques can be achieved by both chemical and physical modification methods. Specific surface area may be increased by steam treatment or acid treatment, like sulfuric or nitric acid (NETL, 2001). Additionally, O'Connor proposed utilization of supercritical water (O'Connor *et al.*, 2000). The results of experimental work shows that higher reactivity of serpentine is possible by increasing specific surface area from 8 to 330  $\text{m}^2/\text{g}$  (Maroto-Valer *et al.*, 2002a).

In case of this pretreatment method, financial considerations – high costs of chemical additives, utilization of acids, energy demand - precludes industrial application.

## OTHER PRE TREATMENT METHODS OF RAW MATERIALS

Different pretreatment methods have been tested. Of interest, ultrasonic treatment and wet grinding in a caustic solution (1 M NaOH, 1 M NaCl) have extensively been investigated by O'Connor *et al.* (O'Connor *et al.*, 2001a). The ultrasonic technique applies ultrasound for increasing chemical reaction and percentage of reacted substances. Wet grinding in a caustic solution consists of milling the material together with suitable amount of water and additive (like NaOH, NaCl) to establish desired pH. Results were not satisfactory, because the desirable mineral activation – significant increment of reaction rates - was not achieved.

A detailed consideration of the problem has revealed that the most favorable pre-treatment option, in terms of economics and energy consumption is conventional grinding (O'Connor *et al.*, 2005). In the current state of art, presented above methods appear as too energy demanding (especially heat treatment). Therefore, research on some of them need to be continued. It is necessary to remember that benefits demonstrated by particular option should be fully balanced by a financial and energetic input and all undesirable side effects should be minimized.

## 2.2 PROCESS ANALYSIS

### 2.2.1 ECONOMIC ANALYSIS

Economic aspects of the process are very important, particularly in case of industrial implementation. To determine the overall cost of mineral carbonation, all stages of process have to be taken into account, along with costs of CO<sub>2</sub> capture.

Mineral carbonation seems to be more expensive than other sequestration methods, because of utilization of complex methods (Huijgen, Comans, 2003). Comparison of components cost of geological sequestration, ocean storage and mineral carbonation was presented in IPCC special report on carbon dioxide capture and storage (IPCC, 2005) (table 2.1 below).

**Table 2.1:** Cost ranges for the components of large scale CCS system (IPCC, 2005).

CCS system components	Cost range	Remarks
<b>Geological storage</b>	0,4 – 6 €/tCO <sub>2</sub> net injected	Excluding potential revenues from EOR or ECBM, monitoring and verification and additional costs for remediation and liabilities
<b>Ocean storage</b>	4 – 23 €/tCO <sub>2</sub> net injected	Including offshore transportation of 100 – 500 km, excluding monitoring and verification.
<b>Mineral carbonation</b>	38 – 77 €/tCO <sub>2</sub> net mineralized	Range for the best case studied. Includes additional energy use for carbonation.

Mineral carbonation cost are very much process dependent. Comparison and estimation of cost of different mineral carbonation methods was prepared by Huijgen and Comans, (2003) (see table below). General costs of mineral sequestration can be divided into investment costs and variable costs. The main one includes:

- excavation of the minerals,
- transportation of the minerals,
- costs of pre treatment techniques and recycling of additives,
- cost directly related to the time for stable binding of carbon dioxide in form of carbonates (Lackner, Worzel, 2010),
- cost of deposition of carbonates,
- costs of land reclamation.

Significant increment of cost may be due to transportation of feedstock (extra emission, cost of transport). This problem might be avoided by close distance of carbonization from point source of the carbon dioxide emission (Folger, 2009).

Very important in case of mineral carbonation are the cost of pretreatment methods, which cover not only use of specific equipment and substances, but additionally costs of recycling of the wastes. Therefore, choice of adequate enhanced method for increasing kinetics, should take into consideration excessive overall process costs.

**Table 2.2:** Costs comparison of different mineral carbon dioxide sequestration routes under the US conditions (Huijgen and Comans, 2003).

CO <sub>2</sub> sequestration method	Fixed costs [€/tonCO <sub>2</sub> ]	Variable costs [€/tonCO <sub>2</sub> ]	Total costs [€/tonCO <sub>2</sub> ]	Source
Acetic acid extraction route	9	54 <sup>1</sup>	63	Kakizawa <i>et al.</i> , 2001
HCl extraction route <sup>2</sup>			30 <sup>3</sup> ÷ 233 <sup>4</sup>	Lackner <i>et al.</i> , 1996
Molten salt process	±11	±52	63	Newall <i>et al.</i> , 1999

To conclude, cost of mineral carbonation process appears to be relatively high. However, Goldberg *et al.*, (2001) and Lackner *et al.*, (1996) claim that it is economically viable option. Costs may be lowered by industrial use of products.

<sup>1</sup> Only energy costs.

<sup>2</sup> Cost estimate based on comparison with existing industrial processes such as copper mining and magnesium production.

<sup>3</sup> Coal fired electric power plants. 30€/ton CO<sub>2</sub> is formulated as the costs objective for mineral CO<sub>2</sub> sequestration. Based on comparisons with the magnesium oxide producing industry, Lackner *et al.* concluded that such costs might be feasible (Lackner *et al.*, 1996).

<sup>4</sup> Assumed: 10% discount rate. Cost estimate based on process flow sheet and general design of equipment. Main costs are the energy consumption related to the dehydration steps and need for make-up chemicals.

### 2.2.2 ENVIRIOMENTAL ANALYSIS

Mineral carbonation requires an Environmental Impact Assessment (EIA). EIA is defined by law (DOE, 2008) as a detailed examination to determine the type and level of possible impacts (negative or positive) that a proposed project would have on the environment. Its role is critical as it enables to make informed decisions, judging the likely impacts of planned projects from an environmental standpoint. However, some scientists claim that mineral carbonation does not require assessment of environmental side effects (McKelevy *et al.*, 2000). To date there is a gap in the literature regarding environmental impact assessment study on mineral carbonation.

In terms of large scale industry investments, several key factors have to be taken into account before judging the relevance of the investment. First, the minerals that may react with carbon dioxide need to be scrutinized. The most suitable ones are the silicate minerals, because they represent the highest carbonation potential. It's crucial that rocks that exhibit the potential of feedstock for mineral carbonation have to be first excavated. All mining operations (both open pit and underground) with further processing of material and related transportation are according to O'Connor's impacting the environment. It is a fact that currently, several operating mines produce those minerals as a byproduct (Huijgen, Comans, 2003). Nevertheless, for industrial implementation of this process, significant increment in mining will be essential. It is worth to note that recommended rock occur in a unique natural neighborhood, what can result in devastation of both landscape and ecosystem (Goff *et al*, 1998).

Pre treatment methods must also be carefully examined from an environmental perspective. The most hazardous seems to be the use of acids, as solvents. Although the acid is being used only during the process, still some amounts may leak, and finally appear in the by- product or/and in the environment. In the same way, grinding of the feedstock material may negatively influence the environment. As mentioned in the section "pretreatment of the raw materials" Kojima *et al.* (1997), evaluate the amount of carbon dioxide that need to be additionally sequestrate due to crashing operations.

Finally, another important aspect is the possible reclamation of the final product. Partly it could be restored to mines as a filling material, so environmental impacts could be confined to a specific side. Unfortunately, the amount of volume increment, caused by carbonation reaction, need to be utilized in a different way (deposition or useful application). Final products could affect the surrounding soil, water and air polluted by deposition. Furthermore erosion, sedimentation and habitat loss may be expected (IPPC, 2005). Therefore a reasonable option would be market application of carbonation products.

## CHAPTER 3

# EVALUATION OF THE MOST FAVOURABLE SOURCE AND METHOD FOR MINERAL CARBONATION OF CARBON DIOXIDE

### 3.1 CHOICE OF SOURCES FOR MINERAL CARBONATION

Several metals elements (e.g. alkali metals, alkali carbonates) are suitable for mineral carbonation. A choice of a proper source of the carbonation must be conducted in order to achieve satisfactory rates of carbon dioxide fixation, reasonably costs, as small as possible negative environmental impacts. Important is as well view at the possibilities within types of products that may be obtained after process due to chemical properties of the sources.

Mineral carbonation considers several different chemical substances that can be suitable for the process application. As regards to their chemistry, particular alkali and alkaline metals, non-alkali, and non-alkaline could be prospects for carbonation.

Based on previous research (Huijgen and Comans, 2003), metals belong to non-alkali and non-alkaline are not considered as viable option because of uncommon occurrence and usefulness. Other metals such as alkali carbonates may be used for CO<sub>2</sub> fixation, but they exhibit a too high solubility in water. Once diluted, they could release carbon dioxide back to the atmosphere. Therefore, they cannot be considered a viable option.

On the contrary, alkaline earth metals, especially calcium or magnesium are the most promising options of binding CO<sub>2</sub> in stable form.

Among alkaline earth metals, calcium and magnesium have been proven to be the most relevant due to their convenient features - abundance and insolubility in nature. The earth's crust is constituted by around 2.1 and 2 mol% calcium and magnesium respectively (Goff *et al.*, 1998). The most preferable chemical compound consisting of calcium or magnesium would be calcium or magnesium oxide. Unfortunately, occurrence of those materials in the nature is rather rare; therefore interest has been focusing on silicates minerals. Silicates minerals represent a wide class of rock-forming minerals. Lackner (Lackner, 2002), has estimated, that storage capacity of silicates minerals is oscillated between 10 thousand and 10 millions Gt of carbon dioxide (see figure 3.1 - below). This value sounds very promising, because it exceeds the cumulative global emission of carbon dioxide (30 GT/year) from fossil fuels (Bleakely, 1994; Tier *et al.*, 2004) for more 300 years. Among all silicate minerals, calcium silicate (wollastonite – CaSiO<sub>3</sub>) and magnesium silicates (xMgO·ySiO<sub>2</sub>·zH<sub>2</sub>O) appear to be the most suitable candidates for mineral carbonation.

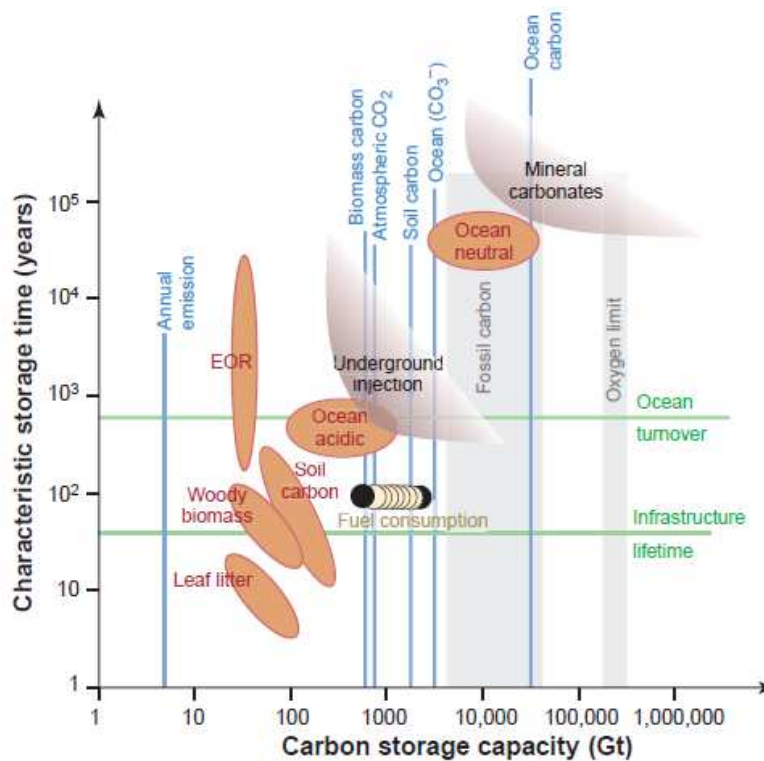


**Figure 3.1:** Estimated storage capacity and time for various sequestration methods. (Lackner, 2003) (“*Oxygen limit* it is the capacity of fossil fuel carbon that by combustion would use all available oxygen: *fossil carbon* includes in its capacity additionally methane hydrates from the ocean floor. *Ocean acids* are related to uptake capacity of carbonic acid; *ocean neutral* means capacity of neutralizing carbonic acids. Limits of mineral carbonation and underground injection due to occurrence of uncertainties are not exactly described; EOR – enhanced oil recovery” (Lackner, 2003)).

Calcium silicate and magnesium silicate are abundant minerals around the globe. Wollastonite occurrence is common in metamorphic limestone and skarns (Tier *et al.*, 2005). Wollastonite is interesting in terms of its high calcium content (48 wt-% CaO). It is formed as a result of two natural processes. The first process is the treatment of silica and limestone by high – 400–450 – temperatures and pressures, caused by deep burial or by their proximity to igneous intrusion. The second process is the direct crystallization from molten, high carbon content, rocks (Van Gosen *et al.*, 2001). Deposits of wollastonite have been found in America: USA (Arizona, Texas, New York, California, Nevada, Idaho, New Jersey), Canada: (Ontario, Quebec), Mexico: Zacatecas, Morelo, Chiapas); Europe: Italy (Sarrabus, Sardinia, Monte Somma and Vesuvius, Campania), Ireland (Dunmorehead, Mourne Mountains, Scawt Hill), Finland (Perheniemi), Germany (Harzburg, Harz Mountains, Auerbach, Odenwald, Hesse), Romania (Dognecea, Csiklova, Banat), Greece, Switzerland; Asia: China (Heilongjiang Province), India (the Belka Bahar); New Zealand (Virta, 2009; Crooks, 2009). World production is estimated at 600,000 tons in 2008 (DiFrancesco, Vitra, 2009).

Magnesium based silicates occur in sufficient quantities (figure 3.2) to be considered as a potential good source for mineral carbonation. Magnesium silicates are divided into many groups. Three of them olivine  $Mg_2SiO_4$ , and serpentine  $Mg_3Si_2O_5(OH)_4$  and forsterite  $Mg_2SiO_4$  are the most attractive due to their natural abundance. They are a base component of ore, mined

for nickel or gold production. Magnesium silicate minerals represent slower kinetics than calcium based silicates (Lackner, 2002). It means that longer time is required for carbon dioxide sequestration to form magnesium carbonates than calcium carbonates.

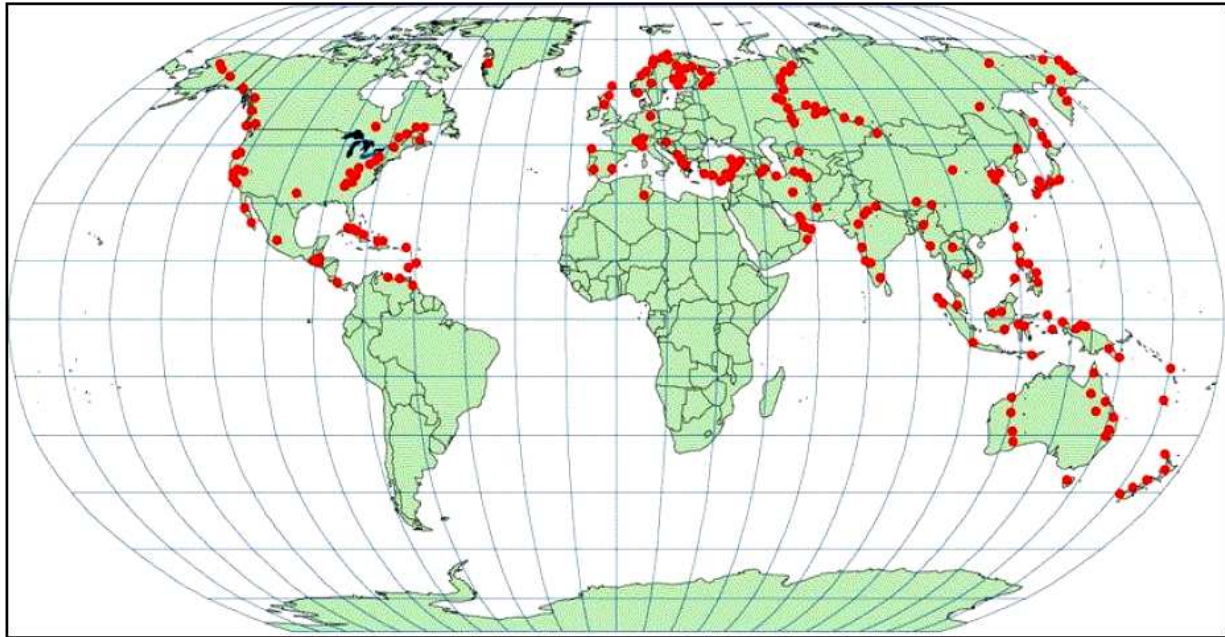


**Figure 3. 2:** Distribution of magnesium silicate mineral deposits worldwide (Ziock, 2000).

To conclude, wollastonite has much higher reactivity than magnesium silicates (Lackner, 2002). Therefore, wollastonite represents the best potential option and availability for conducting the experiment.

### **3.2 CHOICE OF THE EXPERIMENTAL METHOD BASED ON THE CURRENTLY STATE OF AFFAIRS**

Choice of the most optimal condition to perform experiment has been done based on the paper review regarding different process routes for mineral CO<sub>2</sub> carbonation (see graph 3.3 below).

Firstly, investigation of the type of reaction has demonstrated that the process rate aspects (e.g. reaction time, partial pressure of carbon dioxide, reaction temperature, additives, like water, different compounds) are the limiting factors for a successful implementation of mineral carbon sequestration. Secondly, the paper research has pointed out that the choice of appropriated kinetics for the process should be done before making a decision regarding the experimental method. However, it is difficult to compare and interpret the researches that have been carried out

until now. Equipment and boundary conditions used in the experiments (showed in the literature) varies between each other.

As outlined before, the limitations are thermodynamics. They put constraints on the stability of carbonates. Based on the literature, it has been demonstrated that the temperature can only be increased to a certain, pressure dependent level, before which the formation of  $\text{CO}_2$  is favored over carbonates (Lackner *et al.*, 1995).

In addition, for choice of a proper experimental method, the economic aspects have to be considered. For an optimal process, the energy, which is generated by exothermic reaction, could compensate the energy input into process i.e. energy for grinding, stirring ect. In this cost of using additives, drying and de-watering the product should be taken into account.

To recap, the most promising option seems to be the direct mineral carbonation-route in an aqueous solution under elevated pressure and temperature. Among all available methods, this method appears to be more efficient than others mentioned in the literature. Additionally, this method does not require utilization of costly and environmentally unfriendly chemical additives. The detailed description of particular method and its results is detailed later in this chapter.

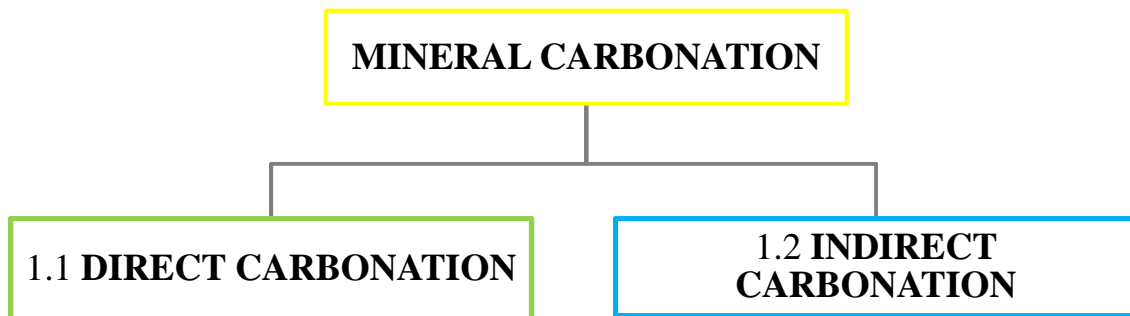


**Figure 3.3 a:** Mineral carbonation routs.

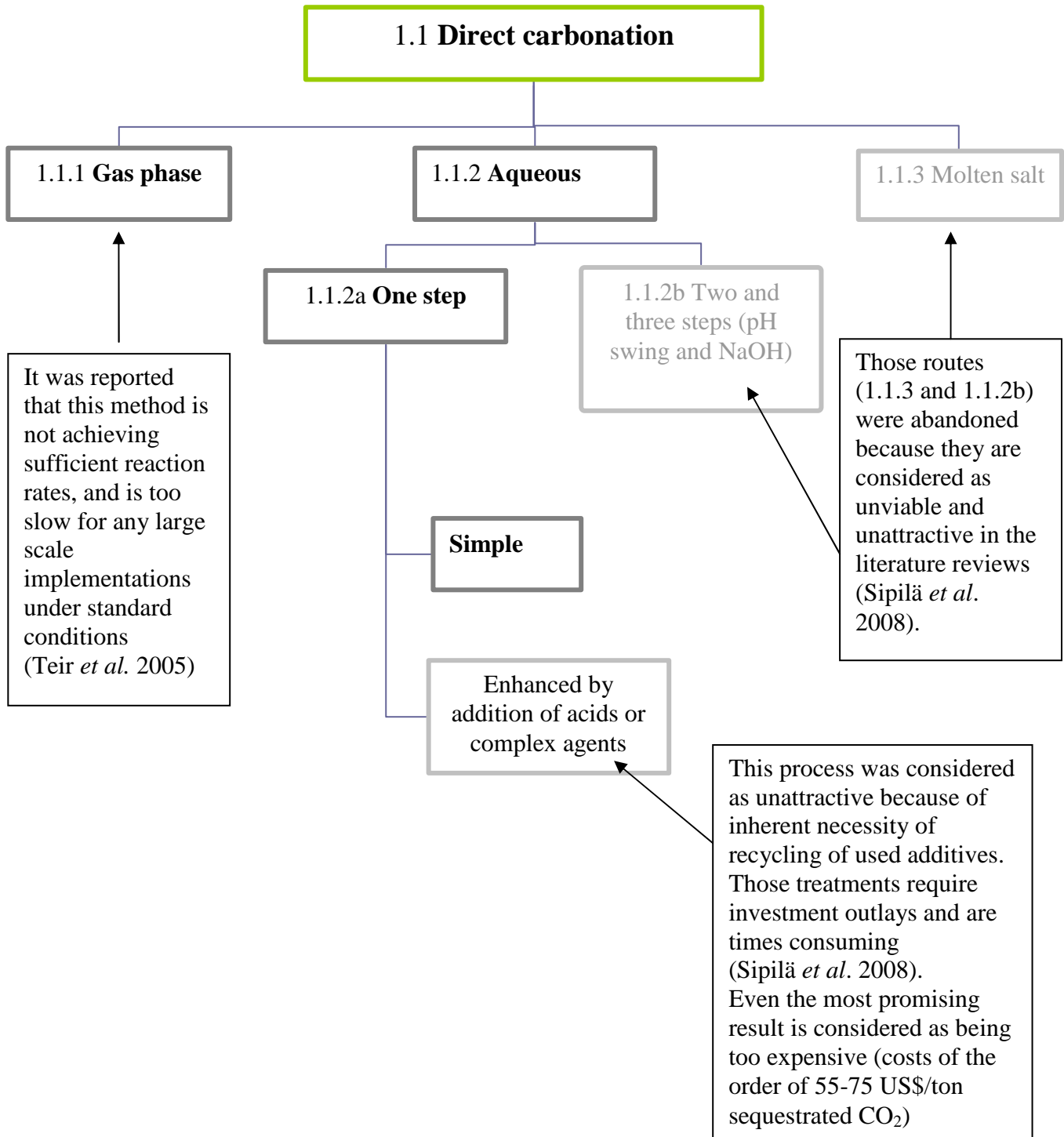


**Figure 3.3 b:** Mineral carbonation routs – direct carbonation.

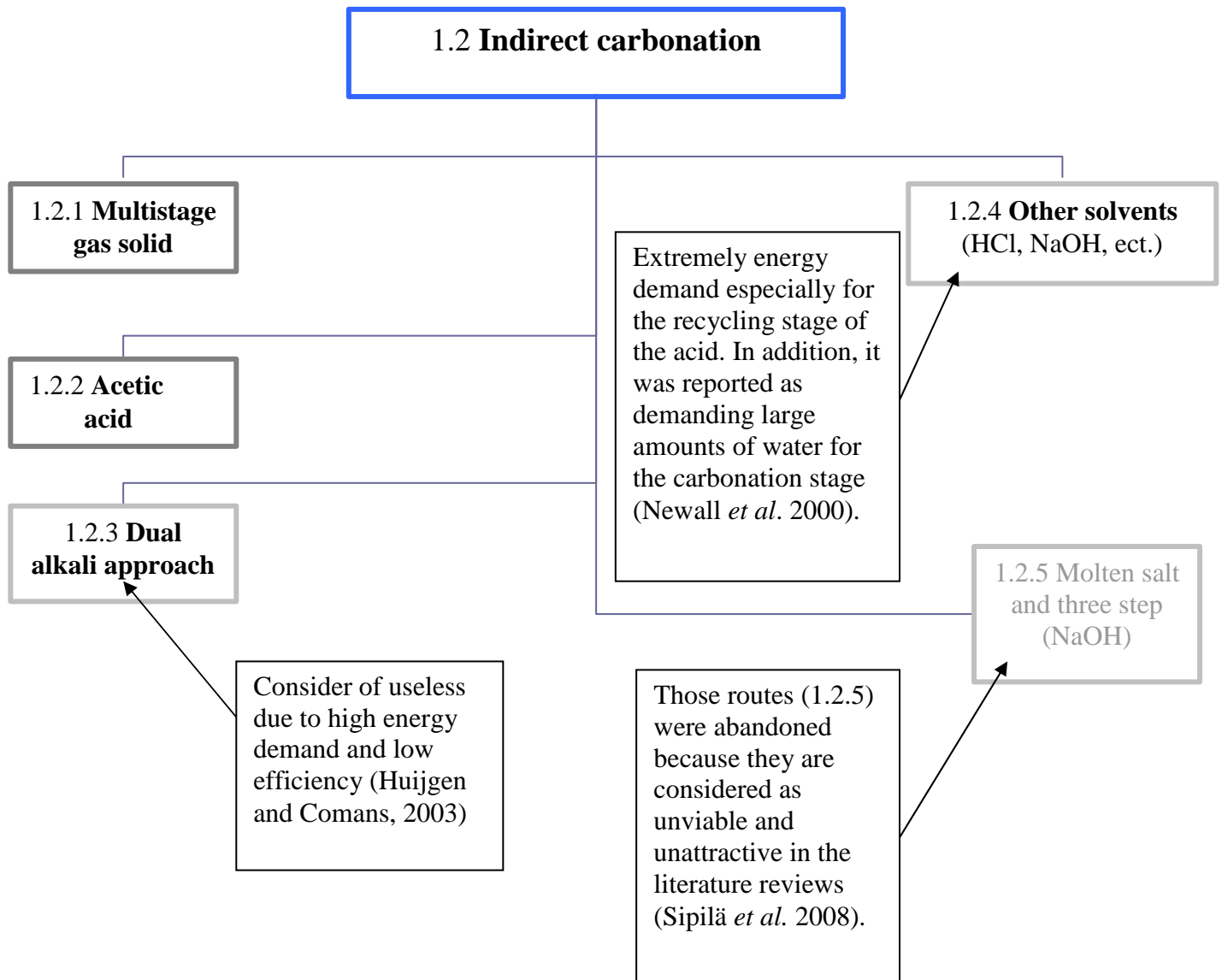


**Figure 3.3 c:** Mineral carbonation routs – indirect carbonation.

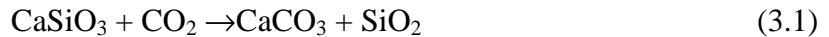
### 3.3.1 DIRECT CARBONATION OF WOLLASTONITE

Direct carbonation of wollastonite is the most straightforward method for conducting mineral carbonation of carbon dioxide. Two processes can be distinguished

- dry (gas-solid phase)
- wet process (aqueous at elevated temperature and pressure).

#### 3.3.1.1 GAS-SOLID PHASE

Gas – solid phase is represented by the following reaction:



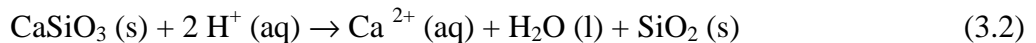
This process was studied by Kojima *et al.* (1997) in a Continuously Stirred Tank Reactor (CSTR) at 25 °C and atmospheric pressure for 0–600 h. The rate of the carbonation process was accounted, as too slow at thermodynamically allowed temperatures.

Based on the above, direct dry mineral carbonation cannot be considered as capable for succession in industrial utilization.

#### 3.3.1.2 DIRECT AQUEOUS AT ELEVATED TEMPERATURE AND PRESSURE

Direct wet carbonation can be presented in the following reaction stages:

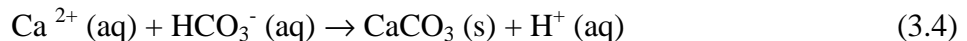
- a. Leaching of Ca:



- b. Dissolution of CO<sub>2</sub> and subsequent conversion of (bi)carbonate species:



- c. Nucleation and growth of calcium carbonate:



This method was investigated by several researchers (inter alia Huijgen, Lackner, Gerdeman) and the following results were published:

- Huijgen *et al.* proposed the most promising process conditions for a reactor (L/S ratio 5 kg/kg, stirrer speed 500 rpm); the conditions were a temperature of 200 °C, a CO<sub>2</sub> partial pressure of 20 bar, a reaction time of 15 min and particle sizes smaller than 38 μm. The process resulted in a carbonation degree of 69%;
- Lackner and coworkers as well implemented direct aqueous carbonation. According to their paper, the optimum carbonation condition for wollastonite are: a conversion (after 1 h) of 81,8 %, with a temperature of 100 °C, a partial pressure of 40,5 bar, and a use of distilled water as carrier solution (Lackner *et al.*, 1997);

- Gerdeman *et al.* have arrived at the conclusion that in the range of temperature 100-200 °C, and at constant pressure (above 50 bar) similar conversion rates are achieved. The decrease of conversion rate occurs below partial CO<sub>2</sub> pressure of 10 bars. It was also reported that the process requires around 8.9 tons of wollastonite for every ton of CO<sub>2</sub> sequestered. The results have not confirmed theoretical prediction of amount of 2.6 ton mineral/ton of CO<sub>2</sub> (Gerdemann *et al.*, 2007). The main disadvantage related to aqueous carbonation is the high energy consumption and the associated cost which, are significant.

### 3.3.2 INDIRECT CARBONATION

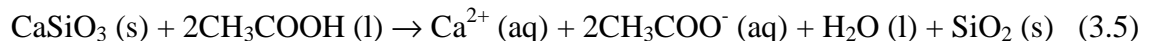
#### 3.3.2.1 MULTI STAGE GAS-SOLID

There is still a lack of industrial viability of this mineral carbonation option. So few result are available.

#### 3.3.2.2 ACETIC ACID

The process can be written by the following two step reaction:

- a. Treating wollastonite with acetic acid (extraction of calcium ions):



- b. Calcium carbonation and recovering of acetic acid:



This theory was developed by Kakizwawa *et al.* as "an improved aqueous carbonation process" by the use of acetic acid as accelerator (Kakizwawa *et al.*, 2009). Their theory suggests that the conversion of 40% can be achieved at the conditions of 25°C and 1 bar, and a conversion of 75% can be reached at 30 bar and at temperature of 25 °C.

There was undertaken another study of Kakizwawa *et al.* that achieved a carbonation conversion of about 20% at 60 min of pressure of 30 bar (Tier *et al.*, 2005).The particle size of calcium silicate obtained from this experiment were smaller than 1 µm. This approach was expanded by Tier *et al.* They showed that the process with the use of acetic acid could produce more 60% CO<sub>2</sub> per kg of calcium carbonate, than process carried out in the conventional route (Tier *et al.*, 2005). It was reported that the reaction could happen spontaneously and would not require large amounts of energy. The approximate energy requirements for producing CaCO<sub>3</sub> were determined as 516 kJ/kg CaCO<sub>3</sub>. The experimental results appear as promising. However the problem of acid recycling sill remains unsolved, which in significant manner, reduce its value.

#### 3.3.2.3 DUAL ALKALI APPROACH

The dual alkali approach is based on the Solvay process. It assumes that sodium carbonate is produced from sodium chloride using ammonia as a catalyst (Huang *et al.*, 2001).

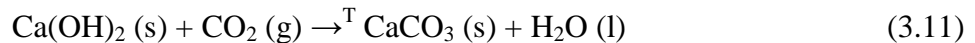
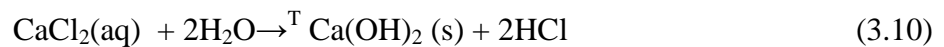
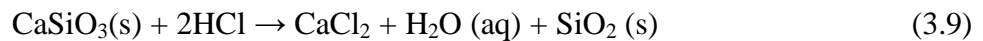
The reaction can be presented in two steps: (1) brine saturation with ammonia and carbon dioxide, and (2) recovery of ammonia by the reaction of lime with ammonium chloride.



The Solvay process is ineffective for industry because it consumes much larger energy and faces the recycling problem of ammonia (one mole CO<sub>2</sub> is produced for every two moles of CO<sub>2</sub> sequestrated because Ca(OH)<sub>2</sub> is used to recycle the ammonia).

### 3.3.2.4 INDIRECT CARBONATION WITH HYDROCHLORIC ACID

This option consists of indirect carbonation with hydrochloric acid for long term storage of CO<sub>2</sub>. It includes a number of stages, starting from precipitation of the calcium hydroxide that subsequently reacts with carbon dioxide and recover of HCl.

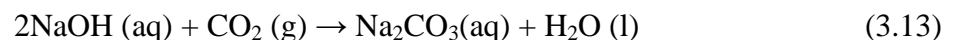
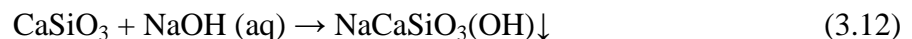


The origin of this process dates back to World War II, because it was developed as a method of producing magnesium. The main disadvantage listed in the literature were first of all the high energy demand for the acid recycling, unsatisfactorily high water demand for the carbonation stage: 840 tH<sub>2</sub>O/t Ca(OH)<sub>2</sub> (Newall *et al.*, 2000) is required. Furthermore exothermic and endothermic steps happen one after the other repeatedly, which make it unfavorable (Newall *et al.*, 2000; Lackner, 2002).

As a result, this option was rejected in the literature review (Huijgen and Comans, 2003).

### 3.3.2.5 MOLTEN SALT

Molten salt, a three steps process represents a route of mineral carbonation with production of carbonate, pectolite from calcium silicate and gaseous carbon dioxide and strong alkaline solution.



Those routes were abandoned because they were considered as unviable and unattractive in the literature reviews (Sipilä *et al.* 2008).

## CHAPTER 4

### EXPERIMENTAL SECTION

#### 4.1 THEORETICAL BACKGROUND OF EXPERIMENT

To fully understand thermodynamics and kinetics of mineral carbonation it is necessary to apprehend mass transfer and transport mechanism.

This section provides the theoretical understanding of the principal processes that occur in mineral carbonation. Mineral carbonation occurs in case of the reaction of metal oxide with carbon dioxide, to produce carbonate and heat evolution, as shown in the reaction below:



Here, M is the indication of divalent metal like magnesium or calcium. In order to cope with heterogeneous reactions as in the case of mineral carbonation, the kinetic approach is required (IPCC, 2005). It is particularly important in the case of reactions involving silica minerals and dissolved carbon dioxide (carbonate minerals and silica bearing mineral are given as a products). Over the past few years many researches were carried out to determine the factors affecting mineral carbonation reaction kinetics. Unfortunately, most of the data gathered were achieved under different laboratory conditions: experimental setup and assumed boundary conditions (temperature and pressure range, presence of catalysts, pH etc.). As a result, comparison and interpretation of data from different experiences is difficult. However, despite the diversity of experiment variety, all of them are classified under a common theoretical basis, presented as the transition state theory (Marini, 2007).

##### 4.1.1 THE MAIN RATE LAWS GOVERING MINERAL CARBONATION

The rate laws governing mineral carbonation (dissolution/precipitation) process are based on connection between the dependent variables (for instance precipitation rate) with other independent variables, like change of temperature, thermodynamic affinity, ionic strength and as well activities or concentrations of species (Marini, 2007).

Mechanism of dissolution/precipitation can be considered in terms of the framework of Transition State Theory (TST), developed by Henry Eyring (1935). It provides an approach to explain how reactants react to form the products and gives possibility of reaction kinetics calculation with a use of statistical mechanisms.

The fundamental principles of TST (called as well activate complex theory) assume occurrence of quasi-equilibrium between particular reactants and activated transition state complexes (IUPAC, 2008). It signifies that reactants have to pass through a high energy state (the transition state), where they form unstable species, also called activated complex. The transition state is defined as “the critical configuration of a reaction system situated at the highest point of the most favorable reaction path on the potential-energy surface” (Fueno, 1999). Furthermore the Transition State Theory assumes that the concentration of the activated complex is in equilibrium with the reactants (Zhang, 2008). An amount of activated complexes and rates of decompositions to yield products are used as bases for computation of the reaction rate by means of statistical mechanisms (Marini, 2007).

The general law regarding the rate of the heterogeneous dissolution-participation reaction was formulated by Lasaga (1995):

$$r = k_0 \cdot A_s \cdot \exp\left(-\frac{E_a}{RT}\right) \cdot a_{H^+}^{n_H} \cdot \prod a_i^{n_i} \cdot g(I) \cdot f(A) \quad (4.2)$$

where  $k_0$  is the rate constant ( $\text{mol m}^{-2}\text{s}^{-1}$ );  $A_s$  represent the reactive surface area of the mineral in contact with the unit volume of aqueous solution ( $\text{m}^2\text{L}^{-1}$ );  $E_a$  express the apparent activation energy of the overall reaction ( $\text{kJ mol}^{-1}$ );  $T$  and  $R$  are correspondingly an absolute temperature (K) and universal gas constant ( $\text{J}/(\text{K mol})$ );  $a_{H^+}^{n_H}$  represents the rate dependence of the pH in the

dissolution precipitation reaction,  $\prod a_i^{n_i}$  express possible effects of the species taking part in formation of precursor complex (catalyst, inhibitor),  $g(I)$  represents the dependence of the rate on the ionic strength  $I$  of aqueous solution and  $f(A)$  represents the dependence of the rate on a distance from the equilibrium state, that may be expressed in terms of the thermodynamic affinity  $A$  for the overall reaction (Marini, 2007).

Moreover, the influence of the temperature changes for the rate of dissolution/precipitation is in the most cases governed by the Arrhenius equation (1889), that describe increment of reaction rate with rising temperature (only if the reaction rate constant indicate exponential dependence on temperature).

## **4.1.2 KINETICS OF MINERAL CARBONATION OF CALCIUM META SILICATE**

Mineral carbonation of calcium silicate represents a complex heterogeneous reaction, due to the mechanisms involved in the reaction between the solid and the solution. During this reaction the following processes may occur: dissolution (release of calcium), nucleation, interface reaction and mass transfer.

Particular steps of mineral carbonation represent different reaction rates. Rate of release of calcium is strongly dependent on the pH of the solution. The slowest rate in dissolution process exhibits diffusion of calcium through an aqueous surface film (Bailey, Reesman, 1971). In the case of nucleation and crystal growth it looks a bit different. Precipitation in its initial step

occurs with relatively fast rate, which in time may be followed by a sudden transition into slow rate, as a result of the gradual release of metal ions (Baker, 1973; Silaban *et al.*, 1995).

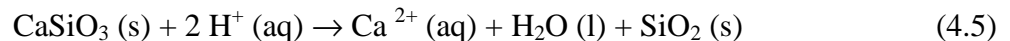
#### 4.1.2.1 CALCIUM DISSOLUTION AND CARBONATE PRECIPITATION

In a general sense the phenomena that occur during aqueous carbonation of wollastonite is a heterogeneous reaction of salt (calcium silicate) reacting with acid (carbonic acid) to produce another salt (calcium carbonate) and acid (silica acid), and as an additional products silica and water. In this case formation of carbonates occurs firstly by the calcium ions separation from crystal matrix and then binding them with carbonic ions. It is multi steps reaction (Guthrie *et al.*, 2001) which can be simplified into following steps - dissolution and precipitation:

- Dissolution of CO<sub>2</sub> and subsequent conversion of bicarbonate, and carbonate ion:



- Leaching of Ca: dissolution of calcium ions from silicate by carbonic acid protons:



- Nucleation and growth of calcium carbonate: precipitation of calcium carbonate by reaction of carbonate ions with calcium ions:



However, the above mentioned model, which describes the experiment, is based on two key assumptions, supported by O'Connor *et al.*, 2000 publication. Firstly, the process does always occur through following steps: dissolution and precipitation. Secondly, this geochemical model of mineral carbonation assumes that dissolution and precipitation occur in the aqueous phase (not in supercritical CO<sub>2</sub> phase). Additionally it should be noted that the components are perfectly mixed, all grains are surrounded by water, and the temperature and ionic strength are uniform.

#### 4.1.2.1.1 SOLUBILITY OF CARBON DIOXIDE IN WATER

The main object of this section is the description of the CO<sub>2</sub>-H<sub>2</sub>O system. Accurate determination of the solubility of CO<sub>2</sub> in pure water is necessary for relevant computations of the CO<sub>2</sub> mass adsorbed by calcium silicate in the mineral carbonation experiment.

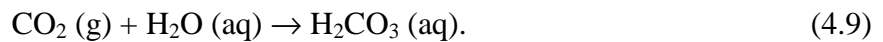
Experimental studies on carbon dioxide dissolution in water have been conducted since many years. Investigations into this phenomenon began already in the end of the XIX<sup>th</sup> century by Wróblewski in 1882, and Bohr in 1899. Later on, the research was conducted by many investigators inter alia Dodds *et al.*, Carroll *et al.* and Crovetto.

Solubility of carbon dioxide is a multistage process. First the CO<sub>2</sub> dissolves according to



The process described by the above expression represents the thermodynamically equilibrium which is reached when the value of fugacity of CO<sub>2</sub> in left and right side of eq. (4.8) is equal.

There is equilibrium established between the dissolved carbon dioxide and carbonic acid (H<sub>2</sub>CO<sub>3</sub>):



Carbonic acid represents a weak acid, which dissociates in two steps



One of the ways of empirical quantification of gas solubility in the water can be calculated based on Henry's law. It states that when a gas is in contact with the surface of a liquid, the solubility of the gas is directly proportional to the partial pressure of that gas above the solution i.e.

$$k_H \equiv \frac{c_a}{p_g}, \quad (4.12)$$

here  $c_a$  represents the concentration of a species in the aqueous phase,  $p_g$  is partial pressure of species in the gas phase (Sander, 1999). The symbol  $k_H$  denote the Henry's constant. It can be varied with change of temperature, but is independent of gas and solvent concentration.

Above relationships (4.12) can be used in presence of ideal condition (or nearly ideal conditions).

#### 4.1.2.1.2 DISSOLUTION

Process of dissolution differs from the precipitation step mainly due to the lower number of steps. There is no need of an initial step – as nucleation in precipitation. It is the result of a dissolving crystal presence in the solution. Basic steps may be distinguished into transfer of the hydrogen ions (fast step) to the surface and a parallel transfer of the calcium (slower step due to diffusion of calcium through an aqueous surface) in the opposite direction – away from the surface (Bailey and Ressman, 1971).

The decomposition reaction between a CO<sub>2</sub> bearing aqueous solution and wollastonite is driven by reaction of hydrogen ion with mineral. It can be characterized as a rapid movement of hydrogen ions among the surface and bulk solution. Moreover the surface concentration of hydrogen ions can be established as a function of the bulk concentration (Bailey and Ressman, 1971).

Dissolution can be transport controlled and surface controlled. For surface controlled reactions the process is slow, and characterize by equal concentration of solute on the surface and in bulk solution. In the case of transport controlled dissolution the concentration of the solute is larger than in the bulk solution (Marini, 2007).

#### **4.1.2.1.3 NUCLEATION AND CRYSTAL GROWTH (precipitation)**

The precipitation of a solid phase consists on nucleation, and subsequently crystal growth. Nucleation is described as a homogenous process where the formation of the nuclei occurs in the bulk solution and as heterogeneous if the process involving a solid surface. This phenomenon is strictly related to the variation of the free energy of precipitation  $\Delta G$ , which depends on the balance of interfacial free energy (the free energy of a system that is developed due to the presence of an interface separating the two coexisting phases at equilibrium (Pfister, 2009), and the bulk free energy, which depends of the cube of radius for a spherical radius. At the nucleation stage the bulk free energy is much smaller than the interfacial free energy, which results in an increment of the net free energy. The subsequent size increment of the critical nucleus (crystal growth) is related to reduction of free energy what takes an effect in transition of process into spontaneous (for  $\Delta G < 0$ ) (Marini, 2007). The rate limitation of crystal growth can be transport- controlled (it is caused by the quick transport of the solute particles from the bulk aqueous solution to the solid surface), surface-reaction controlled (slow process of reaction occurrence at the surface of the growing crystal) or can depend on both – it can be transport and surface- reaction controlled (Marini, 2007).

### **CARBONIC ION CONCENTRATION**

Investigation of the precipitation stage (exactly of its reverse reaction – dissolution of calcium carbonate) has to be conducted. It will enable to better understand the overall conditions of mineral carbonation.

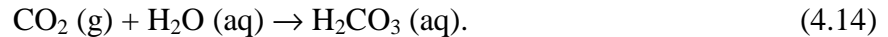


The concentration of ions has to be calculated in view the effect of particular factors like e. g. rising temperature and/or pressure. For calculation purposes, the value of solubility product of calcium carbonate at standard temperature and pressure (STP)<sup>5</sup> equal to  $4,8 \times 10^{-9}$  is taken (Patnaik and Pradyot, 2003).

---

<sup>5</sup> STP – standard conditions assume the value of temperature  $t = 25^\circ$  and pressure  $p = 1$  bar

Calculations of the carbonic ion concentration have to be started by the dissolution step of carbon dioxide in the aqueous phase:

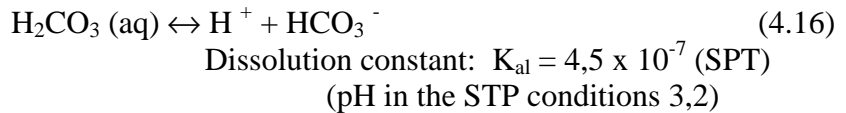


In relation to Henry's Law, the concentration of carbonic acid is proportional to the partial pressure of  $\text{CO}_2$  ( $P_{\text{CO}_2}$ ). As mentioned in section 4.1.2.1.1, the value for Henry's constant is the same for the same temperature, gas and solvent. Further, the concentration of carbon dioxide in the solution can be calculated using Henry's law,

$$\frac{C_1}{P_1} = \frac{C_2}{P_2} \quad (4.15)$$

Henry's constant for  $\text{CO}_2$  at SPT is equal  $K_H = 29,80$  bar/mol/L. Hence, 29,80 bar/mol/L  $\text{CO}_2$  will form a 1M  $\text{CO}_2$  solution. By increasing the pressure of  $\text{CO}_2$  at 25°C the increment of  $\text{H}_2\text{CO}_3$  will be observed.

Carbonic acid is a weak acid that dissociates in two steps,



In the case of equilibrium and absence of any other acid in the solution the following approximation can be written

$$[\text{H}^+] = [\text{HCO}_3^-] = ([\text{H}_2\text{CO}_3 (\text{aq})]K_{a1})^{1/2}. \quad (4.18)$$

By above equilibrium can be concluded that with increasing  $\text{CO}_2$  pressure, the concentration of  $\text{H}_2\text{CO}_3 (\text{aq})$  rises, and consequently concentration of  $[\text{H}^+]$ ,

$$[\text{H}^+] \sim [\text{H}_2\text{CO}_3 (\text{aq})]^{1/2}. \quad (4.19)$$

The situation with pH looks different, because with rising  $\text{CO}_2$  pressure, pH decreases. For instance pH at the conditions: temperature 25°C and  $\text{CO}_2$  pressure 70 bar, is equal 3, and at STP conditions 3.2.

Proceeding with calculations, it is possible to derive from equation (4.17)

$$[\text{CO}_3^{2-}] = \frac{4,7 \times 10^{-11} [\text{HCO}_3^-]}{[\text{H}^+]} \quad (4.20)$$

Thus, based on assumption:  $[\text{H}^+]$  is equal to  $[\text{HCO}_3^-]$ , the concentration is equal to  $[\text{CO}_3^{2-}] \sim 4,7 \times 10^{-11}$ .

According to above presented calculations, increment of carbon dioxide pressure, lowers pH. It can significantly improve the leaching of calcium silicate. Consequently rising the CO<sub>2</sub> pressure, increase both [HCO<sub>3</sub><sup>-</sup>] and [CO<sub>3</sub><sup>2-</sup>] concentration. An elevated level of [CO<sub>3</sub><sup>2-</sup>] is necessary for calcium carbonate precipitation. Moreover if the carbonic ion concentration is low, high calcium ion concentration is necessary for precipitation. This mechanism is very similar to already reported for magnesium silicate (Chen *et al.*, 2001).

### TEMPERATURE DEPENDENCE OF RATE CONSTANT

The calculations conducted in previous point (Carbonic ion concentration), assume the standard temperature conditions (25°C). However, the influence of temperature change cannot be neglected, because it limits the precipitation rate. The temperature has a significant impact on the values of the equilibrium constants K<sub>sp</sub>, K<sub>H</sub>, K<sub>a1</sub>, K<sub>a2</sub>. Based on thermodynamics, the temperature dependence on rate constant can be calculated based on the Gibbs free energy equation (for constant volume)

$$\Delta G = -RT \ln K \quad (4.21)$$

$$\Delta G = \Delta H^\circ - T \Delta S^\circ \quad (4.22)$$

If the equilibrium constant at temperature 25 °C and the value of ΔH are known from Thermodynamic tables (Haywood, 2004), it is straightforward to express value of equilibrium constant for different temperature. For this purpose van Hoff equation<sup>6</sup> can be used

$$\ln \frac{K_1}{K_2} = -\frac{\Delta H^\circ}{R} \left( \frac{1}{T_1} - \frac{1}{T_2} \right) \quad (4.23)$$

Elevation of temperature to 61° changes the equilibrium constants K<sub>H</sub> from 29,8 to 68,9; K<sub>sp</sub> from 4,8 x 10<sup>-9</sup> to 8,2 x 10<sup>-9</sup>, K<sub>a1</sub> from 4,5 x 10<sup>-7</sup> to 6,27x 10<sup>-7</sup>, K<sub>a2</sub> from 4,7 x 10<sup>-11</sup> to 2,47 x 10<sup>-11</sup>. All values of equilibrium constants are listing in table no. 4.1. Above calculations lead to the conclusion that with elevated temperature:

- less carbon dioxide will be in the solution,
- the precipitation of calcium carbonate rises,
- dissociation of aqueous CO<sub>2</sub> to bicarbonate ions and to carbonate ions is higher.

All facts listed above have been already proved by experiments carried by Daval *et al.* and published in 2009.

---

<sup>6</sup> Van Hoff equation is valid for small temperature changes.

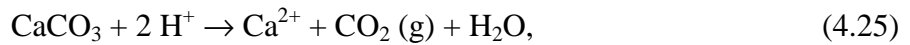
**Table 4. 1:** Equilibrium constants at STP and 65°C.

REACTION	CONSTANT	STP	61°C
$\text{CaCO}_3 \rightarrow \text{Ca}^{2+} + \text{CO}_3^{2-}$	$K_{sp}$	$4,8 \times 10^{-9}$	$8,2 \times 10^{-9}$
$\text{CO}_2(\text{g}) + \text{H}_2\text{O} \rightarrow \text{H}_2\text{CO}_3(\text{aq})$	$K_H$	29,8	68,9
$\text{H}_2\text{CO}_3(\text{aq}) \rightarrow \text{H}^+ + \text{HCO}_3^-$	$K_{a1}$	$4,5 \times 10^{-7}$	$6,27 \times 10^{-7}$
$\text{HCO}_3^- \rightarrow \text{H}^+ + \text{CO}_3^{2-}$	$K_{a2}$	$4,7 \times 10^{-11}$	$2,47 \times 10^{-11}$

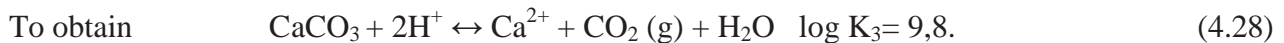
In order to determine the change of  $[\text{CO}_3^{2-}]$ , the procedure is repeated:

$$[\text{CO}_3^{2-}] = \frac{10^{-10} [\text{HCO}_3^-]}{[\text{H}^+]}. \quad (4.24)$$

For better understanding of the problem, investigation of the calcium carbonate formation reaction can also be presented by the phase diagram for calcium carbonate. Starting from the solubility reaction given by



for which the equilibrium constants can be calculated by summation of equations



Hence,

$$\log K_3 = 9,8 = \log[\text{Ca}^{2+}] + \log p_{\text{CO}_2} + 2\text{pH}. \quad (4.29)$$

The equation can be rearranged to obtain relation  $\log[\text{Ca}^{2+}]$  vs. pH:

$$\log[\text{Ca}^{2+}] = 9,8 - \log p_{\text{CO}_2} - 2\text{pH}. \quad (4.30)$$

The above formulas shows that plot of  $\log [\text{Ca}^{2+}]$  vs. pH will be represented by a straight line with a slope of -1, which determinates the phase boundaries between calcite (which is stable on the right side of the graph) and calcium ion in the solution (figure 4.1).

The calculations are made for pressure equal 70 bars.

For 70 bars and 25 °C it gives:

$$\log [\text{Ca}^{2+}] = (9,8 - 1,85_{\log 70\text{bar}}) - 2\text{pH}, \quad (4.31)$$

and for 70 bars and 65 °C (where  $\log K_1 = -8,6$ ,  $\log K_2 = 17,9$ ,  $\log K_3 = 9,3$ )

$$\log[\text{Ca}^{2+}] = 9,3 - \log p_{\text{co}_2} - 2\text{pH} \quad (4.32)$$

$$\log [\text{Ca}^{2+}] = 7,5 - 2\text{pH}. \quad (4.33)$$

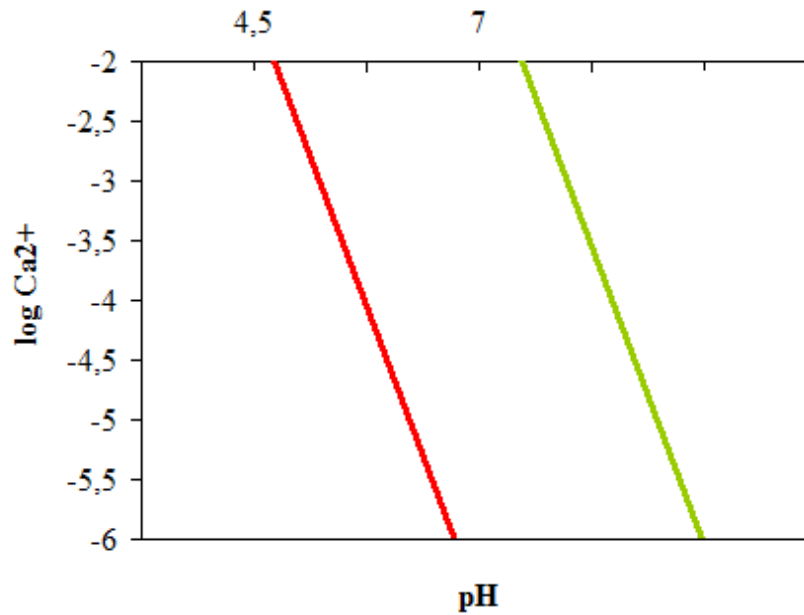


**Figure 4. 1:** Plot of phase boundaries between calcite and calcium ion in the solution. The red line (left) represents the plot for 65°C, and the green line (right) represent plot for 25°C.

The figure shows that the rate of calcium dissolution seems to increase with decrease pH of CO<sub>2</sub>-H<sub>2</sub>O system.

**Table 4. 2:** Carbonic ion concentration at different conditions.

CONDITIONS	pH	[CO <sub>3</sub> <sup>2-</sup> ], mol/l
25°C, 70 bar CO <sub>2</sub> , water	3	4,7 x 10 <sup>-11</sup>
65°C, 70 bar CO <sub>2</sub> , water	2,9	10 <sup>-10</sup>

## **FACTORES AFFECTING REACTION RATES**

As noted above, reaction rates are determined and limited by various factors. The most important factors that determine the mineral carbonation process are:

- reaction time,
- reaction temperature,
- partial pressure of carbon dioxide,
- particle size
- specific surface area.

Regarding the limitate factors, it is worth to mention about passivating layer formation, reaction temperature and pressure and specific surface area. The influence of two, the most significant – reaction temperature and pressure, was discussed in previous section.

The passivating layer formation on the wollastonite suface – silica reach layer- is a complex process. It is a result of the dissolution and decomposition of silica during carbonation reaction.

In the case of heterogeneous reactions, where one of the reactants is solid, specific surface area significant role plays. Proper description of this parameter is necessary for correct interpretation of dissolution (see Appendix 2)

## 4.2. EXPERIMENTAL SETUP

The main objective of the study was to measure the carbon dioxide pressure drop due to the carbonation process. For this purpose suitable laboratory conditions were necessary to investigate the mineral carbonation process. Therefore a set up was made which could be charged with carbon dioxide and be subsequently disconnected from the surroundings. In the reactor pure carbon dioxide was introduced to the adsorbent mineral (wollastonite). A set up is presented in figure 4.2.



**Figure 4. 2:** The experimental setup in the laboratory at TU Delft University.

**SET UP DESCRIPTION**

The set up was designed to measure the mineral carbonation process for different initial pressures. The set-up scheme is given in figure 4.3. The letters in the figure are related to the list of the components of the set up that are described below in figure 4.3.

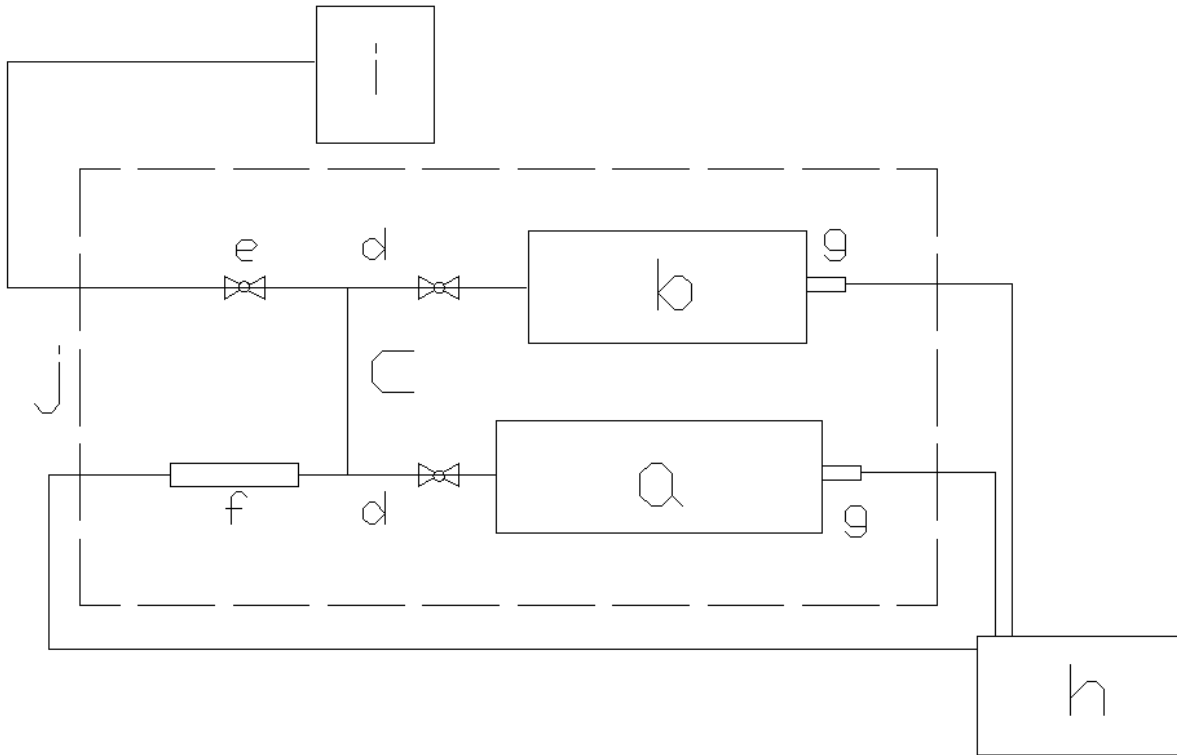


**Figure 4. 3:** Experimental setup for mineral carbonation (explanation of notation a-i below).

- a) A reference cell, which is represented by a double – ended cylinder (304L SS Double-Ended DOT-Compliant Sample Cylinder) with an internal volume of 150 cm<sup>3</sup>, a weight of 0.43 kg. The dimensions are shown in figure 4.4:

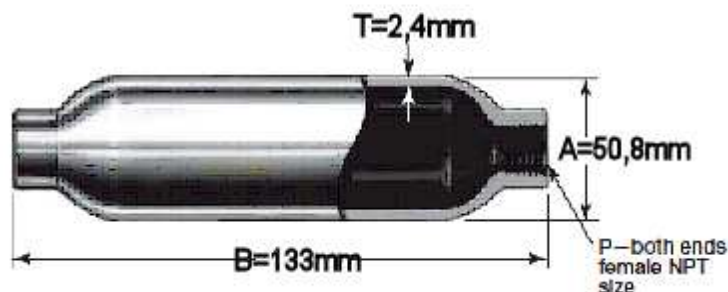


**Figure 4. 4:** Reference cell used in the experimental setup (www.swagelok.com).

- b) A sample cell, which is represented by a double – ended cylinder (304L SS Double-Ended DOT-Compliant Sample Cylinder) with internal volume of 74 cm<sup>3</sup>, weight of 0.28 kg.

The dimensions are shown in figure 4.5:

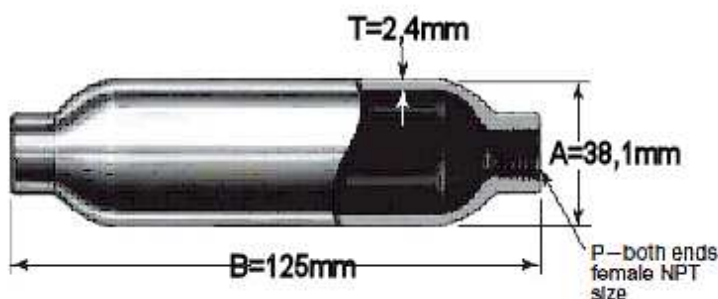


**Figure 4. 5:** Sample cell used in experimental setup (www.swagelok.com).

- c) Tubing;
- d) 2-way on-off valves, which help to control the flow of carbon dioxide and to control the filling of the sample vessel by the gas (carbon dioxide) (Line Loaded Ball Valve 42);
- e) A closing valve, which gives possibility of filling the system with gas from a gas cylinder;
- f) A pressure transducer, which converts pressure into an analog electrical signal;
- g) Thermocouples, which measure temperature in the reference vessel and in the sample cell;
- h) A data acquisition system;
- i) A booster pump and a CO<sub>2</sub> cylinder;
- j) A thermal reactor.

## METHODS USED FOR CHARACTERISATION OF THE REACTANTS AND PRODUCTS

The samples were investigated using a Micro-CT-scanning and an Electron Microprobe both before and after the experiment.

The Micro-CT-scanner analyses were carried out with Phoenix Nanotom Micro-CT-Scanner. It is the 180 kV / 15W nanofocus computed tomography system. It can work with a maximum resolution (depending on object size)  $<0,5\mu$  (3D), and is equipped with a digital 5-megapixel detector.

The Electron microprobe analyses were conducted with a JEOL 8800 M JXA Superprobe (1993). This instrument is equipped with 3 WDS-spectrometers, with LDE1, TAP, PET, and LIF analytical crystals. It may create digital images (secondary and backscattered electron images, and element X-ray photo's). The compositions of the samples were determined using wavelength disperse X-ray spectroscopy.

### **4.3 SAMPLE DESCRIPTION**

Samples of wollastonite used in the carbonation experiment were purchased from the Alfa Aesar GnbH &Co.KG in Karlsruhe in Germany (powdered wollastonite), and from Ankerpoort NV, Mineral Company (Indian A-grade wollastonite). In order to obtain the necessary particle size of the minerals, the Indian A-grade wollastonite was grinded to a grain size of  $715\ \mu\text{m}$ , while powdered wollastonite was ready to use without any pretreatment procedure.

#### **GENERAL INFORMATION**

Wollastonite, calcium metasilicate, with chemical formula  $\text{CaSiO}_3$ , belongs to the class: silicates, the subclass: inosilcatel, and the group: pyroxenoid. It is formed by a reaction between two main components:  $\text{CaO}$  and  $\text{SiO}_2$ .

*Sample no 1* (powder) is a pure calcium meta silicate consisting of  $\text{CaO}$  (in percentage weight of 48.3 %) and  $\text{SiO}_2$  (in percentage weight of 51.7%). It is composed by calcium (34.50%), silicon (24.18%), and oxygen (41.32%). The electron probe micro analysis did not show any trace elements in the composition of mineral (figure 4.6)

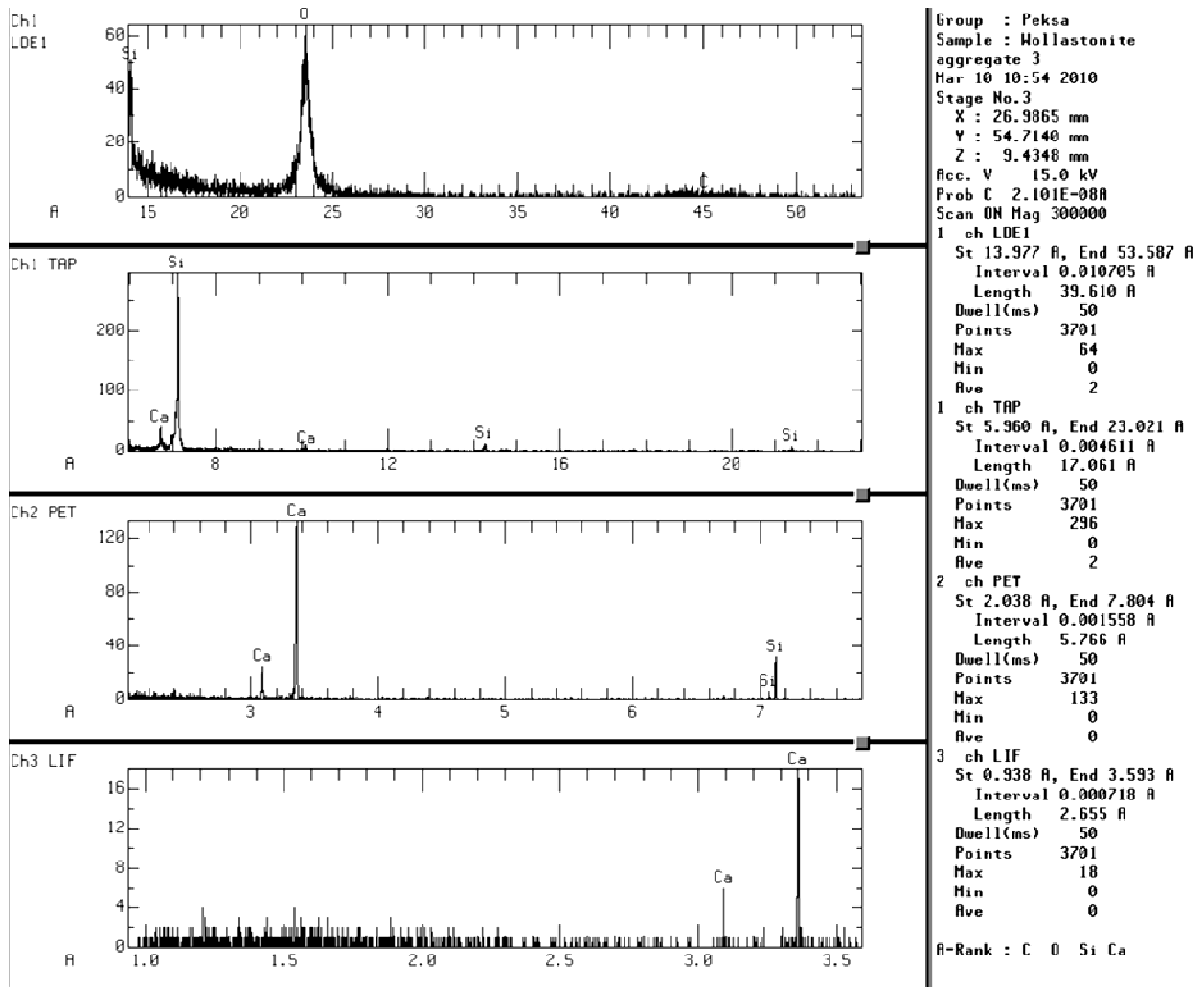


Figure 4. 6: Electron probe analysis of wollastonite (powder) sample.

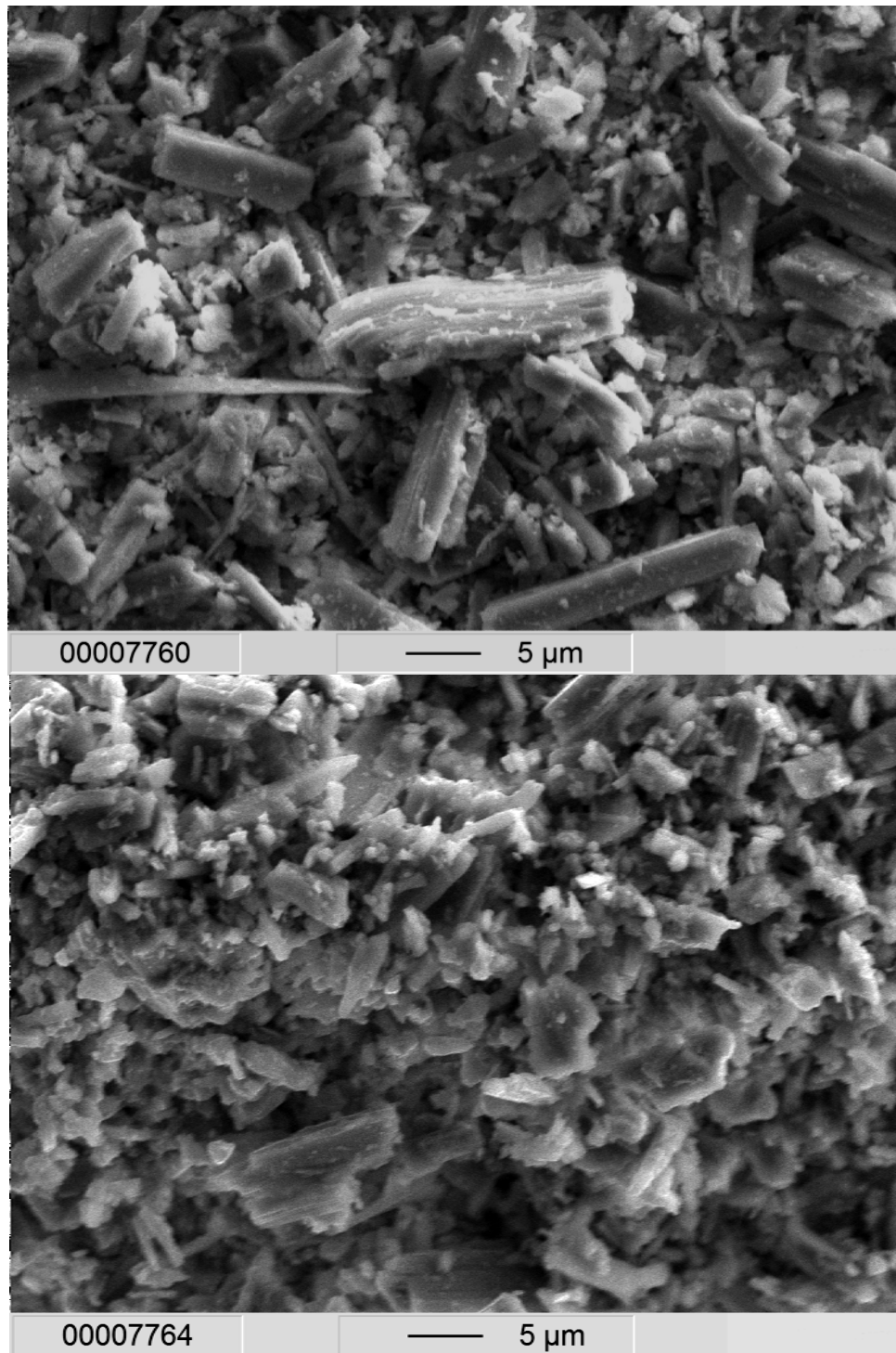
Sample no 2 is a calcium meta silicate consisting of some trace elements (see table 4.3 below).

Table 4. 3: Weight percentage analyses of 2<sup>nd</sup> type of sample (data received due to kindness of Shiva Shayegan Salek).

No.	CaO	MgO	Al <sub>2</sub> O <sub>3</sub>	SiO <sub>2</sub>	FeO	MnO	O	Total
1	47.630	0.025	-	51.870	0.072	0.024	-	99.621
2	0.030	-	-	98.920	0.043	-	-	98.993
3	56.910	-	-	0.007	0.007	-	-	56.917

	CaO	MgO	Al <sub>2</sub> O <sub>3</sub>	SiO <sub>2</sub>	FeO	MnO	O	Total
Min.	0,030	-	-	-	0.007	-	-	56.917
Max.	56.910	0.025	-	98.920	0.072	0.024	-	99.621
Aver.	34.857	0.008	-	50.263	0.040	0.008	-	85.177

The investigation with the Micro Analysis showed that both calcium metasilicates are consists of white, bladed crystal masses, where single crystals show an acicular-shape particles (figure 4.7a and 4.7b).



**Figure 4.7 a:** Electron Probe images, which show needle shaped crystals (Sample no 1). (Scale of 5 $\mu$ m is indicated).

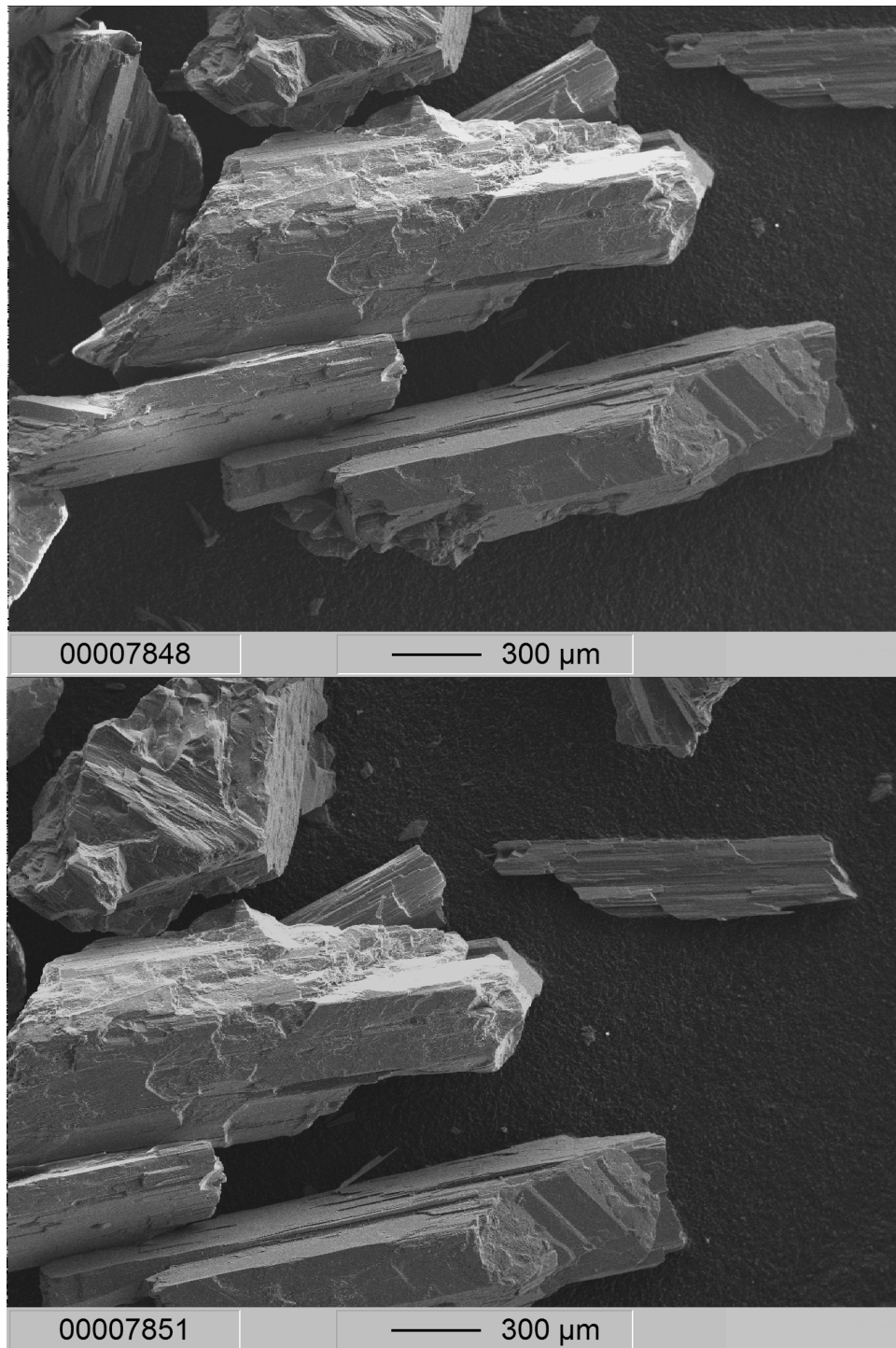


**Figure 4.7 b:** Electron Probe images, which show needle shaped crystals (Sample no 2). (Scale of 300μm is indicated).

## CRYSTALLOGRAPHY

Calcium metasilica represents a single chain silicate. Therefore the  $\text{SiO}_4$  tetrahedral chain has to twist and connect side by side through calcium in octahedral coordination. As a result two edges of  $\text{CaO}_6$  the octahedral have approximately the same length as three  $\text{SiO}_4$  tetrahedral, so the chain, which has a periodicity of three, runs parallel to the octahedral column (Putins, 1992). Wollastonite crystallizes triclinically, with extension along the b axis (lattice constants<sup>7</sup>:  $a = 7.94 \text{ \AA}$ ,  $b = 7.32 \text{ \AA}$ ,  $c = 7.07 \text{ \AA}$ ;  $\alpha = 90,03^\circ$ ,  $\beta = 95,37^\circ$ ,  $\gamma = 103,43$ ) (Buerger *et al.*, 1961). The way how the chains are organized in the triclinic structure was showed by Burge *et al.*(figure 4.8a and 4.8b).

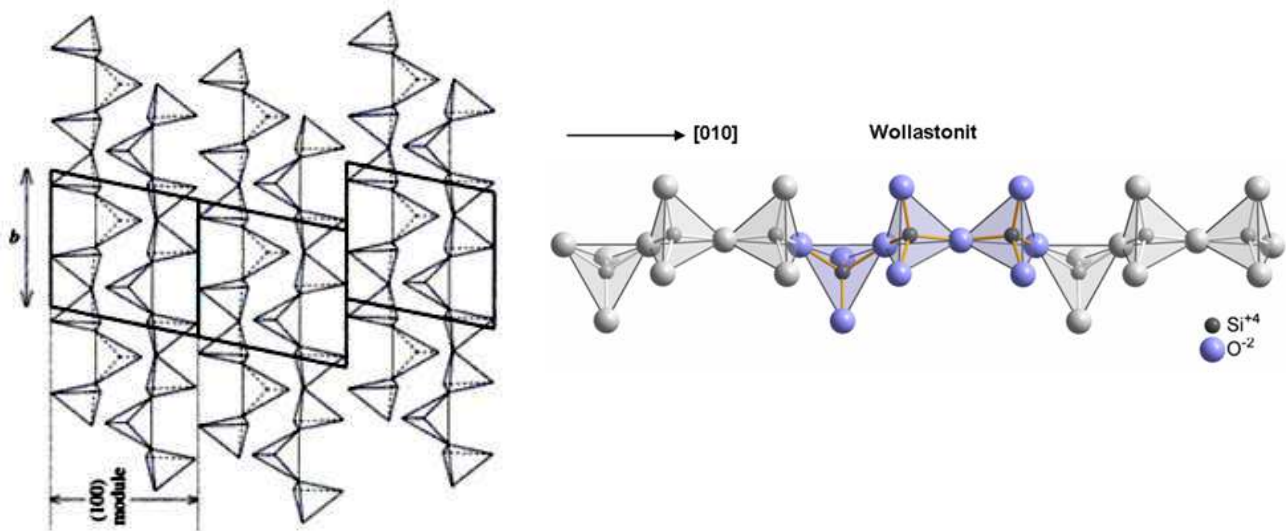


**Figure 4.8 a** (left). The way of chains arrangement in (100) layers in the triclinic structure (Putins, 1992).

**Figure 4.8 b** (right). Structure of wollastonite in a single layer (www.wikipedia.org).

## PHYSICAL PROPERTIES AND SPECIFIC SURFACE AREA

The main physical properties of wollastonite are: the density  $2.9 \text{ g/cm}^3$  ( $2900\text{kg/m}^3$ , hardness (5), and the melting point of  $1540^\circ\text{C}$  (both for sample no 1 and 2). Detailed properties of the sample no 1 are included in the Annex 1.

Specific surface area of the sample was obtained by simple geometric calculations, based on the idealized geometry of mineral grains (Marini, 2009). Main parameters were size and geometry, which were determined from microscopic observation of the sample and by granulometric analysis. For geometric calculation of the specific surface area a suitable geometric shape was

<sup>7</sup> The **lattice constant** represents six constants which are necessary to define size and shape of particular unit cell in a crystal lattice. These are a, b, and c which refer to axial lengths and its inter-axial angles - alpha ( $\alpha$ ), beta ( $\beta$ ), and gamma ( $\gamma$ ).

assumed to be in line with the mineral grains (Oelkers, 2002). The archived results showed that average specific surface area for powder wollastonite is around  $2 \text{ m}^2/\text{g}$ , and for wollastonite, which is represented by grain size  $715 \mu\text{m}$  is  $0.25 \text{ m}^2/\text{g}$ . (See Annex 2)

## 4.4 EXPERIMENTAL METHODS

### Mineral carbonation experiment at elevated pressure and temperature

To establish the process of wollastonite carbonation in different conditions each time a specific sample was prepared (see Table 3) and put into the sample cell. The sample was subsequently exposed to  $\text{CO}_2$  (initially placed in the reference cell and tubing) by a system of valves (see figure 4.3). Carbonation of wollastonite was carried out using the model gas –  $\text{CO}_2$  (4.5 K55OH UN1013 produced by Lindau). The composition of the gas is given by  $\text{CO}_2 \geq 99.995 \text{ vol\%}$ ,  $\text{N}_2 \leq 30 \text{ vpm}$ ,  $\text{O}_2 \leq 15 \text{ vpm}$ ,  $\text{H}_2\text{O} \leq 5 \text{ vpm}$ ,  $\text{C}_x\text{H}_y \leq 2 \text{ vpm}$ .

**Table 4. 4:** Description of samples used in the experiments 1-4.

	Mass of wollastonite	Mass of water
<b>Experiment 1</b>	58.69 (powder)	26.67
<b>Experiment 2</b>	68.53 (powder)	20
<b>Experiment 3</b>	53.38 (powder)	54.82
<b>Experiment 4</b>	102.27 (715 $\mu$ )	36.9

The carbonation was performed in the sample cell at the temperature of  $61^\circ\text{C}$ . The whole set-up was placed in a thermal reactor to achieve elevated temperature conditions. The cylindrical tube that housed a sample was connected to the system by a set of valves to prevent  $\text{CO}_2$  from entering the cell before temperature stabilization of the whole system at an elevated level is secured. The reference cell and tubing were initially pressurized to the desirable level (indicated by a pressure transducer). The initial pressures are presented in table 4.5. The experiment went until the equilibrium pressure was reached. After carbonation these samples were dehumidified at a temperature of  $105^\circ\text{C}$  and then weighted on a laboratory scale.

**Table 4. 5:** Description of the conditions under which the experiments were carried out.

	Initial pressure	Temperature
<b>Experiment 1</b>	81	$61^\circ\text{C}$
<b>Experiment 2</b>	94.95	$61^\circ\text{C}$
<b>Experiment 3</b>	139.1	$61^\circ\text{C}$
<b>Experiment 4</b>	139.21	$61^\circ\text{C}$

In the further analyses of the obtained results, it is assumed that the carbonation occurs only during the reaction time, i.e., at an elevated pressure and temperature and not during additional

steps (like heating, cooling and depressuration). The amount of CO<sub>2</sub>, adsorbed during mineral carbonation process was calculated from: (1) pressure measurements before and after the CO<sub>2</sub> introduction to the sample cell and (2) volume measurements of reference cell, sample cell and tubing.

### **An additional experiment of the adsorption isotherm of carbon dioxide on wollastonite**

An adsorption isotherm of CO<sub>2</sub> on wollastonite was measured at the temperature of 61°C. The sample cell was exposed to carbon dioxide by a system of valves after achieving thermal equilibrium by the whole system. CO<sub>2</sub> was initially placed in the reference cell and tubing at the desirable pressure level. Opening of the valves caused transfer of the gas to the sample cell. After some time adsorption equilibrium was established. The amount of CO<sub>2</sub>, adsorbed during the mineral carbonation process was calculated from pressure measurements before and after the CO<sub>2</sub> introduction to sample cell and volume measurements of reference cell, sample cell and tubing. As base for calculation density of carbon dioxide the equation of state given by Span and Wagner (1996) was used. Subsequently, the pressure in the reference cell and in the tubing was increased and the whole process was repeated. As a result, the adsorption isotherm was obtained.

## 4.5 MODEL OF MASS TRANSPORT IN MINERAL CARBONATION PROCESS

In the process of mineral carbonation mass transport is accompanied with reversible, complex chemical reactions. Equations that represent the mass transfer are sophisticated and in most cases cannot be solved analytically. It is possible to achieve an approximate analytical solution of the problem (method proposed by van Krevelen and Hoftijzer (1948)), but then numerical verification of the results is required. For that reason, in order to obtain an accurate description of the process, numerical techniques are utilized (Perry and Pigford, 1953).

### 4.2.1 MODEL

We consider a sample cell, which is a cylindrical tube with an inner diameter of  $d_2 = 0.032$  m and a length of  $l_2 = 0.125$  m with a volume  $V_2$ . Tubing above the vessel has a volume of  $V_{2t}$ . The cylindrical tube is filled with a  $\text{CaSiO}_3$  sample, and constant connate water saturation  $S_{wc}$ . There is equilibrium between the  $\text{CO}_2$  dissolved in the water and  $\text{CO}_2$  in the gas phase. We ignore the presence of water vapor. The flow of carbon dioxide is governed by Darcy's law. The carbon dioxide is designated as component 1. The porosity is  $\phi$ . There is a reference cell with an inner diameter of  $d_1 = 0.045$  m and a length  $l_1 = 0.133$  m filled with glass beads. The reference cell is connected to the entrance valve of the sample cell by tubing with a volume  $V_{1t}$ . The pore volumes of the reference cell and tubing have a volume  $V_r$ . The reference cell and connected tubing are filled with  $\text{CO}_2$ . The pressure in the reference cell and the connected tubing is only a function of time. There is a valve between the two vessels that is opened at  $t=0$  after the temperature is stabilized at  $T=61^\circ\text{C}$ . Temperature effects due to adiabatic compression or expansion are disregarded.

At  $t=0$  the pressure is distributed between the upper vessel and the pores in the bottom vessel containing the  $\text{CaSiO}_3$ , and the tubing connecting the vessels.

The transport equation in the sample cell reads:

$$\phi(1-S_{wc})\partial_t\rho_{g1} + \phi S_{wc}\partial_t\rho_{w1} = \partial_x \left( \frac{k_g \rho_g}{\mu} \partial_x P \right) - R \quad (4.33)$$

The fact that the two fluids jointly fill the voids implies the relation  $S_{wc} + S_g = 1$ , where  $S_{wc}$  and  $S_g$  are the saturation of water and the saturation of the gas phase, respectively.

Based on the assumption that the chemical reaction follows the mass action law and expresses the transient state of process, the term  $R$  represents the reaction rate. The reaction rate model is used according to Lasaga. The Lasaga applied the detailed balancing for describing the relationship between reaction rate and equilibrium. The microscopic reversibility follows the forward reaction by backward reaction. Thus, it is convenient to represent the reaction rate  $R$  as a difference of the forward rate  $r_f$  and the backward rate  $r_b$

$$R = r_f - r_b \quad (4.34)$$

Hence, the rate of forward reaction (adsorption) is denoted, as

$$r_f = k_f P (\rho_{\max} - \rho_{s1}) \quad (4.35)$$

and rate of the backward reaction (desorption) is express as

$$r_b = k_b \rho_{s1} \quad (4.36)$$

The complete transport equation is represented by

$$\varphi(1 - S_{wc}) \partial_t \rho_{g1} + \varphi S_{wc} \partial_t \rho_{w1} = \partial_x \left( \frac{k_g \rho_g}{\mu} \partial_x P \right) - k_f P (\rho_{\max} - \rho_{s1}) + k_b \rho_{s1} \quad (4.37)$$

The ratio of the rate constants of these reactions is related to equilibrium constants, which is given by:

$$K_{eq} = \frac{k_f}{k_b} \quad (4.38)$$

The equilibrium assumes the specific conditions at which the overall reaction has to be equal to zero, so as follows:

$$R = r_f - r_b = 0 \quad (4.39)$$

$$r_f = r_b = k_f P (\rho_{\max} - \rho) = k_b P \quad (4.40)$$

hence the equilibrium constant is represented by

$$K_{eq} = \frac{\rho}{P (\rho_{\max} - \rho)} \quad (4.41)$$

The above equation consists of two parameters, i.e., the equilibrium constant  $K_{eq}$ , and the adsorption capacity  $\rho_{\max}$ , which fully define the adsorption kinetics and the adsorption equilibrium. In this work adsorption equilibrium can be represented by the Langmuir equation. The constant parameters can be specified according to a Langmuir type adsorption isotherm that is shown in section 4.2.2.1.

According to the foregoing, the adsorbed carbon dioxide concentration is given by:

$$\varphi(1 - S_{wc}) \partial_t \rho_{s1} = k_f P (\rho_{\max} - \rho_{s1}) - k_b \rho_{s1} \quad (4.42)$$

The equilibrium density in the water phase is related to the gas density, i.e.,

$$\rho_{w1} = H \rho_{g1} \quad (4.43)$$

The density of CO<sub>2</sub> is given by the law of corresponding states as

$$\rho_{g1} = \frac{MP}{ZRT}, \quad (4.44)$$

where  $Z=Z(P_R, T_R)$ .

The boundary conditions are:

$$\partial_x P(x = l_2, t) = 0, \quad (4.45)$$

and at the top, i.e.  $x=0$

$$V_1 \partial_t \rho_{g1}^{ref} = -\frac{k \rho_{g1}^{ref} A}{\mu} \partial_x P(x = 0, t) \quad (4.46)$$

#### 4.2.2.1 DETERMINATION OF LANGMUIR PARAMETERS

The Langmuir parameters were determined based on the experiment results. In order to obtain the Langmuir parameters, the general equation describing the adsorption process in mineral carbonation has to be presented. Firstly, the expression for adsorption density  $\rho$  in a given time has to be written. By applying the law of conservation in a given time the density  $\rho$  can be represented by the following equation:

$$\rho(t) = (C_{g,0} - C_g) \cdot \frac{M_g}{w_a} \quad \text{where } w_a = \frac{W}{V}, \quad (4.47)$$

here the  $C_{g,0}$  is the initial concentration of carbon dioxide (adsorbate) in the system,  $C_g$  denotes the concentration of carbon dioxide at a time  $t$ ,  $M_g$  is molecular mass of carbon dioxide and  $w_a$  – adsorption dosage, which is function of mass of adsorbent  $M_a$  and overall volume of the solution  $V$ .

Assuming a uniform distribution of the adsorbent through the system, and taking into consideration the relation between initial concentration of the active sites and chemical kinetics of reversible reactions, the equation (4.48), can be established as:

$$\frac{d\rho}{dt} = \left(\frac{k_{f1}}{M_{CO_2}}\right)(\rho_{\max} - \rho)(M_{CO_2} C_{g,0} - w_a \rho) - k_b \rho \quad (4.48)$$

By changing the units from molar to technological the general equation describing the adsorption process in mineral carbonation is given by:

$$\partial_t \rho = k_f (\rho_{\max} - \rho)(C_{g,0} - w_a \rho) - k_b \rho \quad (4.49)$$

At the equilibrium  $\rho = \frac{C_{g,0} - C_{g,e}}{w_a}$ , and the kinetic equation reduced to equation, which represents

the general form of Langmuir adsorption isotherm

$$\rho = \frac{\rho_{\max} K_{eq} C_{g,e}}{1 + K_{eq} C_{g,e}} \quad (4.50)$$

where  $\rho$  states for amount of adsorbate on the adsorbent at the equilibrium. The Langmuir model assumes that each molecule of the adsorbate occupies a single active site, so called mono – layer coverage of the surface;  $C_e$  is the concentration of adsorbate at equilibrium;  $\rho_{\max}$  represent the maximum adsorption capacity, which occurs for complete monolayer coverage on the adsorbate,  $K_{eq}$  is an empirical Langmuir constant.

Langmuir parameters are independent on the initial concentration, volume of the solution and amount of adsorbent. They are constant for a given temperature type of solution.

The values of the  $\rho_{\max}$  and  $K_{eq}$  can be determined from the slope and intercept of the linear form of the Langmuir equation:

$$\frac{1}{\rho} = \frac{1}{\rho_{\max} K_{eq}} \cdot \frac{1}{C_e} + \frac{1}{\rho_{\max}} \quad (4.60)$$

The achieved results are:

$$K_{eq} = 20 \text{ cm}^3/\text{g}$$

$$\rho_{\max} = 0,17 \text{ gCO}_2/\text{gCaSiO}_3$$

### PROCEDURE FOR DETERMINATION OF $k_f$ and $k_b$ PARAMETERS

The values of reaction rate constant can be obtained by solving the equation

$$\frac{1}{w_a(X_1 - X_2)} \ln \frac{(\rho - X_1)X_2}{(\rho - X_2)X_1} = k_f t \quad (4.61)$$

$$X_1 = \frac{b + \sqrt{b^2 - 4ac}}{2a} \quad X_2 = \frac{b - \sqrt{b^2 - 4ac}}{2a} \quad (4.63)$$

Here,

$$\text{and} \quad a = w_a \quad ; \quad b = C_{g,0} + w_a \rho_{\max} + \frac{1}{K_{eq}} \quad ; \quad c = \rho_{\max} C_{g,0} \quad (4.64)$$

The  $k_b$  value is determined from the relation  $k_b = k_f/K$

The achieved results are:

$$k_b = 0,014 \text{ 1/s}$$

$$k_f = 0,27 \text{ cm}^3/\text{g*s}$$

## CHAPTER 5

### RESULTS AND DISCUSSION

The process of wollastonite mineral carbonation conducted in our experiments is represented by time dependent CO<sub>2</sub> pressure. Four investigations were carried, which distinguish themselves by different compositions of the starting material (solid/liquid ratio) and by different initial pressures (see table 5.1 - below).

**Table 5. 1:** Characteristic data of particular experiments.

	Mass of wollastonite [g]	Mass of water [g]	Initial pressure [bar]
<b>Experiment 1</b>	58.69 (powder)	26.67	81
<b>Experiment 2</b>	68.53 (powder)	20	94.95
<b>Experiment 3</b>	53.38 (powder)	54.82	139.2
<b>Experiment 4</b>	102.27 (715 $\mu$ )	36.9	129

The conceptual model (see Section 4) assumes that the mineral carbonation reactions take place in the aqueous phase, or near the reacting wollastonite. The carbon dioxide reacts with water, dissolves and forms carbonic acid. As a result of subsequent dissociation the hydrogen cations and bicarbonate (carbonate) anions, are formed, and hydrogen ions attack wollastonite, which releases calcium cations. Carbonate ions diffuse in the opposite direction of the concentration gradient - from the particle surface to the core, and then CO<sub>2</sub><sup>2-</sup> reacts with free Ca cations forming stable carbonates. At this stage, a limitation of the process occurs because with time, the mass transfer rate of dissolved carbon dioxide drops down in the direction of the core.

This mineral carbonation process may be presented graphically by plotting the pressure in the closed system vs. time (Figures 5.1 – 5.4).

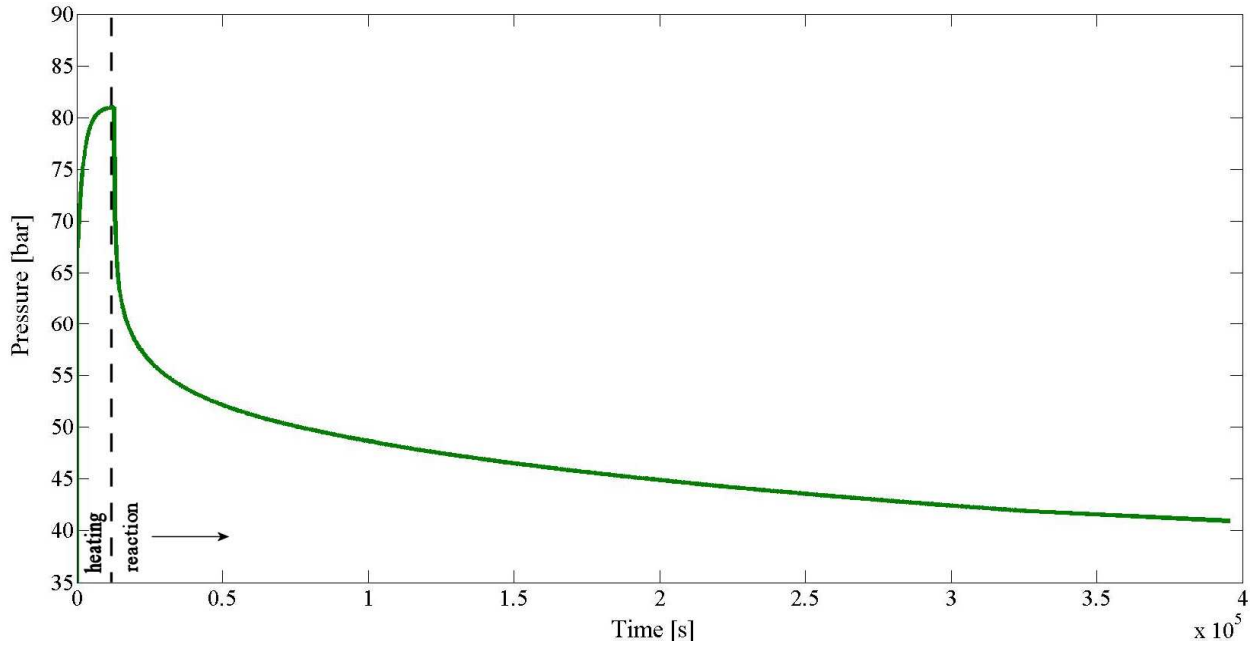


**Figure 5.1 a:** Pressure vs. time during a carbonation experiment 1. The initial mass of wollastonite was 58.69 grams, 26 grams of water and an initial pressure of 81 bars. This experiment was carried out with powder wollastonite. Until the dashed vertical line the temperature was increased to 61°C. The pressure continues to decline at the end of the experiment. The density decrease is 120 [kg/m<sup>3</sup>]. The free volume is 30 cm<sup>3</sup>.

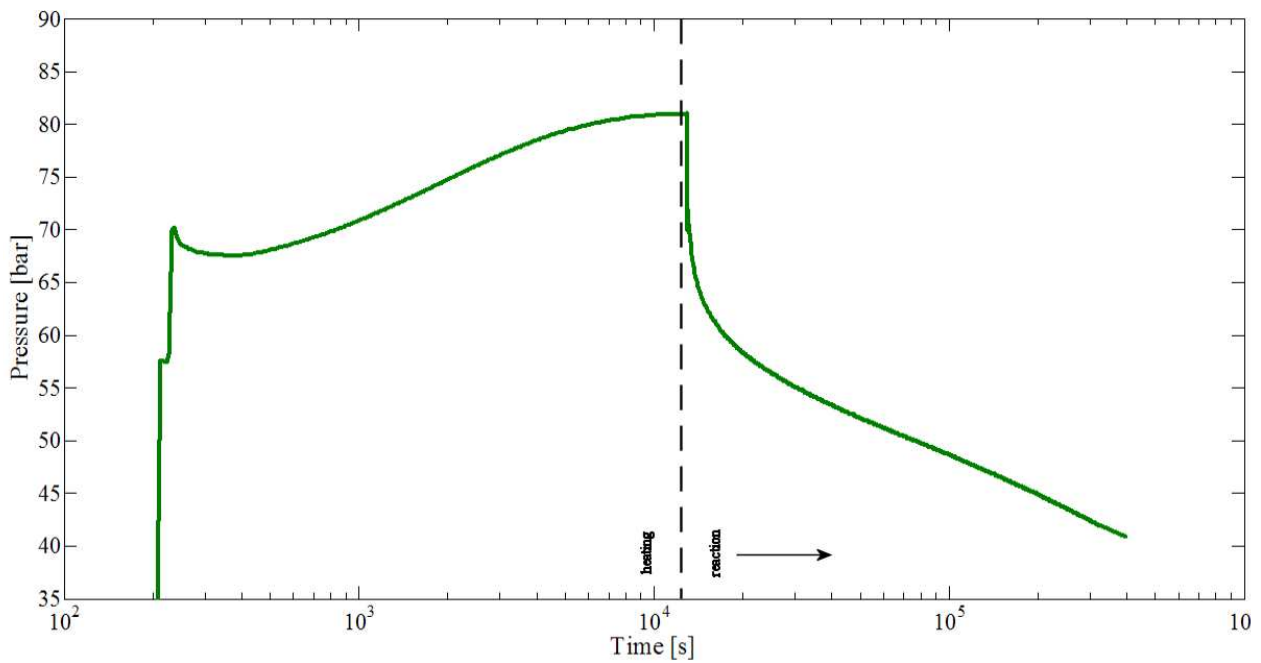


**Figure 5.1 b:** Pressure vs. log time during a carbonation experiment 1. The same as figure 5.1a, but now for a logarithmic time scale. There is an initial fast decline followed by a slow decline at later times.

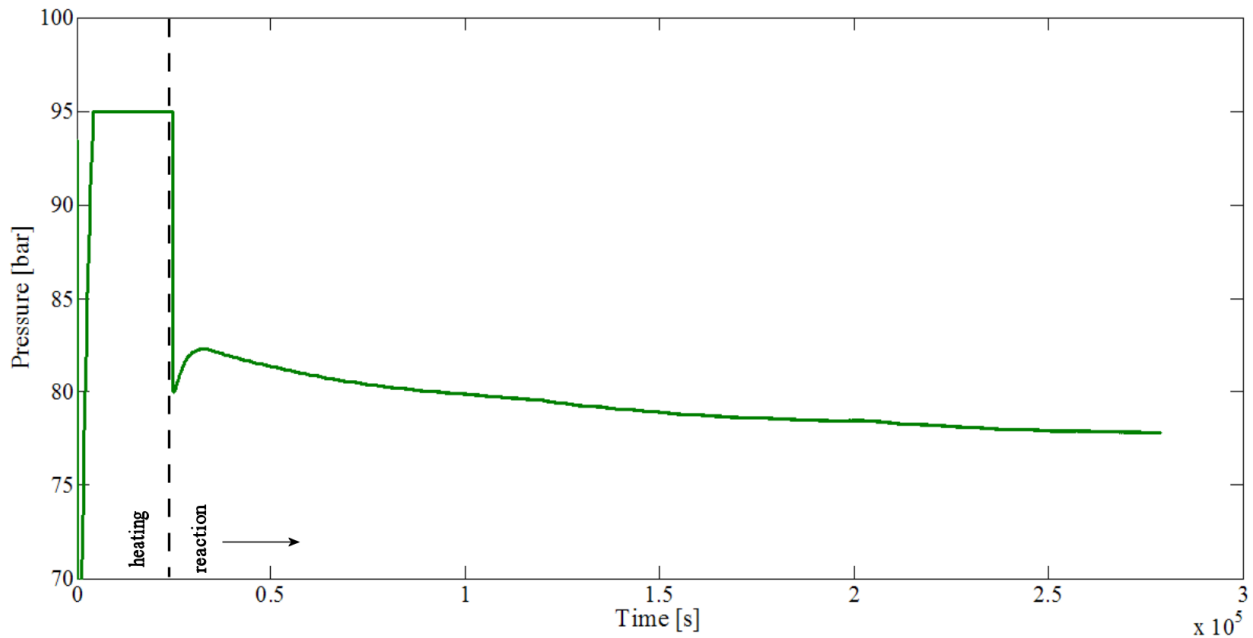


**Figure 5.2 a:** Pressure vs. time during a carbonation experiment 2. The initial conditions are 68.53 grams of wollastonite, 20 grams of water and an initial pressure of 94.95 bar. This experiment was carried out with powder wollastonite. The density decrease is  $70 \text{ kg/m}^3$ . The free volume is  $30 \text{ cm}^3$ .

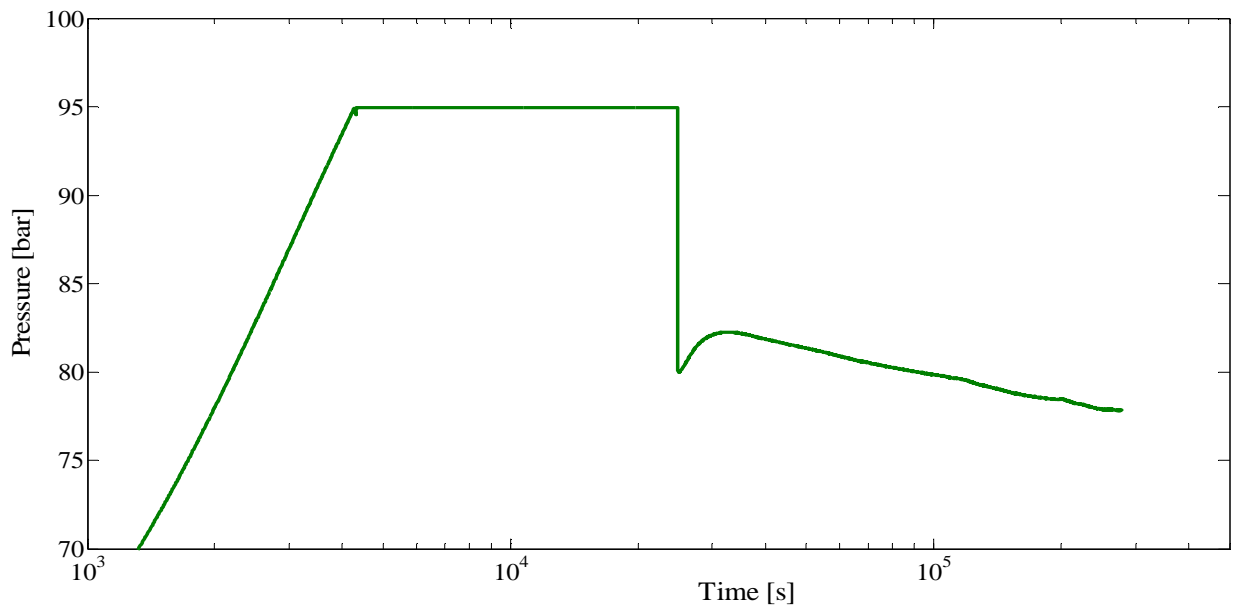


**Figure 5.2 b:** Pressure vs. log time during a carbonation experiment 2. The same as figure 5.2a, but now for a logarithmic time scale. There is an initial decline, which is instantaneous followed by a much slower decline than in figure 5.1b.

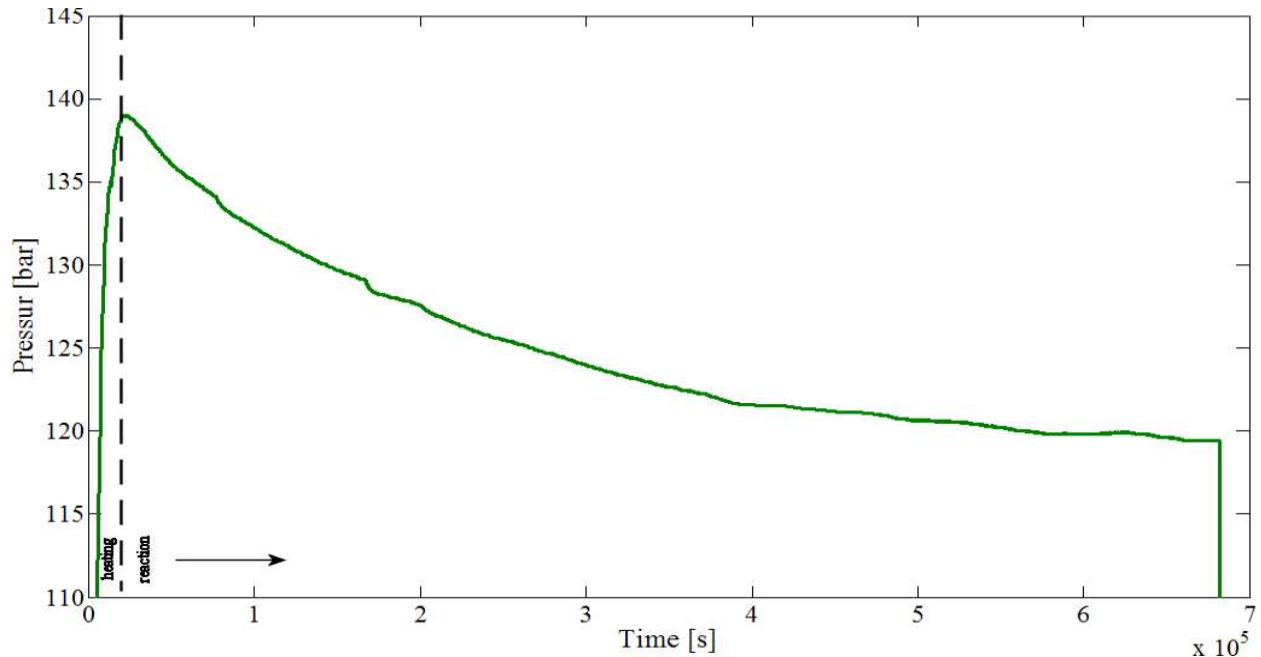


**Figure 5.3 a:** Pressure vs. time during a carbonation experiment 3. The initial conditions are: mass of wollastonite 53.38 grams, mass of water is 54.82 grams and the initial pressure is 139.2 bars. This experiment was carried out with powder wollastonite. There is no initial fast decline. The density decline is  $140 \text{ kg/m}^3$ . The free volume is  $4 \text{ cm}^3$ .

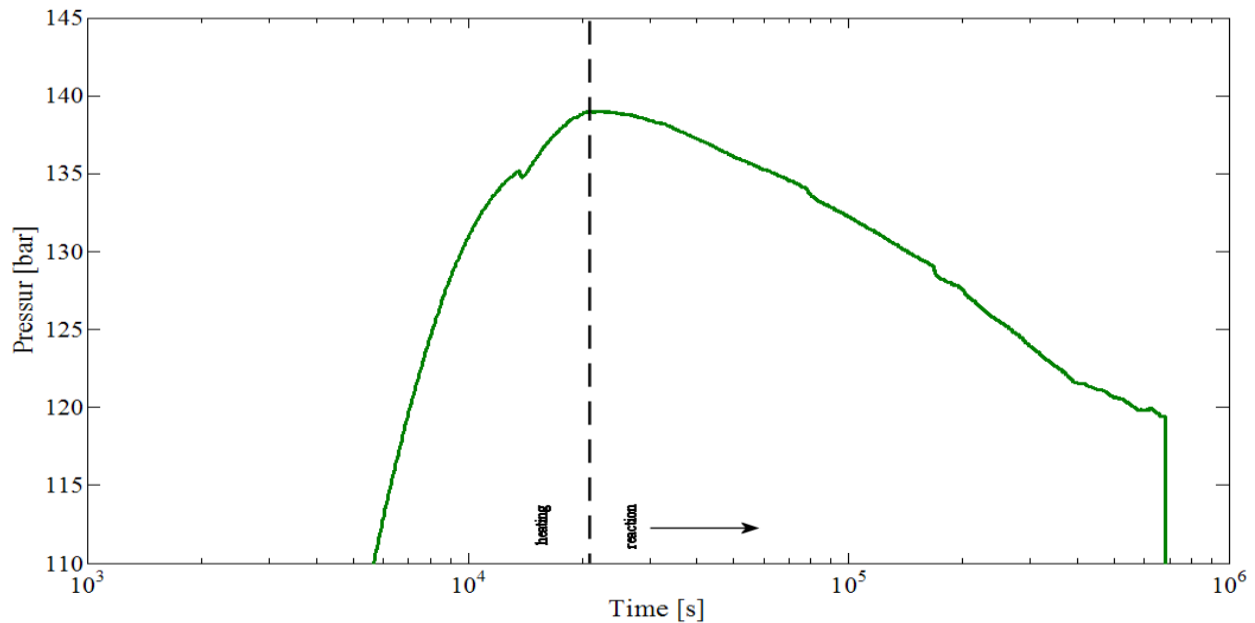


**Figure 5.3 b:** Pressure vs. log time during a carbonation experiment 3. The same as figure 5.3 a, but now for a logarithmic time scale. There is no initial fast decline.

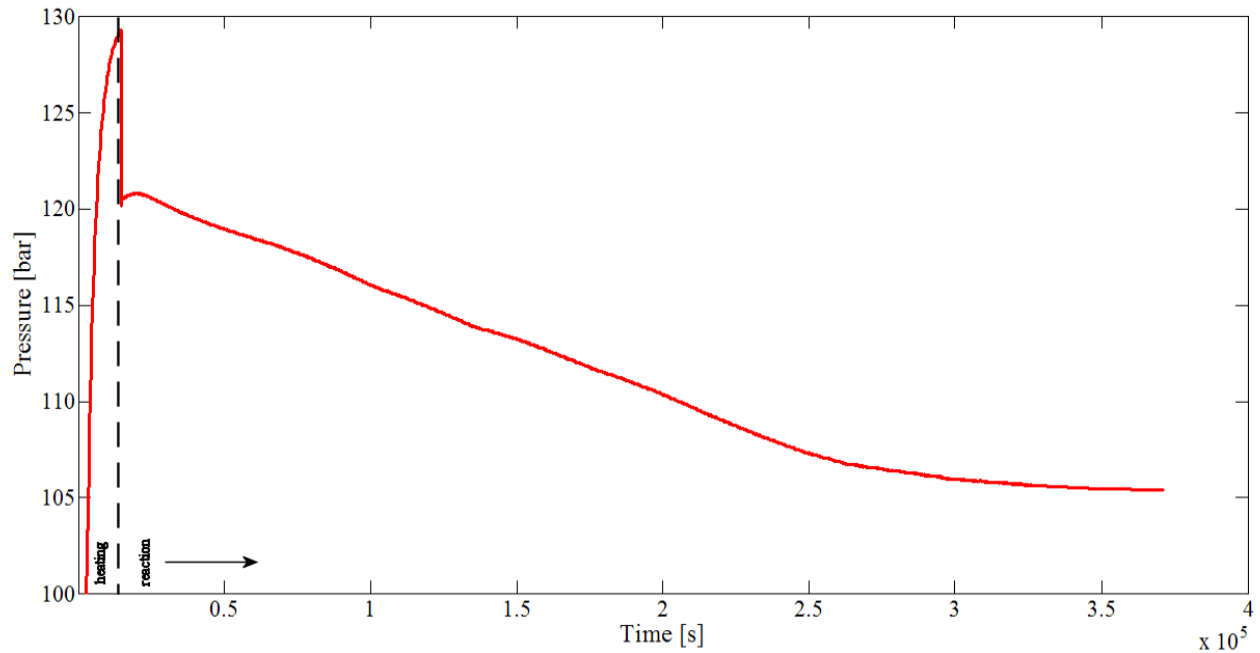


**Figure 5.4 a:** Pressure vs. time during a carbonation experiment 4. Initial conditions are: 102 g of wollastonite, water 36.9 and initial pressure 129 bars. This experiment is carried out with grains 715  $\mu\text{m}$ . There is an instantaneous initial decline followed by a slow decline.

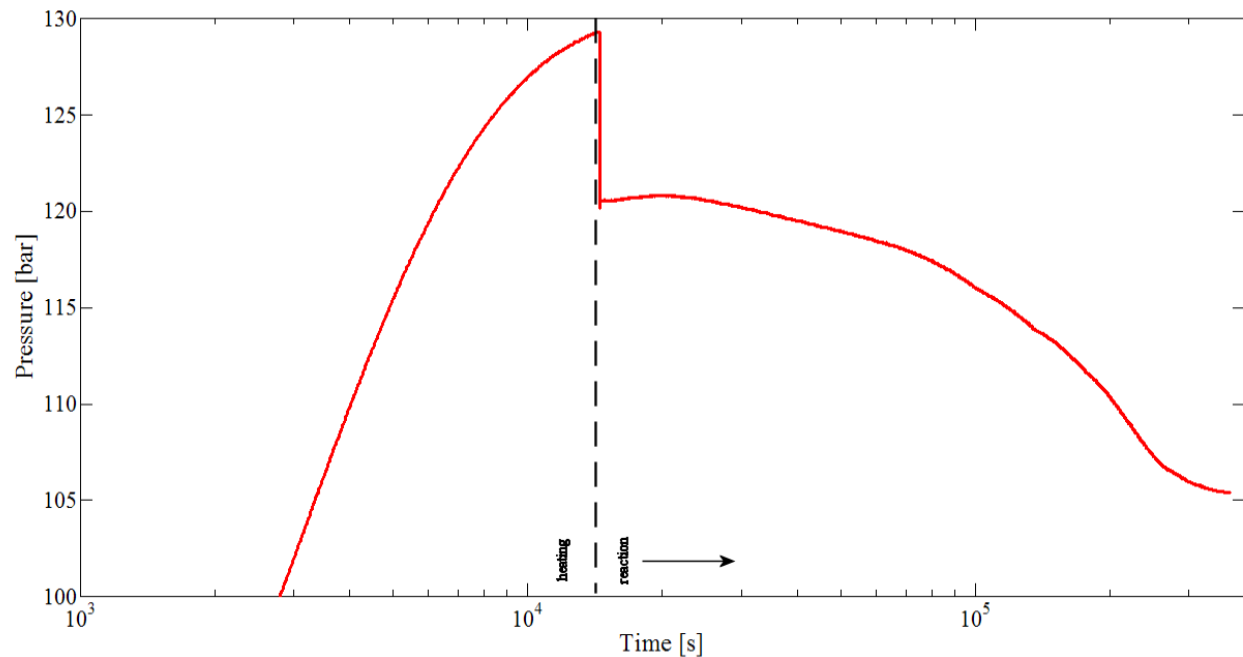


**Figure 5.4 b:** Pressure vs. log time during a carbonation experiment 4. The same as figure 5.4 a, but now for a logarithmic time scale. There is an initial fast decline followed by a slow decline at later times and an even slower decline towards the end of the experiment.

In all experiments, the first stage of the procedure was heating to the desired temperature of 61°C. During this period of time, pressure of carbon dioxide was increasing due to temperature change and stabilized after reaching the temperature set in the thermal reactor. In all experiments presented above, carbon dioxide was introduced to sample above critical conditions (temperature 304.2 K (31.05°C) and pressure 73.8 bar). Before introduction to the sample the temperature was below the critical point. As the temperature was rising, the density of liquid carbon dioxide was decreasing due to its expansion and the gas density was increasing due to evaporation. At the critical point both densities become equal, resulting in the supercritical phase formation. Graphical interpretation of density-pressure phase diagram of carbon dioxide is shown in Figure 5.5.

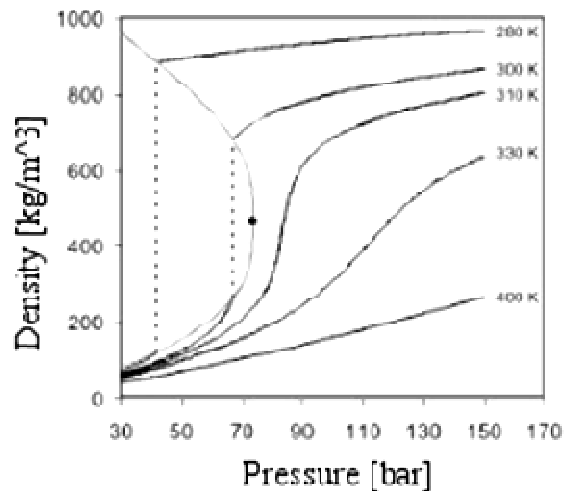


**Figure 5. 5:** Density-pressure phase diagram of carbon dioxide (after Jacobs, 2005).

Just after opening of the valves the gas expansion in the reference cell and compression in the sample cell are observed. It represents an adiabatic process, in which effectively no heat is exchanged with the outer environment (the temperature monitoring system did not show any changes in the temperature of the vessel). It can be deduced that in case of these experiments the process happened very fast or/and the change of temperature occurred inside the vessel. For that reason the measuring equipment was unable to record any changes. This phenomenon can be observed in the experiments 1, 2 and 4 in which the pressure transducer showed a slight gas pressure increment just after a significant drop. It happened due to the adiabatic process, which caused (not visible by record data) a decrease of temperature. Subsequently temperature equilibration took place at 61°C (figure 5.6 and 5.7 – below).

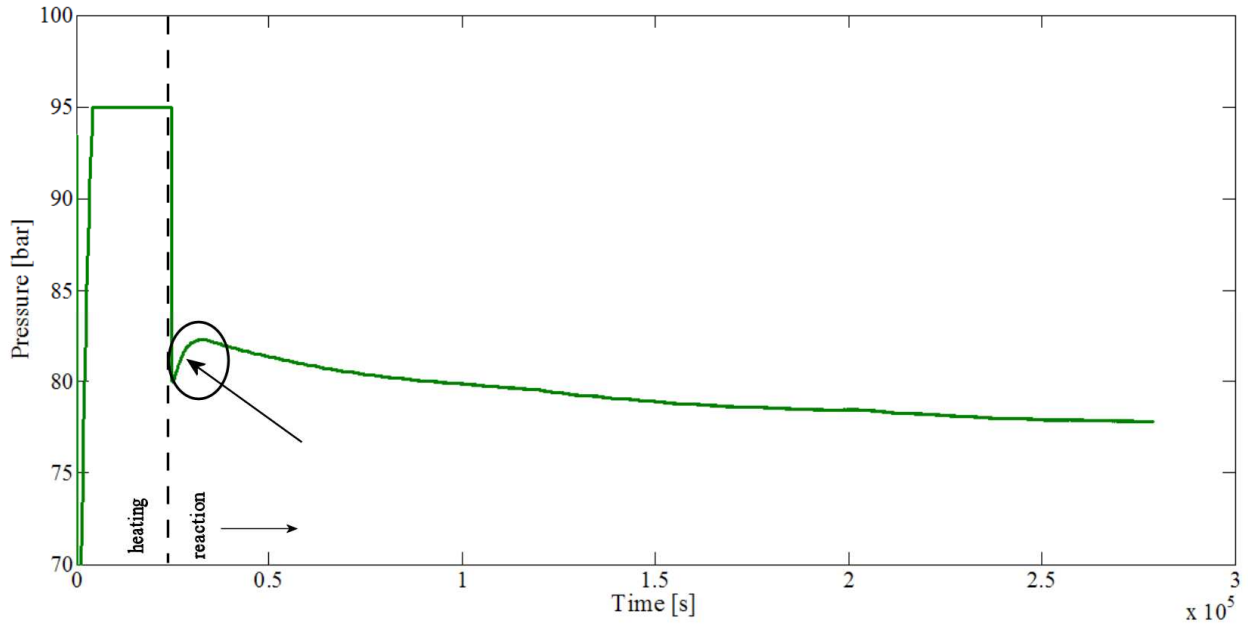


**Figure 5.6:** The same as figure 5.2 but with indication of the adiabatic expansion of carbon dioxide in experiment 2.

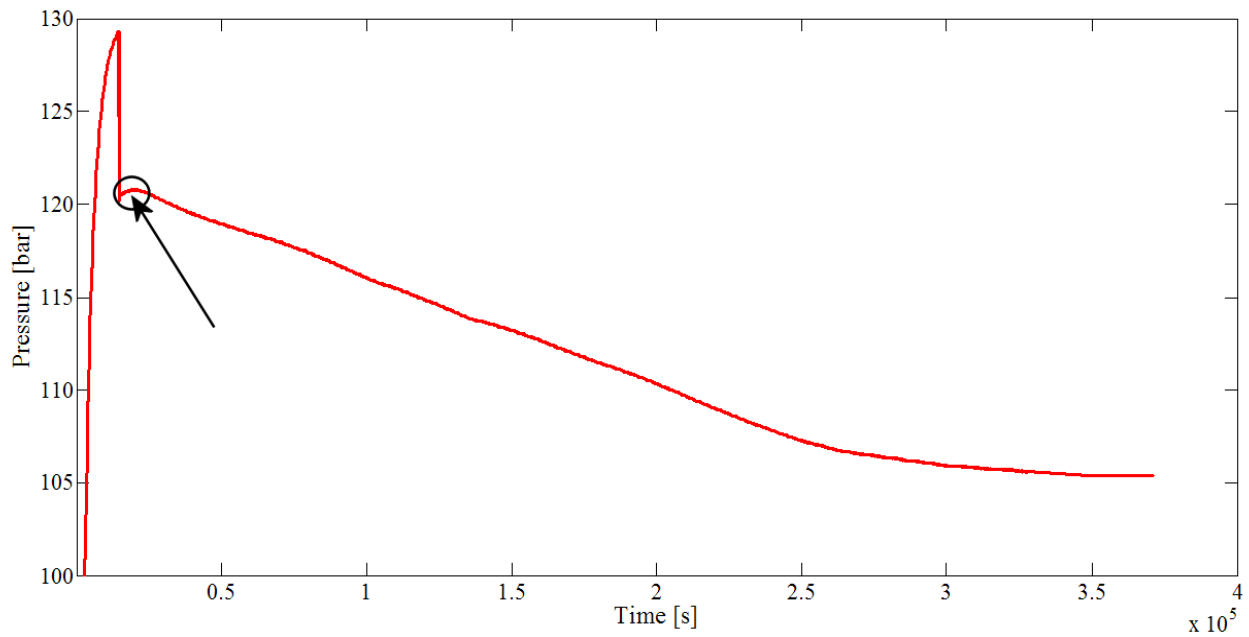


**Figure 5. 7:** The same as figure 5.4, but with indication of the adiabatic expansion of carbon dioxide in experiment 4.

## SEM and CT SCANNER EXAMINATION OF THE SAMPLES

According to CT scanner and SEM examination of the samples before and after exposure to the carbon dioxide, the distinction between three types of chemical compounds in the final product of the reaction can be made: starting wollastonite –  $\text{CaSiO}_3$ ,  $\text{CaCO}_3$  and silicon dioxide  $\text{SiO}_2$  (possibly even the fourth one – partly reacted wollastonite). Initially the sample consisted of pure calcium silicate.

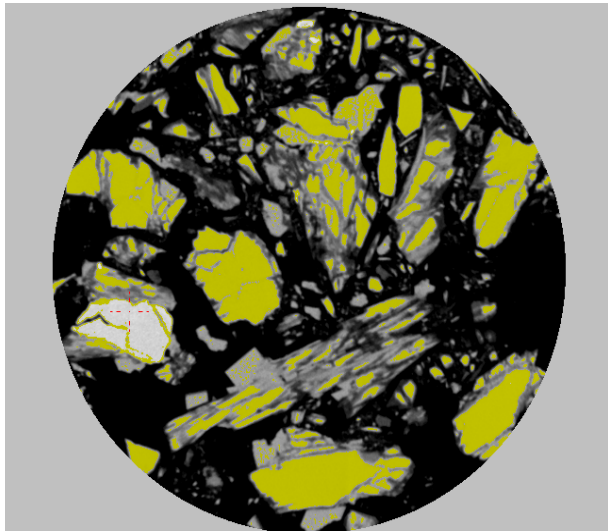


Figure 5.8a: Presence of  $\text{CaSiO}_3$  in the sample indicated by yellow color. Grey parts cover  $\text{SiO}_2$  and  $\text{CaCO}_3$ .

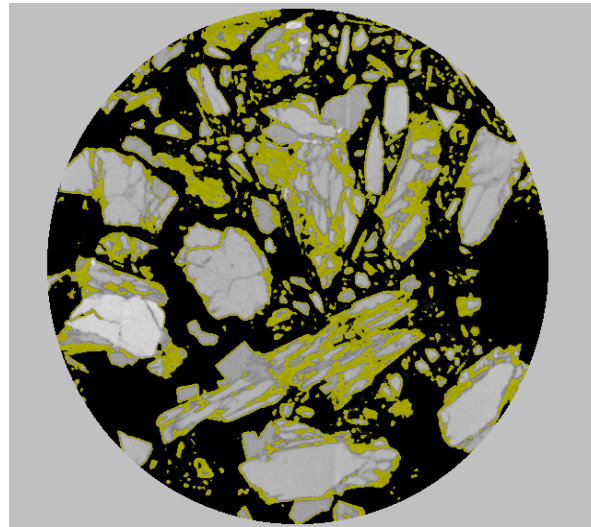


Figure 5.8b: Presence of  $\text{SiO}_2$  in the sample indicated by yellow color. Grey parts cover  $\text{CaSiO}_3$  and  $\text{CaCO}_3$ .

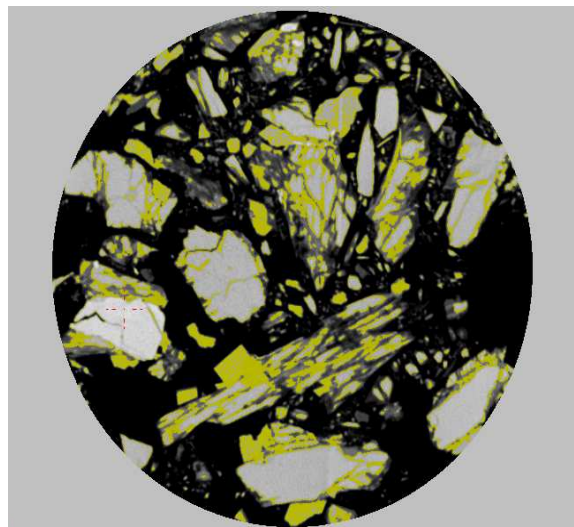
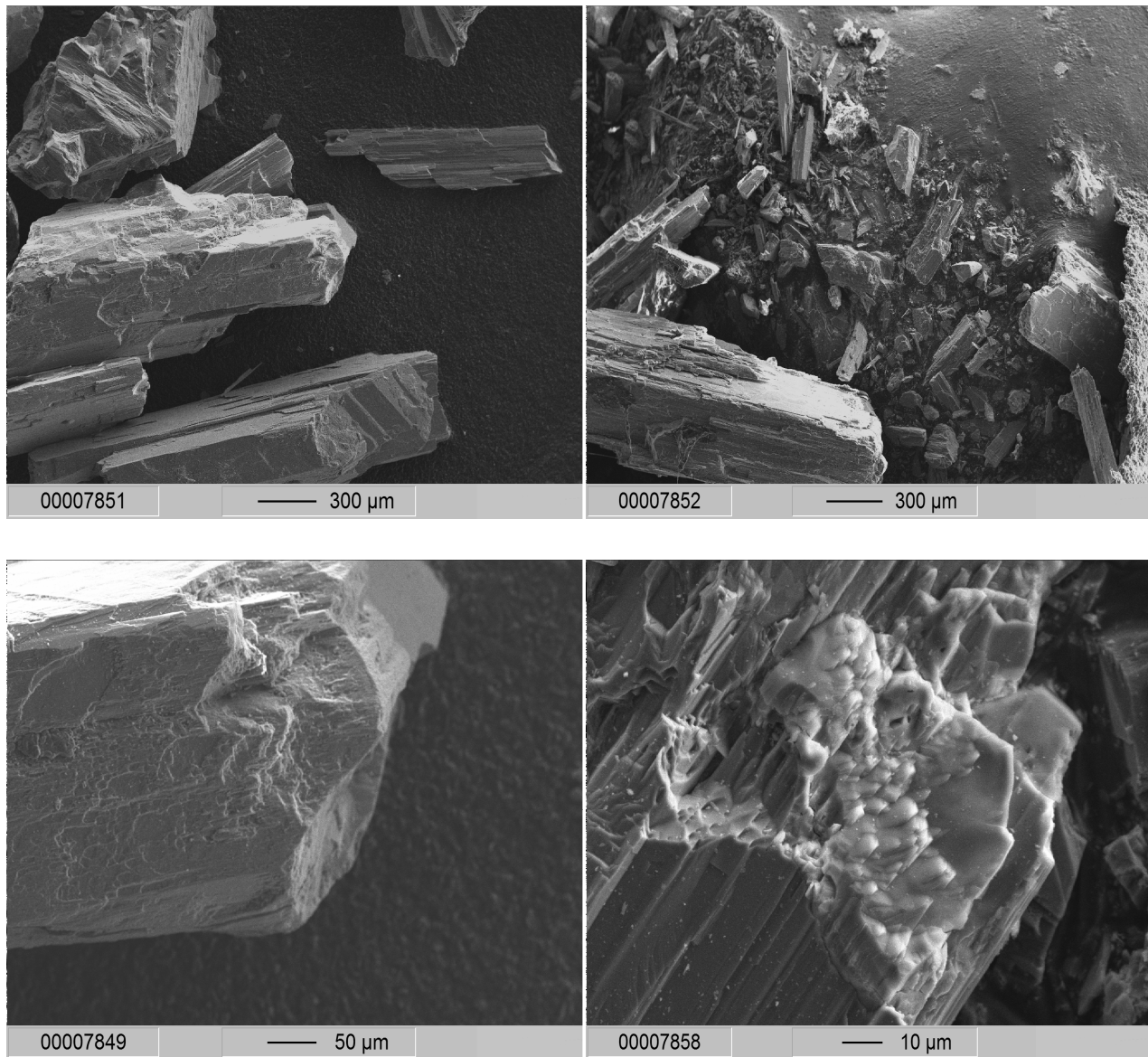


Figure 5.8c: Presence of  $\text{CaCO}_3$  in the sample indicated by yellow color. Grey parts cover  $\text{CaSiO}_3$  and  $\text{SiO}_2$ .

**Figure 5. 8 a-c:** CT scanner photos presenting three different types of chemical compounds in the reaction product.

The CT scanner analyses showed that investigated sample contains 42.04 % of  $\text{SiO}_2$ , 28.67 % of  $\text{CaCO}_3$  and 30.02 % of  $\text{CaSiO}_3$ .

The SEM electro probe analyses showed that minerals exhibit changes in the shape after the mineral carbonation process. The particles tend to have a rhombohedron shape - typical for calcite. The starting material exhibits predominantly acicular (needle like) particles shapes (figure 5.7 –left). Most of them, as a result of reaction, disappeared and were replaced by crystals with rhombohedron shapes. This phenomenon proved the carbonation reaction (figure 5.7 below).



**Figure 5.7:** SEM photos of the wollastonite samples before (left) and after (right) experiment. Photos on the left side represent particles with needle like shape. In the pictures on the right side some particles, which have a rhombohedron shape appears. It shows presence of calcite. Bottom right picture shows silica rich layer.

Figure 5.7 (bottom right picture) shows that nucleation of calcite is associated with parallel formation of silica. This phenomenon leads to passivating layer formation, what can significantly limit the reaction rate of the process.

## 5.2 THE CONVERSION OF WOLLASTONITE TO CALCIUM CARBONATE

Estimation of conversion rate of wollastonite ( $\text{CaSiO}_3$ ) to calcium carbonate ( $\text{CaCO}_3$ ) was based on the weight increment ( $\Delta W$ ), obtained from the measurement of the sample mass by using a precision laboratory scale and by empirical calculation of carbon dioxide mass adsorbed during the carbonation process.

The conversion can be calculated from the following equation:

$$X(\%) = \frac{(\Delta W / A_{\text{RCO}_2}) \times A_{\text{RCa}}}{(W_R / M) \times A_{\text{RCa}}} \times 100 \quad (5.1)$$

In the above equation  $X$  denotes the degree of conversion and  $\Delta W$  denotes the weight increment caused by the composition of  $\text{CaCO}_3$  in at temperature of  $61^\circ\text{C}$  for a range of pressures. The value of  $\Delta W$  is obtained from the mass measurement of the sample before the experiment and by a volumetric calculation of carbon dioxide mass adsorbed.  $W_R$  is the weight of the original sample (without water) at the beginning of the experiment.  $A_R$  represents the atomic weight  $\text{CO}_2$  ( $A_{\text{RCO}_2} = 44$ ) and  $\text{Ca}$  ( $A_{\text{RCa}} = 40$ ).

The term  $M$  represents the weight of wollastonite, which contains 1 gmol of calcium. 1gmol is 40 g of calcium. In the case of a rock composed of pure wollastonite,  $M$  is equal to 116.16 g/gmol of calcium, which is the molecular weight of  $\text{CaSiO}_3$  (Clifford *et al.*, 2005).

Accordingly, the expression  $\Delta W / 44$  represents the number of moles of  $\text{CO}_2$  that react during experiment. The results are given in the table 5.2.

**Table 5. 2:** Estimated conversion percentage of particular experiments.

	Initial pressure [bar]	Conversion [%]
<b>Experiment 1</b>	81	66
<b>Experiment 2</b>	94.95	28
<b>Experiment 3</b>	139.2	24
<b>Experiment 4</b>	129.21	21

### 5.3 THE EFFECT OF PRESSURE ON THE CARBONATION OF WOLLASTONITE REACTED AT 334K DURING 3 DAYS

None of the experiments described here were performed in duplo and therefore the interpretation must be considered as tentative.

The aim of the test was to study the influence of pressure on the conversion rate keeping all other variables the same (solid/liquid ratio, temperature). A series of four experiments were performed (data in table 5.3):

**Table 5. 3:** Conversion rate achieved during 3 days experiment (data for experiments a – d).

	Initial pressure [bar]	Conversion [%]
<b>Experiment a</b>	37	13.20
<b>Experiment b</b>	48	22.40
<b>Experiment c</b>	82	71
<b>Experiment d</b>	145	74

Figure 5.9 indicates that the reaction rate is strongly dependent on the critical point of carbon dioxide. Below the pressure of 73.8 bar (critical point), the experimental results indicate that the reaction is very slow. However, when the pressure was elevated above the critical point (to the supercritical condition of carbon dioxide) then the reaction rate increased.

From above, it can be concluded that conditions favorable for mineral carbonation process include a pressure above the critical point of the gas.

Based on the experimental results and research from Vorholz *et al* on the equilibrium of the CO<sub>2</sub>–H<sub>2</sub>O binary system (Vorholz *et al*, 2000) we can assume that the mole fraction of CO<sub>2</sub> at a temperature of 61°C (334K) in the pressure range 80 - 150 bar is almost independent of pressure. Vorholz *et al* conducted an experiment that demonstrated the independence of the mole fraction of CO<sub>2</sub> of the conditions of pressure at the temperature 394K in the pressure range 80 - 150 bar. Based on above it can be stated that the effect of pressure on conversion (in the range 80 - 150 bars) is rather small.

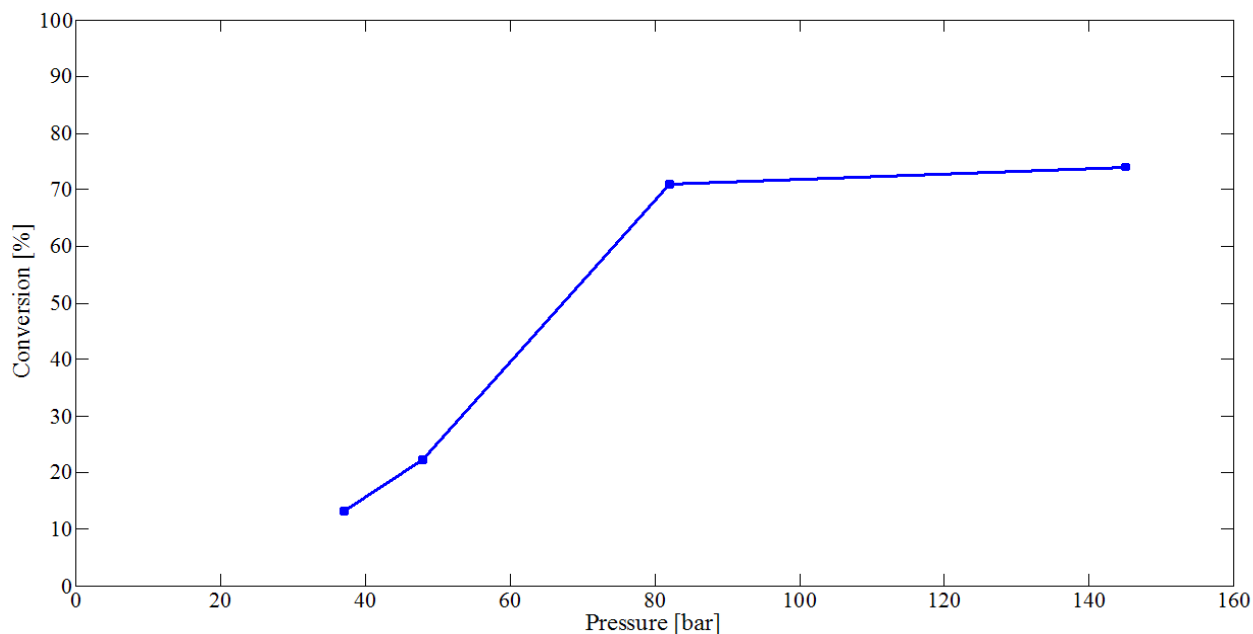


**Figure 5. 9:** The effect of pressure on the carbonation conversion percentage of wollastonite reacted at 334K after 3 day for series of experiments (similar water conditions).

#### **5.4 THE EFFECT OF WATER ON THE CARBONATION OF WOLLASTONITE REACTED AT 334K**

Figures 5.10 – 5.13 show that pressure of carbon dioxide initially decreases rapidly (See fragment of the curve on the red background). This decrease may indicate the expansion of gas into empty spaces and the dissolution process of  $\text{CO}_2$  in water. The “breaking point” at which both dissolution and adsorption occur can be calculated using of mass balance and Henry’s law. After this point (indicated on the graphs by a black dot) adsorption of carbon dioxide takes place.

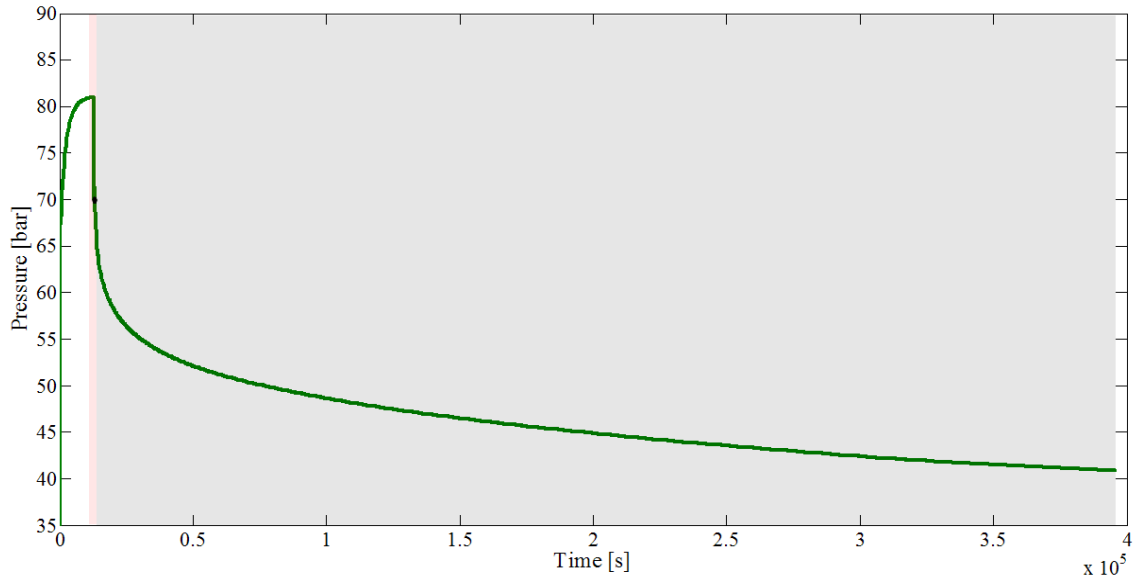


**Figure 5. 10:** Pressure vs. time during a carbonation experiment 1. The same as figure 5.1a, but with indication of dissolution of carbon dioxide in water (part of graph on the red background) and carbonation region (part of graph on gray background). Experimental conditions: mass of wollastonite 58.69g (powder), mass of water 26.67 g, initial pressure 81 bar.

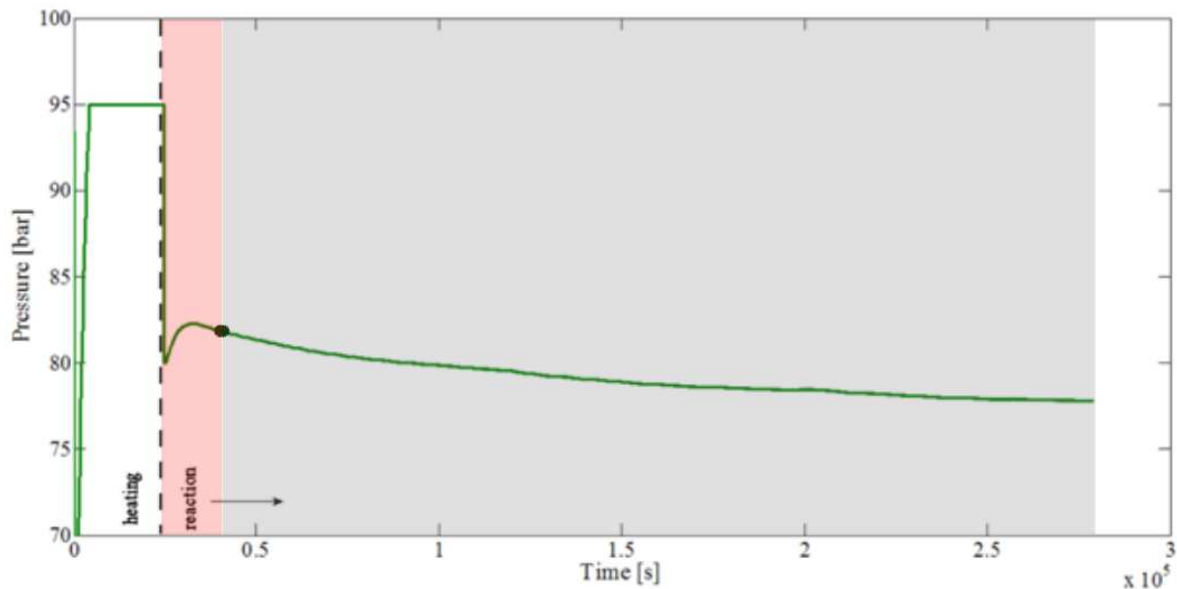


**Figure 5. 11:** Pressure vs. time during a carbonation experiment 2. The same as figure 5.2a, but with indication of dissolution of carbon dioxide in water (part of graph on the red background) and carbonation region (part of graph on gray background). Experimental conditions: mass of wollastonite 68.53 (powder), mass of water 20 g, and initial pressure 94.95 bar.

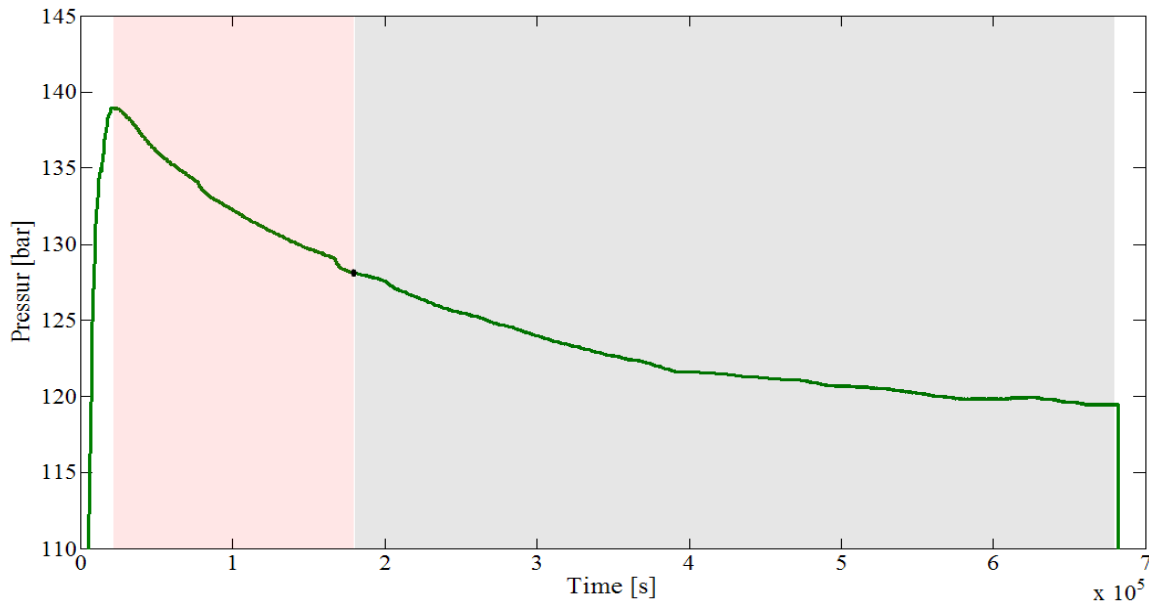


**Figure 5. 12:** Pressure vs. time during a carbonation experiment 3. The same as figure 5.3a, but with indication of dissolution of carbon dioxide in water area (part of graph on the red background) and carbonation region (part of graph on gray background). Experimental conditions: mass of wollastonite 53.38 (powder), mass of water 54.82 g, initial pressure 139.2 bar.

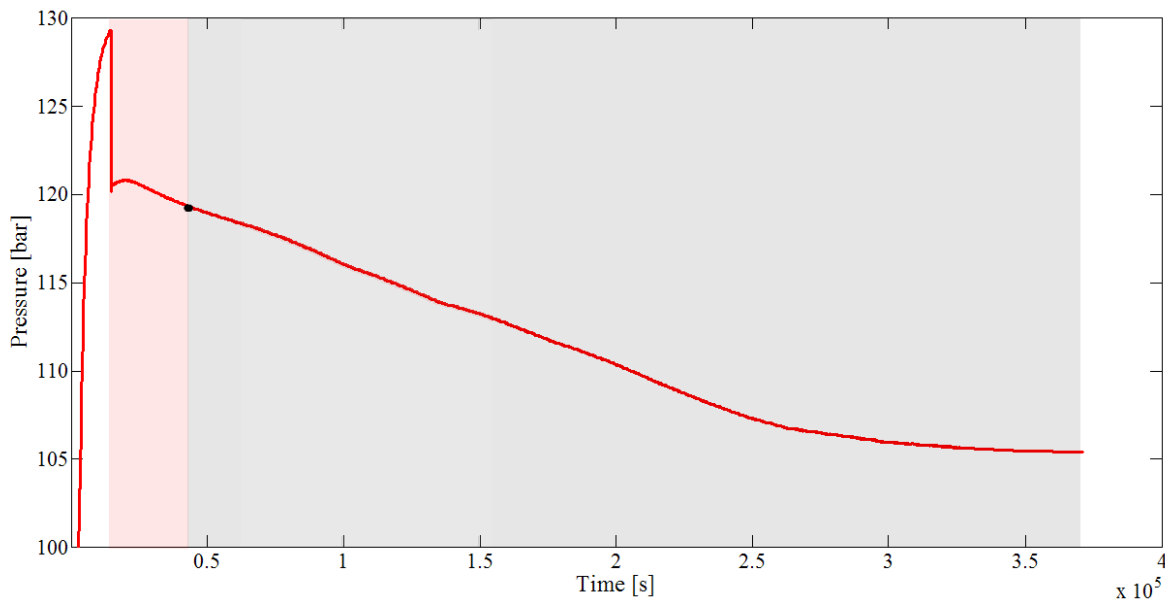


**Figure 5. 13:** Pressure vs. time during a carbonation experiment 4. The same as figure 5.4a, but with indication of dissolution of carbon dioxide in water area (part of graph on the red background) and carbonation region (part of graph on gray background). Experimental conditions: mass of wollastonite 102.27 (715 $\mu$ ), mass of water 36.9 g, and initial pressure 129.21 bar.

Comparison of the particular test (with different solid/liquid ratio) shows that with a decrease of the ratio of solid/liquid, the time of “dissolution part” process increases (see figure of experiment 1 and 3 and experiment 2 and 3). This phenomenon makes it possible that the rate of dissolution of  $\text{CO}_2$  and dissociation of carbonic acid is a limiting factor of the process.

## 5.5 MASS OF CARBON DIOXIDE CAPTURED IN THE EXPERIMENT

This section shows the result of the calculation of the mass of the carbon dioxide solute in the aqueous phase and of the adsorbed mass by wollastonite (to form calcium carbonate).

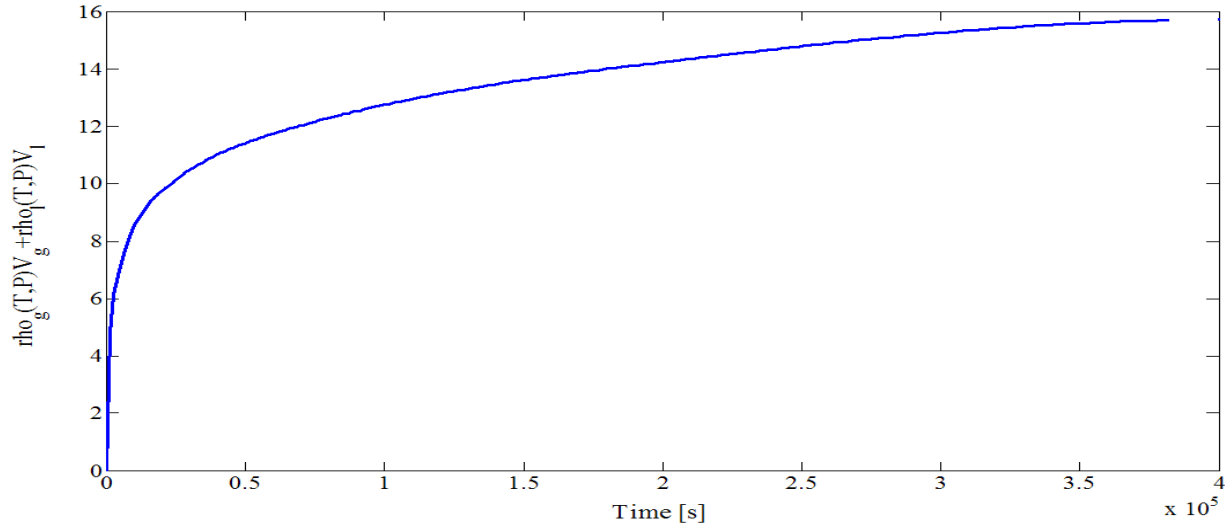


**Figure 5. 14:** Mass of carbon dioxide adsorbed by wollastonite and dissolved in water ( $\rho_g(T,P)V_g + \rho_l(T,P)V_l$ ) vs. time (exp1). See also figure 5.1.

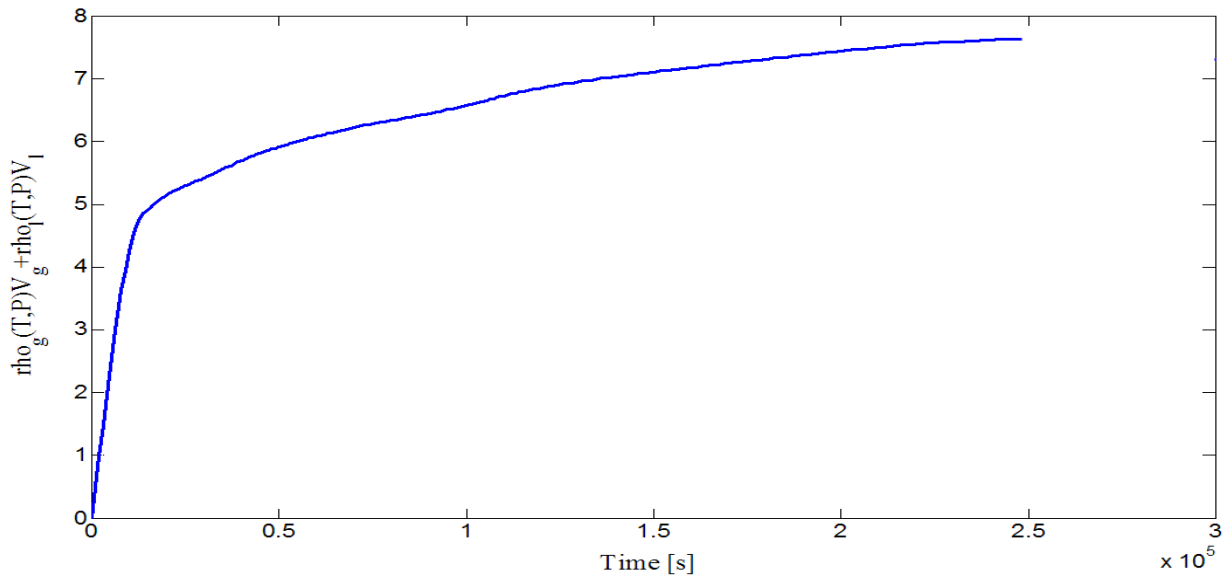


**Figure 5. 15:** Mass of carbon dioxide adsorbed by wollastonite and dissolved in water ( $\rho_g(T,P)V_g + \rho_l(T,P)V_l$ ) vs. time (exp 2). See also figure 5.2.

Figures 5.14 and 5.15 show the sum of the mass of carbon dioxide adsorbed on wollastonite and dissolved in water ( $\rho_g(T,P)V_g + \rho_l(T,P)V_l$ ) vs. time for experiment 1 and 2 respectively. In the experiment 1 the initial pressure was 81 bars, the temperature 61°C, and the mass of the sample

58 grams; in the experiment 2 the initial pressure was 94.95 bars, the temperature 61°C, and the mass of the sample was 68 grams. Initially the graphs show a square root of time behavior, but it does not lead to a single straight line indicating that there are various processes the occur. The process is still continuing beyond  $4 \times 10^5$  seconds in case of the first experiment and  $3 \times 10^5$  seconds in the case of the second experiment. The mass of CO<sub>2</sub> adsorbed is almost 25% (experiment 1) and 10% (experiment 2) of the initial mass of wollastonite. Based on the results presented in section 5.3 the difference in adsorbed mass in experiment 1 and 2 is not only influenced by different initial pressures, but rather by different solid/liquid ratios of the samples (experiment 1 ~2/1, experiment 2 ~ 3.5/1). For example for  $1.5 \times 10^5$  seconds, the mass adsorbed in the first experiment is double the mass adsorbed in second one. The curve representing mass adsorbed in the first experiment is very smooth.

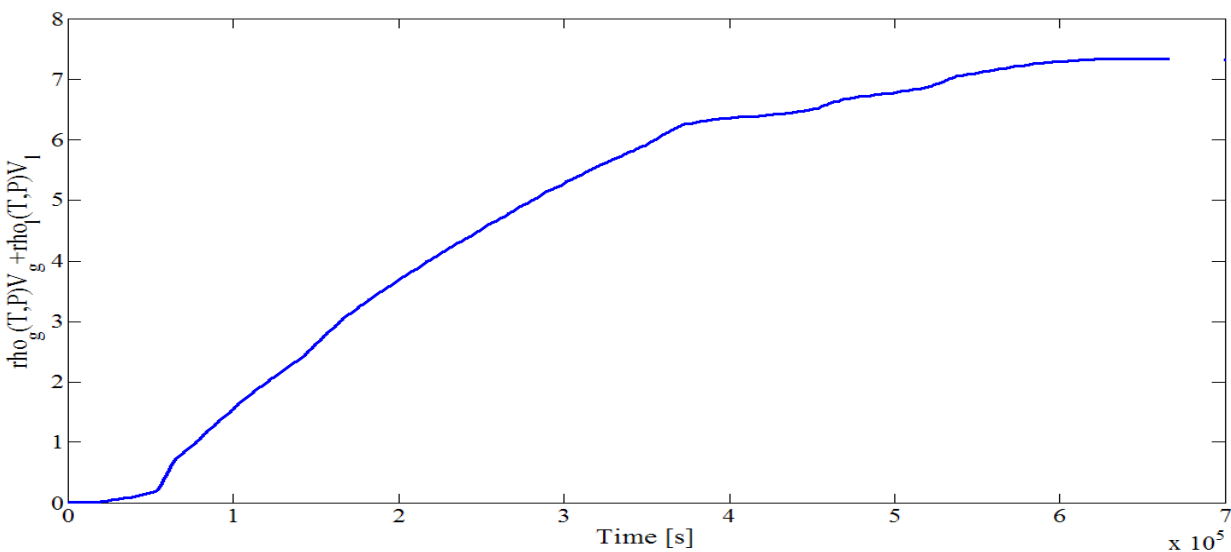


**Figure 5. 16:** Mass of carbon dioxide adsorbed by wollastonite and dissolve in water ( $\rho_g(T,P)V_g + \rho_l(T,P)V_l$ ) vs. time (exp 3)

Figures 5.16 shows the sum of the mass of carbon dioxide adsorbed on wollastonite and dissolved in water ( $\rho_g(T,P)V_g + \rho_l(T,P)V_l$ ) vs. time for experiment 3. The initial pressure was 139.2 bars, the temperature 61°C, and the mass of the sample 53.58 grams. The process, like in case of experiment 1 and 2 is still continuing, beyond  $7 \times 10^5$  seconds. The mass of CO<sub>2</sub> adsorbed is almost 15% of the initial mass of wollastonite. The plot shows that the adsorption is much slower than in the case of experiment 1 and 2. Plots 5.14 and 5.15 are very steep ( $\sim 85^\circ$ ) at the beginning (first  $0.5 \times 10^5$  seconds), whereas the plot 5.16 is more flat ( $\sim 45^\circ$ ). This is possibly due to low solid/liquid ratio 1/1. Up to  $2 \times 10^5$  seconds only diffusion controls the carbonation process, because only dissolution of the carbon dioxide in the water occurs (See graph 5.12).

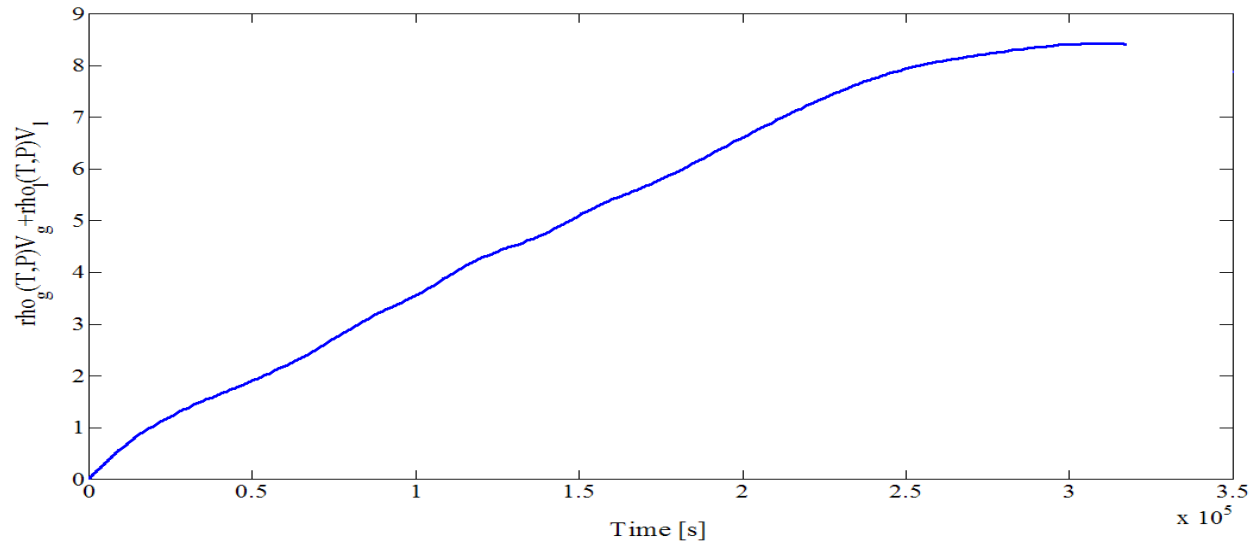


**Figure 5. 17:** Mass of carbon dioxide adsorbed by wollastonite and dissolve in water ( $\rho_g(T,P)V_g + \rho_l(T,P)V_l$ ) vs. time (exp 4).

Figure 5.17 shows the sum of the mass of carbon dioxide adsorbed on wollastonite and dissolved in water ( $\rho_g(T,P)V_g + \rho_l(T,P)V_l$ ) vs. time for experiment 4. The initial pressure was 129 bars, the temperature 61°C, and the mass of the sample 102.2 grams. The process, like in case of experiment 1, 2 and 3 is still continuing, beyond  $3.5 \times 10^5$  seconds. The mass of CO<sub>2</sub> adsorbed is almost 7% of the initial mass of wollastonite. The plot shows that the adsorption is much slower than in the case of experiment 1 and 2, even if the ratio of solid/liquid is more or less similar. It is possible a result of larger grain size (experiment 1, 2 – powder around 1 – 15 μm, experiment 4 – 715μm). With increasing grain size, the adsorption of the calcium carbonate by wollastonite decrease.

## 5.6 FIRST (FAST) STAGE OF CARBONATION

The following test was conducted in order to show the comparison of the reaction rate. The results used to the CT scanner analysis were obtained after the first 15 minutes and after 168 hours of the experiment. Based on the results from the CT scanner analysis, it can be concluded that carbonation occurs quite fast already during the initial time of the experiment. As a consequence 18.40% of the sample was converted into calcium carbonate. Then the carbonation process slows down attaining 30.02% of calcium carbonate (after 168 hours) and then approaching adsorption with very slow rate after relatively long time (comparable to 30% after one week).

CT scanner results were recorded for the first time after 15 minutes and later after 168 hours after exposing a sample of wollastonite to CO<sub>2</sub>. CT scanner analyses showed that after 15 minutes of the process the sample contains 5.47% of SiO<sub>2</sub>, 18.40 % of CaCO<sub>3</sub> and 53.08 % of CaSiO<sub>3</sub> and after one week 42.04 % of SiO<sub>2</sub>, 28.67 % of CaCO<sub>3</sub> and 30.02 % of CaSiO<sub>3</sub>. The scan image of

pure sample before experiment (Figure 5.18) does not exhibit any differences in the density (sample uniformly gray).

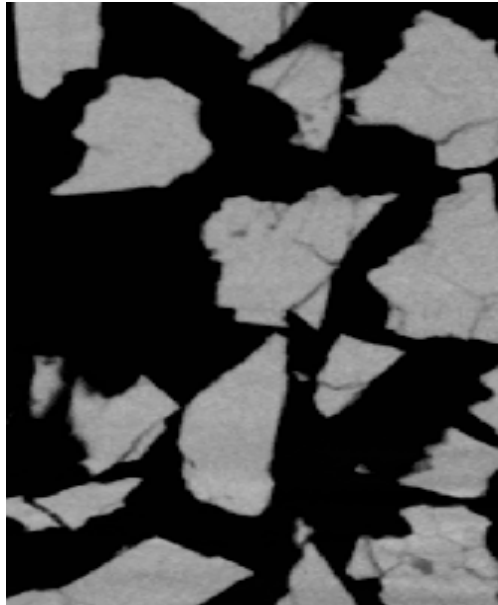


**Figure 5. 18:** CT scanner image of the pure sample of wollastonite before experiment.

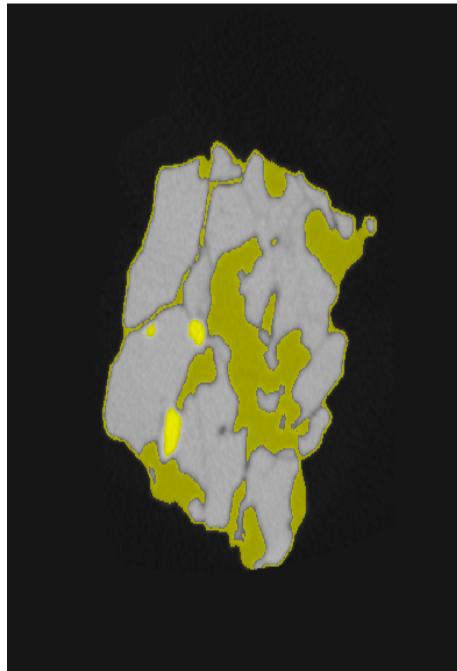


**Figure 5. 19:** CT scanner image of the sample of wollastonite after 15 minutes of carbonation process. The yellow parts indicate the presence of CaCO<sub>3</sub>. The gray part covers CaSiO<sub>3</sub> and SiO<sub>2</sub>.



**Figure 5. 20:** Image of the wollastonite sample after 168 hours of carbonation process. The yellow parts indicate the presence of CaCO<sub>3</sub>. The gray covers presence of CaSiO<sub>3</sub> and SiO<sub>2</sub>.

## 5.6 ADSORPTION ISOTHERM TEST RESULTS

For the purpose of the adsorption isotherm test, the following operational parameters were determined: the temperature 61°C and the pressure up to 90 bar. The amount of carbon dioxide adsorbed by a unit of wollastonite and pressure data obtained from the experiment lead to generation of an adsorption curve. The results from test become input data to obtain parameters of the Langmuir model (figure 5.21), which seems to be adequate for characterization of the CO<sub>2</sub> adsorption process on wollastonite. The procedure for adsorption density calculations is presented in Annex 3.

The adsorption isotherm presented below (figure 5.21) is steep at the range of low pressures and subsequently flattens out with increasing pressure at the moment when the total surface of the wollastonite is covered with carbon dioxide. Additionally this adsorption isotherm provides information about maximum adsorption density that corresponds to the maximum amount of carbon dioxide that can be adsorbed by 1 kg of wollastonite.

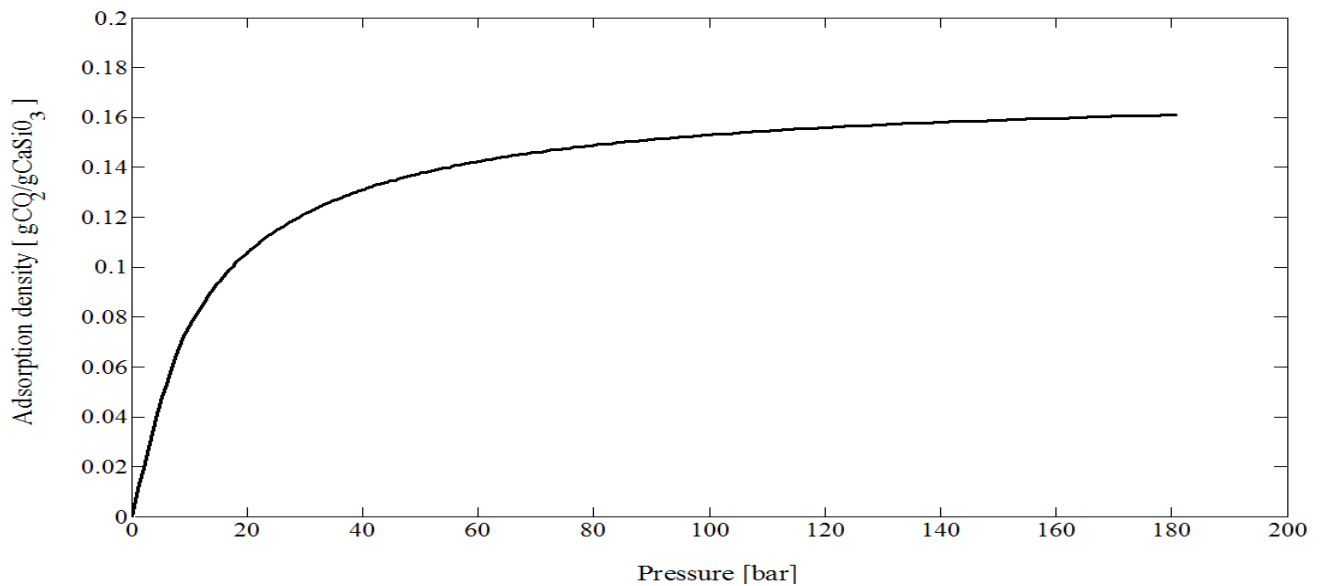


**Figure 5. 21:** Adsorption isotherm curve: adsorption density vs. pressure.

## **5.7 MAJOR LIMITATIONS OF THE MINERAL CARBONATION PROCESS CONDUCTED IN THE EXPERIMENTAL SETUP**

The experimental results from mineral carbonation of wollastonite highlight a number of limitations of the experimental set-up.

The most significant limitation was the impossibility to introduce an additional amount of carbon dioxide to the closed system during the process while the carbonation reaction was preceding. Introduction of additional amount would influence the speed of the reaction.

Another important limitation was lack of stirring equipment installed in the sample vessel. Improvement of the process may be achieved by a use of the magnetic stirrer. Firstly, it would be very applicable in samples with higher liquid to solid ratio. It would allow achieving perfectly uniform conditions in whole sample cell. Additionally, agitation might have significant impact on increasing carbonation by mechanical removal of silica rich passivating layer around the calcium silicate. SiO<sub>2</sub> coating surface of wollastonite could be sloughed off during the reaction by means of stirring that would cause abrasion of particles.

## CHAPTER 6

### MODEL SIMULATIONS

#### Simulations

After creating the reacting flow model including the complex reversible reaction, the model equation can be solved using COMSOL Multiphysics 4.0. COMSOL Multiphysics is a software package that can be dedicated for simulation of a process of mineral carbonation, because it allows creating interactive transport models. Using COMSOL Multiphysics 4.0 software, a number of simulations were done to study on the influence of changing operational parameters like pressure and time. All figures are presented in the Annex 4.

#### Influence of time on transport phenomenon

Attached plots (Figure A4.1a-i) from Comsol Multiphysics simulations show how transport of CO<sub>2</sub> occurs. Figure A4.1 presents the mineral carbonation under a temperature of 61 °C and a pressure 95 bar. After a time of 1e5 [s] (around 1 day and 4 h) diffusing carbon dioxide almost reached the bottom of sample cell, the concentration decreases gradually from top to bottom of the sample vessel (Figure A4.1f). Figure A4.1i presents that after a time of 5e5 [s] (5 days 19 h) the concentration in whole system almost is equal and reached level of 150 [kg/m<sup>3</sup>]. The adsorption density increases with time (see Figure A4.1a-e) reaching 352 [kg/kg] at the time 5e5 [s] (Figure A4.1d). The adsorbed density increases with the time to certain point that is limited to the maximum adsorption density. Change in the concentration in time in the reference vessel and sample vessel is presented in the figure A4.1f-i.

#### Influence of change of pressure at constant temperature

Attached plots (Figure A4.2a – A4.2.i) show how the adsorption density changes with changing pressure. The simulations collaborated with the experimental results that the increment of the pressure above 120 bars (up to 300 bar) influences slightly the final density (see Figure A4.2a – A4.2.i).

#### Some major limitations of Comsol Multiphysics 4.0:

Comsol Multiphysics 4.0 is not adequate to give reliable results. The following problems were encountered:

- Errors in calculations of the influence of time on transport phenomenon. The same

- model have to be created in a new file couple of times to achieve correct results;
- Errors in plotting graphs – graphs are not plotted or wrong data are plotted;
  - The numerical effects – negative values of concentration.

Due to above, achieve results are presented in the annex 4.

## CHAPTER 7

### CONCLUSIONS

- The wollastonite carbonation is a viable option for stable and safe fixation of carbon dioxide. It uses, as a source, abundant minerals around the globe and utilizes already existing technologies. However to determine the viability in practice one has to take into account that activation methods are needed for increasing the reaction rates, and decreasing the demand of minerals, which is directly connected to a larger energy demand, and higher overall costs of the process. Also the environmental consideration, like additional emission of the carbon dioxide, as a result of transportation and use of pretreatment methods and devastation of both landscape and ecosystem may lower the value of this option.
- The aqueous mineral carbonation is a complex heterogeneous reaction that involves dissolution (release of calcium), nucleation, interface reaction and mass transfer. The dissolution and nucleation may be transport controlled and surface-reaction controlled.
- In this study the operational parameter were investigated, both experimentally and with use of the modeling software, i.e., partial pressure of carbon dioxide, solid/liquid ratio, particle size, reaction time. The model is in principal capable to deal with different partial pressures and reaction times and is limited with adsorption and rate constants. The experimental results showed that amount of water and particle sizes have the strongest influence on the carbonation process. Water behaves as a catalyst; however in the case of low solid/liquid ratios it may limit the conversion rate in time due to diffusion. Such a diffusion limitation will be absent is stirring equipment is available; the experiments show that the conversion rate does not strongly depend on the pressure in the range above critical point.
- The computed storage capacity of the wollastonite, based on the experimental results, is equal to  $0.17 \text{ kgCO}_2/\text{kgCaSiO}_3$ , which is in agreement with the work of Goff and Lackner (1998). They show that rocks contacting calcium exhibit lower storage capacity than rocks containing magnesium. The value given by Groff and Lackner for magnesium bearing rocks is  $0.55 \text{ kgCO}_2/\text{kg}$  of rock.
- Our result of  $0.17 \text{ kgCO}_2/\text{kgCaSiO}_3$  (for operational parameters:  $T=61^\circ\text{C}$ ,  $S/L \sim 3$ ) is larger than  $0.11 \text{ kgCO}_2/\text{kgCaSiO}_3$  reported by Gardeman et al. (2007). Possibly it is due to different conditions.
- The change in the grain shape is observed due to the carbonation reaction. The starting material exhibits predominantly acicular particles shapes, while some of the product particles tend to have a rhombohedron shape - typical for calcite. Additionally formation of silica reach layers is observed on the wollastonite surface.

## TABLE OF FIGURES

Figure 3.1: Estimated storage capacity and time for various sequestration methods .....	16
Figure 3.2: Distribution of magnesium silicate mineral deposits worldwide .....	17
Figure 3.3 a: Mineral carbonation routs.....	18
Figure 3.3 b: Mineral carbonation routs – direct carbonation.....	19
Figure 3.3 c: Mineral carbonation routs – indirect carbonation.....	20
Figure 4. 1: Plot of phase boundaries between calcite and calcium ion in the solution.....	32
Figure 4. 2: The experimental setup in the laboratory at TU Delft University.....	35
Figure 4. 3: Experimental setup for mineral carbonation.....	35
Figure 4. 4: Reference cell used in the experimental setup.....	36
Figure 4. 5: Sample cell used in experimental setup.....	36
Figure 4. 6: Electron probe analysis of wollastonite (powder) sample.....	38
Figure 4.7 a: Electron Probe images, which show needle shaped crystals (Sample no 1).....	40
Figure 4.7 b: Electron Probe images, which show needle shaped crystals (Sample no 2) .....	41
Figure 4.8 a: The way of chains arrangement in (100) layers in the triclinic structure .....	42
Figure 4.8 b: Structure wollastonite in a single layer .....	42
Figure 5.1 a: Pressure vs. time during a carbonation experiment 1.....	50
Figure 5.1 b: Pressure vs. log time during a carbonation experiment 1.....	50
Figure 5.2 a: Pressure vs. time during a carbonation experiment 2.....	51
Figure 5.2 b: Pressure vs. log time during a carbonation experiment 2.....	51
Figure 5.3 a: Pressure vs. time during a carbonation experiment 3.....	52
Figure 5.3 b: Pressure vs. log time during a carbonation experiment 3.....	52
Figure 5.4 a: Pressure vs. time during a carbonation experiment 4.....	53
Figure 5.4 b: Pressure vs. log time during a carbonation experiment 4.....	53
Figure 5. 5: Density-pressure phase diagram of carbon dioxide.....	54
Figure 5.6: The same as figure 5.2 but with indication of the adiabatic expansion of carbon dioxide in experiment 2.....	55
Figure 5. 7: The same as figure 5.4, but with indication of the adiabatic expansion of carbon dioxide in experiment 4.....	55
Figure 5. 8 a-c: CT scanner photos presenting three different types of chemical compounds in the reaction product.....	56
Figure 5. 9: The effect of pressure on the carbonation conversion percentage of wollastonite reacted at 334K after 3 day for series of experiments .....	60
Figure 5. 10: Pressure vs. time during a carbonation experiment 1.....	61
Figure 5. 11: Pressure vs. time during a carbonation experiment 2.....	61
Figure 5. 12: Pressure vs. time during a carbonation experiment 3.....	62
Figure 5. 13: Pressure vs. time during a carbonation experiment 4.....	62
Figure 5. 14: Mass of carbon dioxide adsorbed by wollastonite and dissolved in water ( $\rho_g(T,P)V_g +$ $\rho_l(T,P)V_l$ ) vs. time (exp1).....	63
Figure 5. 15: Mass of carbon dioxide adsorbed by wollastonite and dissolved in water ( $\rho_g(T,P)V_g +$ $\rho_l(T,P)V_l$ ) vs. time (exp 2).....	63
Figure 5. 16: Mass of carbon dioxide adsorbed by wollastonite and dissolve in water ( $\rho_g(T,P)V_g +$ $\rho_l(T,P)V_l$ ) vs. time (exp 3).....	64
Figure 5. 17: Mass of carbon dioxide adsorbed by wollastonite and dissolve in water ( $\rho_g(T,P)V_g +$ $\rho_l(T,P)V_l$ ) vs. time (exp 4).....	65

Figure 5. 18: CT scanner image of the pure sample of wollastonite before experiment. ....	66
Figure 5. 19: CT scanner image of the sample of wollastonite after 15 min of carbonation .....	66
Figure 5. 20: Image of the wollastonite sample after 168 hours of carbonation process.....	67
Figure 5. 21: Adsorption isotherm curve: adsorption density vs. pressure. ....	68
Figure A4.1 a: Adsorption density reached after 1e5 seconds.....	83
Figure A4.1 b: Adsorption density reached after 2.5e5 seconds.....	83
Figure A4.1 c: Adsorption density reached after 4e5 seconds .....	82
Figure A4.1 d: Adsorption density reached after 5e5 seconds .....	82
Figure A4.1 e: Adsorption density change in time from 1e5 to 5e5 seconds .....	83
Figure A4.1 f: Concentration change in the reference vessel and sample vessel in time 1e5 .....	83
Figure A4.1 g: Concentration change in the reference vessel and sample vessel in time 2.5e5.....	84
Figure A4.1 h: Concentration change in the reference vessel and sample vessel in time 4e5.....	84
Figure A4.1 i: Concentration change in the reference vessel and sample vessel in time 5.5e5 .....	85
Figure A4.2 a: Adsorption density reached after 2.5e5 seconds.....	85
Figure A4.2 b: Adsorption density reached after 2.5e5 seconds.....	86
Figure A4.2 c: Adsorption density reached after 2.5e5 seconds.....	86
Figure A4.2 d: Adsorption density reached after 2.5e5 seconds.....	87
Figure A4.2 e: Adsorption density reached after 2.5e5 seconds.....	87
Figure A4.2 f: Adsorption density reached after 2.5e5 seconds .....	88
Figure A4.2 g: Adsorption density reached after 2.5e5 seconds.....	88
Figure A4.2 h: Adsorption density reached after 2.5e5 seconds.....	89
Figure A4.2 i: Adsorption density reached after 2.5e5 seconds.....	89

## TABLE OF TABLES

Table 2.1: Cost ranges for the components of large scale CCS system . . . . .	12
Table 2.2: Costs comparison of different mineral carbon dioxide sequestration routes under the US conditions . . . . .	13
Table 4. 1: Equilibrium constants at STP and 65°C. . . . .	31
Table 4. 2: Carbonic ion concentration at different conditions. . . . .	32
Table 4. 3: Weight percentage analyses of 2 <sup>nd</sup> type of sample . . . . .	38
Table 4. 4: Description of samples used in the experiments 1-4. . . . .	43
Table 4. 5: Description of the conditions under which the experiments were carried out. . . . .	43
Table 5. 1: Characteristic data of particular experiments. . . . .	49
Table 5. 2: Estimated conversion rate of particular experiments. . . . .	58
Table 5. 3: Conversion rate achieved during 3 days experiment . . . . .	59

## REFERENCES

- BAILEY, A., REESMAN, L. (1971) A survey study of the kinetics of wollastonite dissolution In the H<sub>2</sub>O-CO<sub>2</sub> and buffered system At 25°C, American Journal of Science, vol. 271
- BAKER, R., (1973) Reversibility of the reaction  $\text{CaCO}_3 = \text{CaO} + \text{CO}_2$ . J. Appl. Chem. Biotechnol, 23 (10), 733–742
- BOSLOUGH, M. B., WELDON, R. J., ARHENS, T. J., (1980) Impact induced water loss from serpentine, nontronite and kernite. Proceedings of the 11th lunar and planetary science conference
- BOUDART, M., DJEGA-MARIADASSOU, G.,(1984) Kinetics of Heterogeneous Catalytic Reactions, Princeton University Press, Princeton, New Jersey
- BROWNLOW, A.H., (1979) Geochemistry, Prentice–Hall, New York
- BUERGER, M. J., PREWITT, C. T. (1961) The crystal structures of wollastonite and pectolite. Proceedings of the National Academy of Sciences, U.S.A., 47, 1884–1888
- CHEN, Z-Y., O’CONNOR, W. K., GERDEMANN, S. J., (2001) Chemistry of aqueous mineral carbonation for carbon sequestration and explanation of experimental results
- CLIFFORD, Y., TAI, W., CHEN, R., SHIN-MIN, S., (2005) Factors affecting wollastonite carbonation under CO<sub>2</sub> supercritical conditions, DOI 10.1002/aic.10572
- DAHOWSKI, R.T., DOOLEY, J.J., DAVIDSON, C.L., BACHU S., and GUPTA, N., (2004) A CO<sub>2</sub> Storage Supply Curve for North America. IEA Report PNWD- 3471, IEA GHG R&D Programme, Cheltenham, UK
- DAVAL, D., MARTINEZ, I., GUIGNER, J.-M., HELLMANN, R., CORVISIER, J., FINDLING, N., DOMINICI, CH., GOFFE, B., GUYOT, F., (2009) Mechanism of wollastonite carbonation deduced from micro- to nanometer length scale observations. American Mineralogist. 94: 1707-1726
- DUNSMORE H.E., (1992) A geological perspective on global warming and the possibility of carbon dioxide removal as calcium carbonate mineral, Energy Convers. Mgmt, 33 (5-8), 565-572
- FOLGER, P., (2009) Carbon Capture and Sequestration (CCS)
- GERDEMANN, S.J., DAHLIN, D. C., O’CONNOR, W., and PENNER, L., (2003) Carbon dioxide sequestration by aqueous mineral carbonation of magnesium silicate minerals
- GERDEMANN, S.J., O’CONNOR, W.K., DAHLIN, D.C., PENNER, L.R., Rush, H., 2007, Ex situ aqueous mineral carbonation, Environ. Sci. Technol. (41), pp. 2587-2593

GUTHRIE, G.D., Jr., CAREY, J.W., BERGFELD, D., BYLER, D., CHIPERA, S., and ZIOCK, H.-J., (2001) Geochemical Aspects of the Carbonation of Magnesium Silicates in an Aqueous Medium, Proceedings of the 1st National Conference on Carbon Sequestration, Washington, DC

HAYWOOD R.W., (2004) Thermodynamic Tables in SI (metric) Units

HOWARD, H., (2002) Carbon sequestration via mineral carbonation: Overview and assessment, MIT Laboratory for Energy and the Environment

HUANG, H. P., SHI, Y., Li, W. CHANG, S. G. (2001) Dual alkali approaches for the capture and separation of CO<sub>2</sub>, Energy and Fuels/15, pp. 263-268

HUIJGEN, J. J. W., WITKAMP, G-J., COMANS, N. J., Mechanism of aqueous wollastonite carbonation as a possible CO<sub>2</sub> sequestration process, Chem. Eng. Sci., vol. 61, issue 13, pp 4242-4251 (2006)

HUIJGEN, J. J.W., COMANS N, J., (2003) Carbon dioxide sequestration by mineral carbonation, Literature Review

IEA GHG (International Energy Agency Greenhouse Gas), (2000), CO<sub>2</sub> storage as carbonate minerals, PH3/17, CSMA Consultants Ltd, United Kingdom, Cheltenham

LACKNER, K.S., (2002) Carbonate chemistry for sequestering fossil carbon. Annual Review of Energy and the Environment, 27, 193-232

LACKNER, K.S., BUTT, D.P., WENDT, C.H., (1997), Progress on binding CO<sub>2</sub> in mineral substrates. Energy Conversion and Management, 38, S259 – 264

LACKNER, K.S., BUTT, D.P., WENDT, C.H., JOYCE, E.L., SHARP. D.H., (1995). Carbon dioxide disposal in carbonate mineral. Energy, 20 (11), 1153 – 1170

LACNER, K.S, WORZEL, E., (2010) Air capture and mineral sequestration: Tools for fighting climate change. The Earth Institute and School of Engineering and Applied Sciences, Columbia University, New York

KAKIZAWA, M., YAMASAKI, A., YANAGISAWA, Y., (2001) A new CO<sub>2</sub> disposal process using artificial rock weathering of calcium silicate accelerated by acetic acid, Energy/26, pp. 341-354

KOJIMA, T., NAGAMINE, A., UENO, N., UEMIYA, S., (1997) Absorption and fixation of carbon dioxide by rock weathering. Energy Conversion and Management vol. 38, p. 461–466

MAROTO-VALER, M.M., KUCHTA, M.E., ZHANG, Y., ANDRESEN, J.M., (2002) Integrated carbonation: a novel concept to develop a CO<sub>2</sub> sequestration module for power plants, 6th International Conference on Greenhouse Gas Control Technologies, Kyoto, Japan

NETL (National Energy Technology Laboratory) (2001) Workshop NETL Mineral CO<sub>2</sub> Sequestration

NEWALL, P., CLARKE, S., HAYWOOD, H., SCHOLES, H., CLARKE, N., KING, P., (2000) CO<sub>2</sub> storage as carbonate minerals. IEA Greenhouse Gas R&D Programme, report number PH3/17

O'CONNOR, W.K., DAHLIN, D. C., NILSEN, D. N., GERDEMANN, S.J., RUSH, G.E., WALTERS, R.P. and TURNER, P. C. (2001a) Research status on the sequestration of carbon dioxide by direct aqueous mineral carbonation, 18th Annual International Pittsburgh Coal Conference, Newcastle, Australia

O'CONNOR, W.K., DAHLIN, D. C., NILSEN, D. N., RUSH, G.E., WALTERS, R.P. and TURNER, P. C. (2001b) Carbon dioxide sequestration by direct mineral carbonation: results from recent studies and current status, 1st National Conference on Carbon Sequestration, Alexandria, VA, USA

O'CONNOR, W.K., DAHLIN, D. C., NILSEN, D. N., WALTERS, R. P. and TURNER, P. C. (2000b) Carbon dioxide sequestration by direct mineral carbonation with carbonic acid, 25th International Technical Conference on Coal Utilization and Fuel Systems, Clearwater, FL, USA

O'CONNOR, W.K., DAHLIN, D. C., NILSEN, D. N., RUSH, G.E., and COLLINS, W.K. (2002) Carbon dioxide sequestration by direct mineral carbonation: process mineralogy of feed and products, *Minerals & Metallurgical Processing* 19(2), 95-101

O'CONNOR, W.K., DAHLIN, D. C., Rush, G.E., GERDEMANN, S.J., PENNER, L.R. and NILSEN, D.N. (2005) Aqueous mineral carbonation: mineral availability, pretreatment, reaction parametric and process studies, DOE/ARC-TR-04- 002, Albany Research Center, Albany, OR, USA

O'CONNOR, W.K., DAHLIN, D. C., NILSEN, D. N., GERDEMANN, S.J., RUSH, G.E., WALTERS, R. P and TURNER, P. C. (2002a) Continuing studies on direct aqueous mineral carbonation for CO<sub>2</sub> sequestration, 27th International Technical Conference on Coal Utilization, Clearwater, FL, USA

OELKERS, 20

PRADYOT, P., (2003) *Handbook of Inorganic Chemical Compounds*. McGraw-Hill

PENNER, L., O'CONNOR, W., DAHLIN, D. C., GERDEMAN, S., RUSH, G.E., (2004) Mineral Carbonation: Energy Costs of Pretreatment Options and Insights Gained from Flow Loop Reaction Studies, Albany Research Center, Office of Fossil Energy, US DOE

PERRY, R.H., PIGFORD, R.L., (1953) Kinetics of gas-liquid reactions. Simultaneous adsorption and chemical reaction. *Ind. Engng. Chem.*, 1247-1253

PFISTER, C.-E., (2009) Interface free energy or surface tension: definition and basic properties

- PUTNIS, D. A., (1992) Introduction to Mineral Sciences, Cambridge University Press
- SANDER, R., (1999) Compilation of Henry's law constants for inorganic and organic species of potential importance in environmental chemistry, Germany
- SCHUILING, R.D., (2002) Versnelde verwerking. De natuurlijkste manier om kooldioxide te binden. *Natuur. & Techniek*: pp. 55-57
- SEIFRITZ, W., (1990) CO<sub>2</sub> disposal by means of silicates. *Nature*, 345, 486
- SILABAN, A.; HARRISON, D. P., (1995) High temperature capture of carbon dioxide: Characteristics of the reversible reaction between CaO(s) and CO<sub>2</sub>(g). *Chem. Eng. Commun.*, 137, 177-190
- SIPILÄ, J., TEIR, S., ZEVENHOVEN, R.(2008) Carbon dioxide sequestration by mineral carbonation Literature review update 2005-2007
- TAKAYUKI, F., (1999) The transition state: a theoretical approach, CRC Press
- TEIR, S., ELONEVA, S., ZEVENHOVEN, R., (2005) Production of precipitated calcium carbonate from calcium silicates and carbon dioxide, *Energy Conversion and Management* 46 2954-2979
- TEIR, S., ELONEVA, S., FOGELHOLM, C.-J., ZEVENHOVEN, R., (2006) Stability of calcium carbonate and magnesium carbonate in rainwater and nitric acid solutions, *Energy Conversion and Management*. (47), pp. 3059-3068
- TKACOVA, K., (1989) Mechanical activation of minerals
- VISION 21, (1998) Clean Energy for the 21st Century, U.S. Department of Energy, Office of Fossil Energy DOE/FE-0381
- VORHOLZ., J., HARISMIADIS VI, RUMPF, B., PANAGIOTOPOULOUS, A.Z., MAURE, G., (2000) Vapor liquid equilibrium of water, carbon dioxide, and the binary system, water - carbon dioxide, from molecular simulation. *Fluid Phase Equilib.* 170:203-234
- WHITE, A.F., and PETERSON, M.L. (1990) The role of reactive surface areas in chemical weathering, Washington, DC: American Chemical Society
- YEGULALP, T.M., LACKNER, K.S. and ZIOCK, H.S., (2000) A review of emerging technologies for sustainable use of coal for power generation," presented at Sixth International Symposium on Environmental Issues and Waste Management in Energy and Mineral Production, Calgary, Alberta, Canada
- ZEVENHOVEN, R., KOHLMANN, J. (2002) CO<sub>2</sub> sequestration by magnesium silicate mineral carbonation in Finland, Recovery, Recycling & Re-integration, Geneva, Switzerland
- ZHANG, Y., (2008) Geochemical kinetics, Princeton University Press

ZIOCK, H. S, (2000) Zero emission coal to hydrogen.

# ANNEX 1- Wollastonite specification

Veiligheidsinformatieblad volgens 1907/2006/EG, Artikel 31		Bladzijde 2/3
datum van de druk: 09.06.2009		Herziening van: 09.06.2009
Handelsnaam: <b>Calcium silicate, meta</b>		
Ademhalingsbescherming: Oogbescherming: Lichaamsbescherming:	Aanraking met de ogen vermijden Aanraking met de ogen en de huid vermijden Adembescherming bij hoge concentraties Veiligheidsbril Gezichtsbescherming Draag geschikte beschermende arbeidskleding	(voorzorg van stof)
<b>9 Fysische en chemische eigenschappen</b>		
<b>Algemene gegevens</b>		
Vorm:	Poeder	
Kleur:	Wit	
Reuk:	Reukloos	
Toestandverandering		
- Smeltpunt/smeltbereik:	1540 °C	
- Kookpunt/kookpuntbereik:	Niet bepaald	
- Sublimeringstemperatuur/-begin:	Niet bepaald	
Vlampunt:	Niet ontvankelijk	
Ontstekingstemperatuur:	Niet bepaald	
Ontbindingstemperatuur:	Niet bepaald	
Ontploffingsgevaar:	Het product is niet ontploffingsgevaarlijk	
Ontploffingsgrenzen: onderste: bovenste:	Niet bepaald Niet bepaald	
Stoomdruk:	Niet bepaald	
Dichtheid bij 20 °C:	2,9 g/cm <sup>3</sup>	
<b>10 Stabiliteit en reactiviteit</b>		
Thermische ontbinding / te vermijden omstandigheden: te vermijden stoffen: Gevaarlijke reacties: Gevaarlijke ontledingsproducten:	Geen afbraak bij opslag en handling volgens voorschrift No information known Geen gevaarlijke reacties bekend Metaaloxiden	
<b>11 Toxicologische informatie</b>		
Acute toxiciteit: Primaire aandoening op de huid: aan het oog: Overgevoeligheid: Aanvullende toxicologische informatie:	Proxakt de huid en de slijmvliezen. Irriterend Groot effect van oorsmergeligheid bekend Voor zonneculter verwondt is de acute en chronische toxiciteit van deze stof niet volledig bekend Er zijn geen data beschikbaar over kankerverwekkende eigenschappen van dit materiaal bronchaal EPA / IARC / ITP / OSHA of ACGIH	
<b>12 Ecologische informatie</b>		
Algemene informatie:	Zwaar te zwaar vloed (NL) 10. Kan in het aquatisch milieu op lange termijn schadelijke effecten veroorzaken. Gevaar voor water klasse 1. D1. Zelfontsteking: gevaar voor water klasse 1 Wat overvloed of in grote hoeveelheden lezen in grondwater, in oppervlaktewater of in de omgeving Licht het materiaal niet in het milieu vrijkomen zonder specifieke verontreiniging van de omgeving	
<b>13 Instructies voor verwijdering</b>		
Product: Aanbeveling:	Volg de plaatselijke of nationale reglementeringen voor de juiste afvalverwerking Aanbeveling bij afnemers van zwaarlijst-gedieren of afgeven bij inzamelpunt van gevaarlijke stoffen Moet onder nadere bepalingen van overheidsoverheidsinstellingen een speciale behandeling ondergaan	
Niet gereinigde verpakkingen: Aanbeveling:	Afvalverwijdering volgens overheidsoverheidsinstellingen	
<b>14 Informatie met betrekking tot het vervoer</b>		
Vervoer over land ADR/RID en GGVV/GGVV (grensoverschrijdend/binnenland): ADR/GGVV/E klasse:	Geen	
Vervoer per zeeschip (MDG/GGVVSee): MDG/GGVVSee-klasse:	Geen	
Luchtvervoer (ICAO-TI en IATA-DGR): ICAO/IATA-klasse:	Geen	
Transportverdere gegevens:	Geen groen overeenkomstig de bovengenoemde verordeningen	
<b>15 Wettelijk verplichte informatie</b>		
Kenmerking volgens EEG-richtlijnen: Kenletter en gevaaromschrijving van het product:	<b>X</b> - Irriterend	
R-zinnen: S-zinnen:	R11: Irriterend voor de ogen S53: Bij aanraking met de ogen: spoel ogen af met overvloedig water afspoelen en dekschild afdoeken S60: Waarschuwen voor de ogen	
Nationale voorschriften: Aanwijzingen m.b.t. lewerkstelligheidsbeperking:	Tevens niet oplosbaar in water voor de algemene bevolking Een veiligheidsinformatieblad (SIF) is beschikbaar	
Gevaarklasse v. water:	Watervervuilingsklasse (WV) 10 - Geringe verontreiniging	

**ANNEX 2 - Specific surface area calculation**

Wollastonite is represented by tabular crystals. For simplification of calculation it can be assumed to be cylindrical. In this case the surface area  $A_c$  can be written as

$$A_c = 2\pi r_c^2 + 2\pi r_c h_c, \quad (\text{A.2.1})$$

where  $A_c$  denotes surface area, [ $\text{cm}^2$ ];  $r_c$  is radius of cylinder, [ $\text{cm}$ ];  $h_c$  represents height of the cylinder, [ $\text{cm}$ ].

The specific surface area of the assumed cylinder  $a_c$  of radius  $r_c$  and height  $h_c$  can be calculated as follows:

$$a_c = \frac{A_c}{M_s} = \frac{2}{\rho_c} \cdot \left( \frac{1}{h_c} + \frac{1}{r_c} \right). \quad (\text{A.2.2})$$

The density of the sample is equal to  $2.9 \text{ [g/cm}^3\text{]}$ . Cylindrical model is only approximate for real crystals. Thus the specific surface area, which was derived by a simple geometric approach, has to be corrected by a parameter called surface roughness. The surface roughness is defined as ratio of

$$\text{true surface area/ geometric surface area.} \quad (\text{A.2.3})$$

As surface roughness was characterized as independent of particle size, White and Peterson (1990) publicize surface roughness value equal to 7 for all silicates. Hence the calculated specific surface area will be larger.

The achieved results showed that average specific surface area for powder wollastonite is around  $2 \text{ m}^2/\text{g}$ , and for wollastonite, which is represented by grain size  $715 \mu\text{m}$  is  $0.25 \text{ m}^2/\text{g}$ .

### ANNEX 3 - The procedure of determination amount of CO<sub>2</sub> adsorbed during the mineral carbonation process

The amount of carbon dioxide absorbed by wollastonite can be calculated by a mass balance. The mass of carbon dioxide initially prepared in the reference vessel and tubing ( $m_{IC}$ ) is equal to sum of carbon dioxide mass adsorbed in an experiment ( $m_a$ ), the mass of carbon dioxide in the adsorption equilibrium state ( $m_f$ ) and the mass of carbon dioxide dissolved in the water ( $m_{ds}$ ).

$$m_{IC} = m_a + m_f + m_{ds} \quad (A3.1)$$

Hence,

$$m_a = m_{IC} - (m_f + m_{ds}) \quad (A3.2)$$

The mass of carbon dioxide initially prepared in the reference vessel and tubing can be expressed as a function of the temperature ( $T_{int}$ ), the initial pressure ( $p_{int}$ ), and the volume that occupied ( $V_{1t}$ ):

$$m_{IC} = m_{IC}(p_{int}, T_{int}, V_{1t}), \quad (A3.3)$$

where  $V_{1t}$  (assumed to be constant) refers to the volume of void space in the reference vessel, between glass beads and the volume of the tubing:

$$V_{1t} = V_{VS} + V_t. \quad (A3.4)$$

The mass of carbon dioxide in the adsorption equilibrium state ( $m_f$ ) can be calculated from the equation of state.

The volume  $V_f$  of carbon dioxide can be calculated from following relation:

$$V_f = V_{1t} + V_2 - V_3, \quad (A3.5)$$

where,  $V_2$  is the volume of sample vessel and  $V_3$  stands for the sorbent and sorbent phase that cannot be penetrate by CO<sub>2</sub> molecules.

The mass of carbon dioxide dissolved in the water can be calculated with Henry's law.

For the more accurate determination of the isotherm adsorption model, the excess amount of CO<sub>2</sub> adsorbed per mass of wollastonite was calculated. The excess sorption can be expressed as (Marov *et. al* 2004):

$$m_{exc} = m_{abs} \left(1 - \frac{\rho_f}{\rho_a}\right), \quad (A3.6)$$

where  $\rho_a$  is density of the gas in the sorbed phase, which is assumed to be constant;  $m_{abs}$  is the total amount of carbon dioxide adsorbed per unit mass.

**ANNEX 4 – COMSOL Multiphysics 4.0**

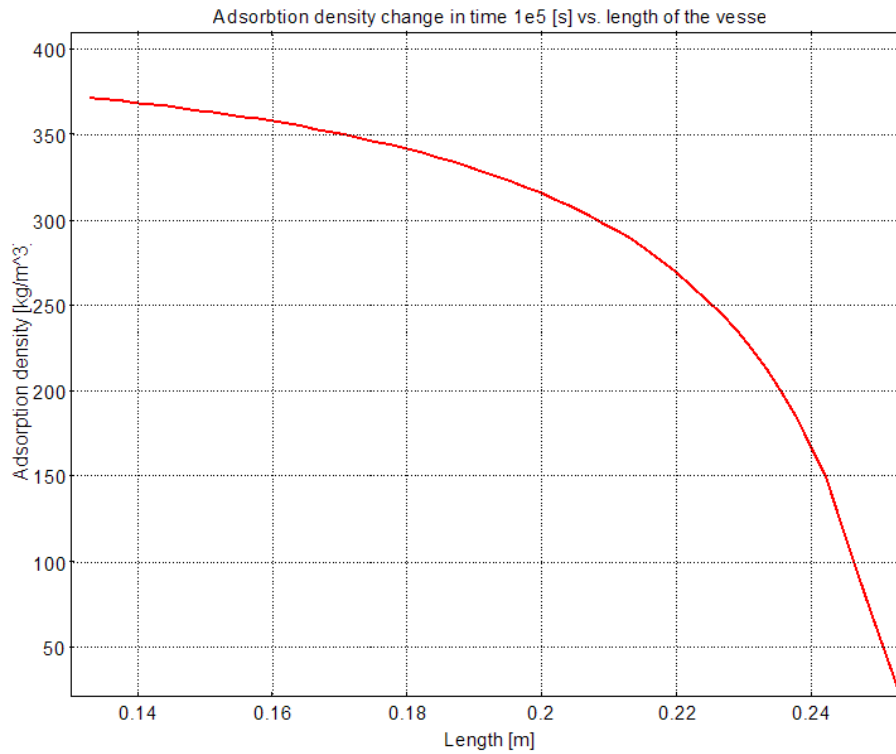


**Figure A4.1 a:** Adsorption density reached after 1e5 seconds (T=61°C, p=95bar). Chart corresponds to the sample vessel – length 0.125m.

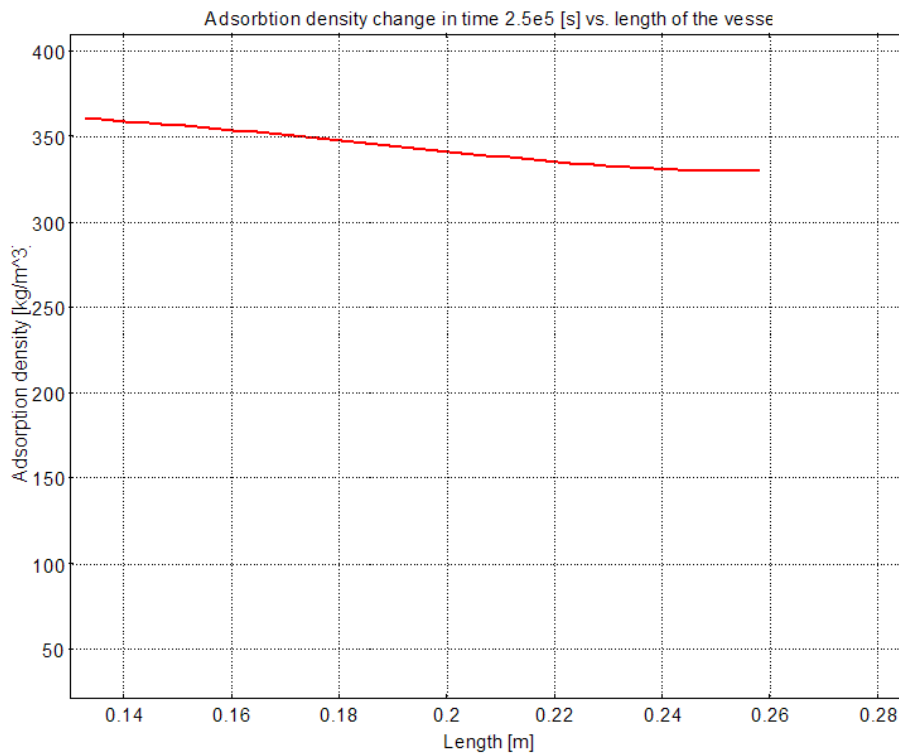


**Figure A4.1 b:** Adsorption density reached after 2.5e5 seconds (T=61°C, p=95bar). Chart corresponds to the sample vessel – length 0.125m.

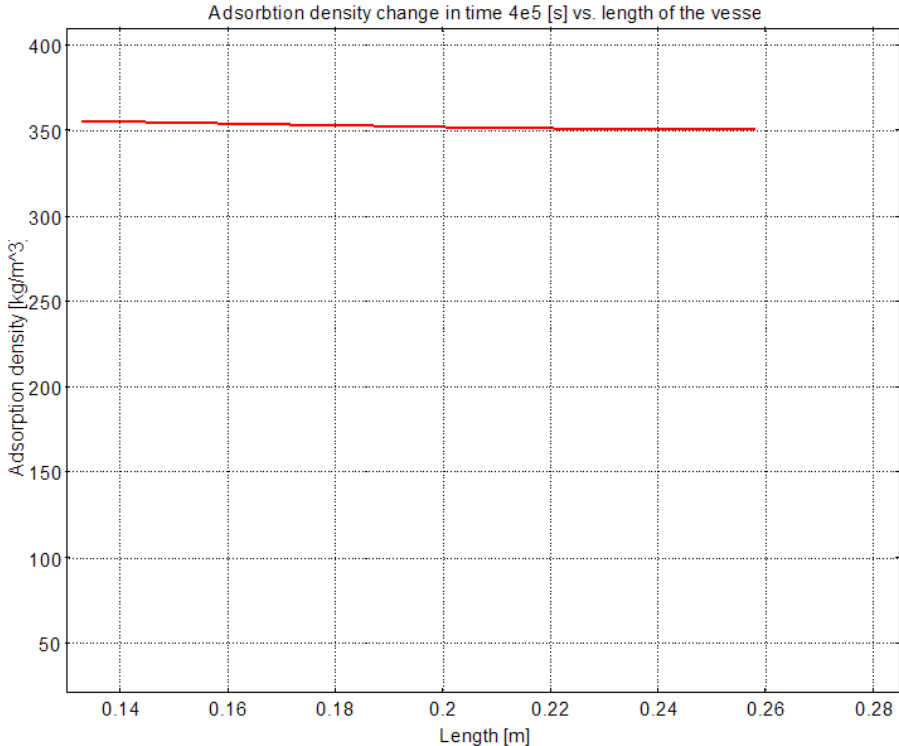


**Figure A4.1 c:** Adsorption density reached after 4e5 seconds (T=61°C, p=95bar). Chart corresponds to the sample vessel – length 0.125m.

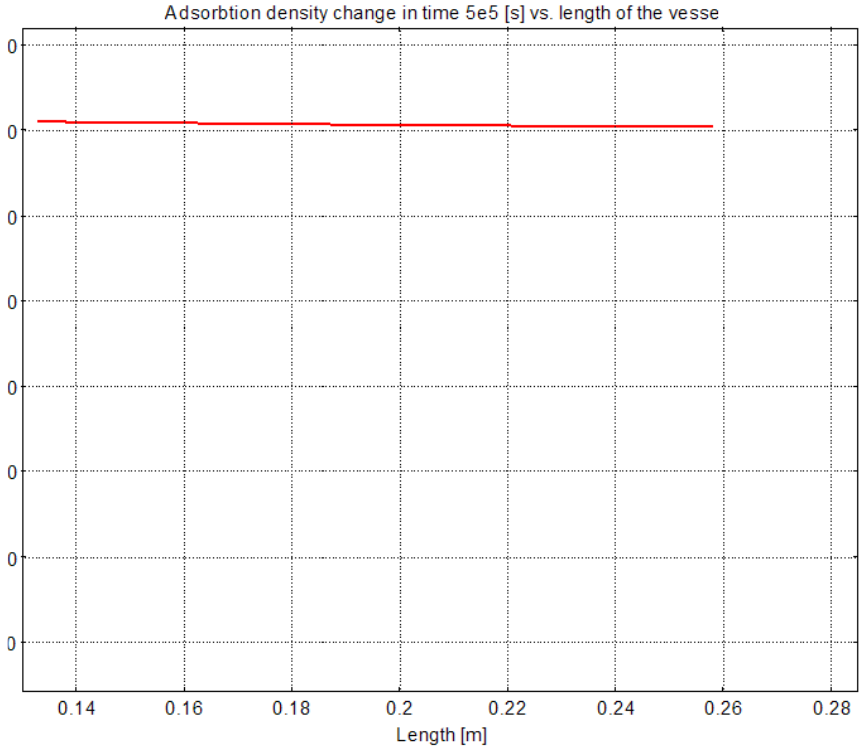


**Figure A4.1 d:** Adsorption density reached after 5e5 seconds (T=61°C, p=95bar). Chart corresponds to the sample vessel – length 0.125m.

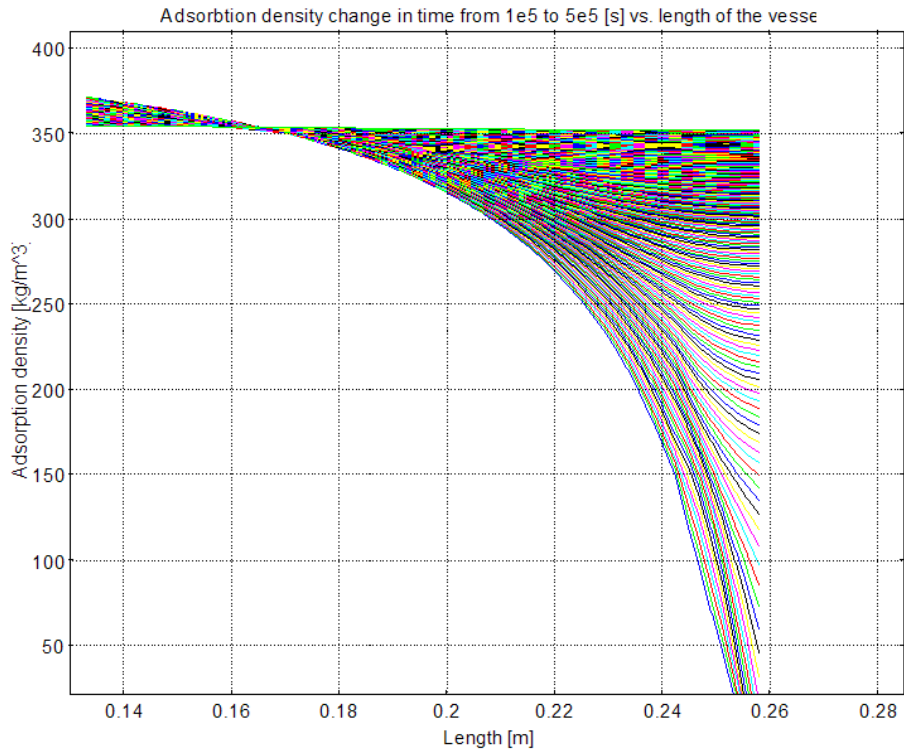


**Figure A4.1 e:** Adsorption density change in time from 1e5 to 5e5 seconds ( $T=61^{\circ}\text{C}$ ,  $p=95\text{bar}$ ). Chart corresponds to the sample vessel – length 0.125m.

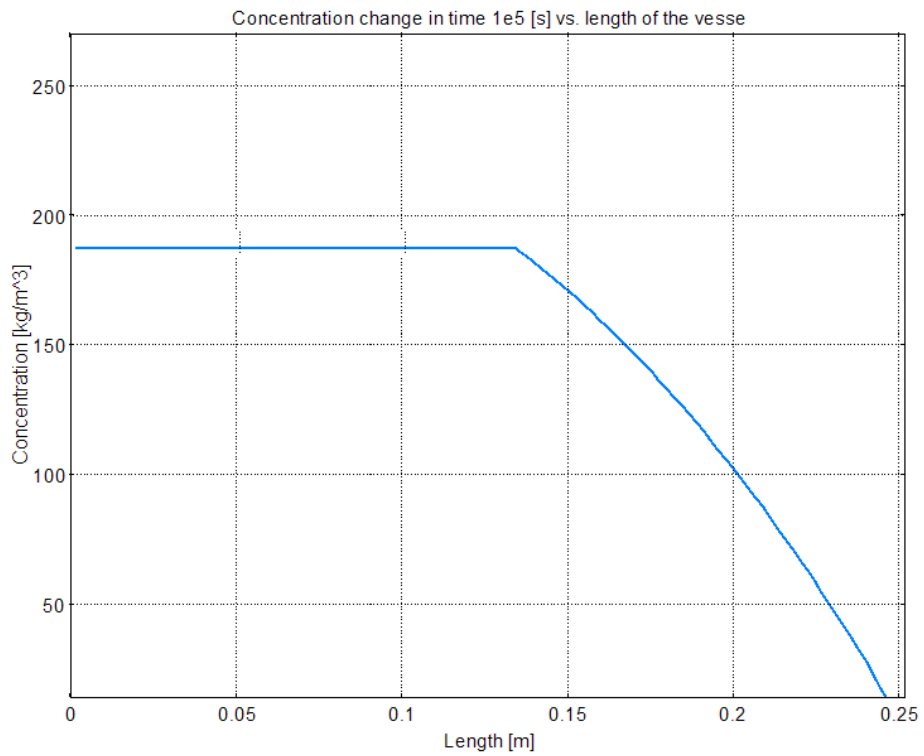


**Figure A4.1 f:** Concentration change in the reference vessel (represented by length 0 – 0.133m) and in the sample vessel (represented by length 0.133 – 0.258m) in time 1e5 ( $T=61^{\circ}\text{C}$ ,  $p=95\text{bar}$ ).

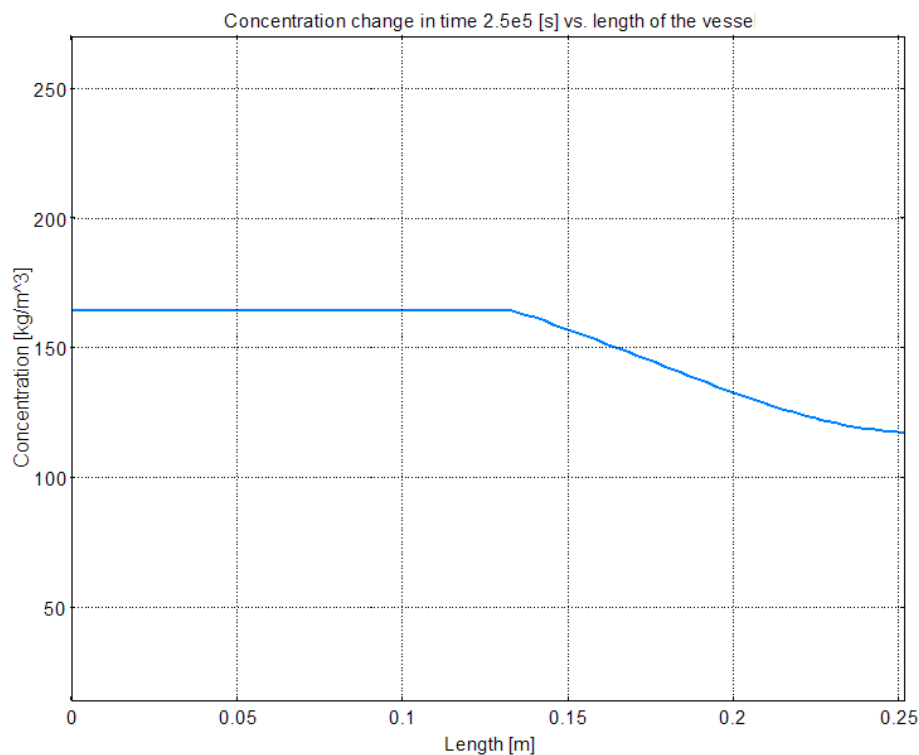


**Figure A4.1 g:** Concentration change in the reference vessel (represented by length 0 – 0.133m) and in the sample vessel (represented by length 0.133 – 0.258m) in time 2.5e5 (T=61°C, p=95bar).

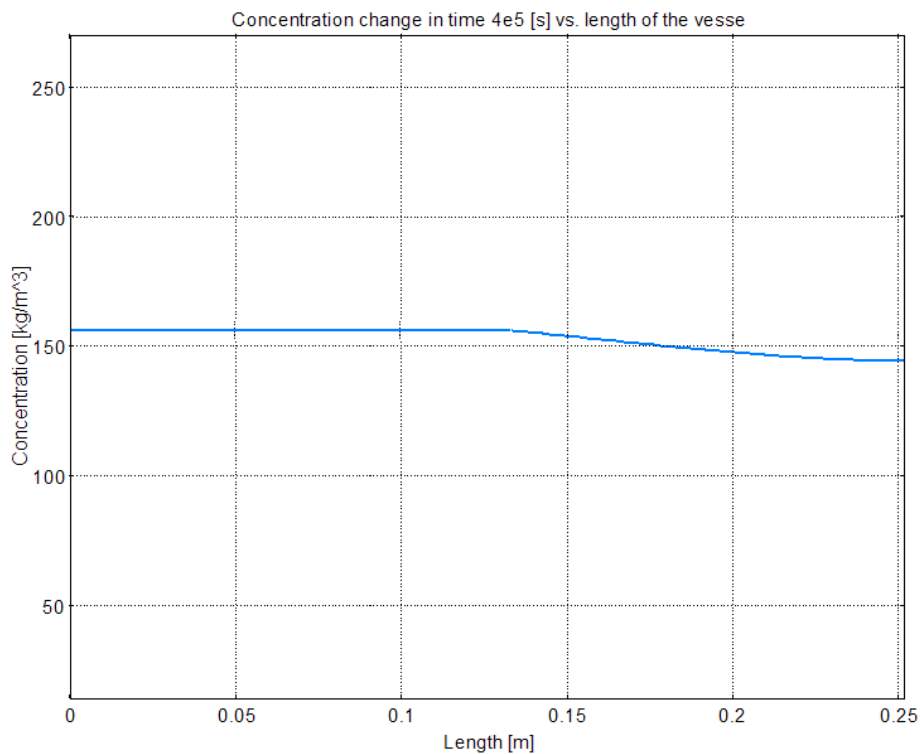


**Figure A4.1 h:** Concentration change in the reference vessel (represented by length 0 – 0.133m) and in the sample vessel (represented by length 0.133 – 0.258m) in time 4e5 (T=61°C, p=95bar).

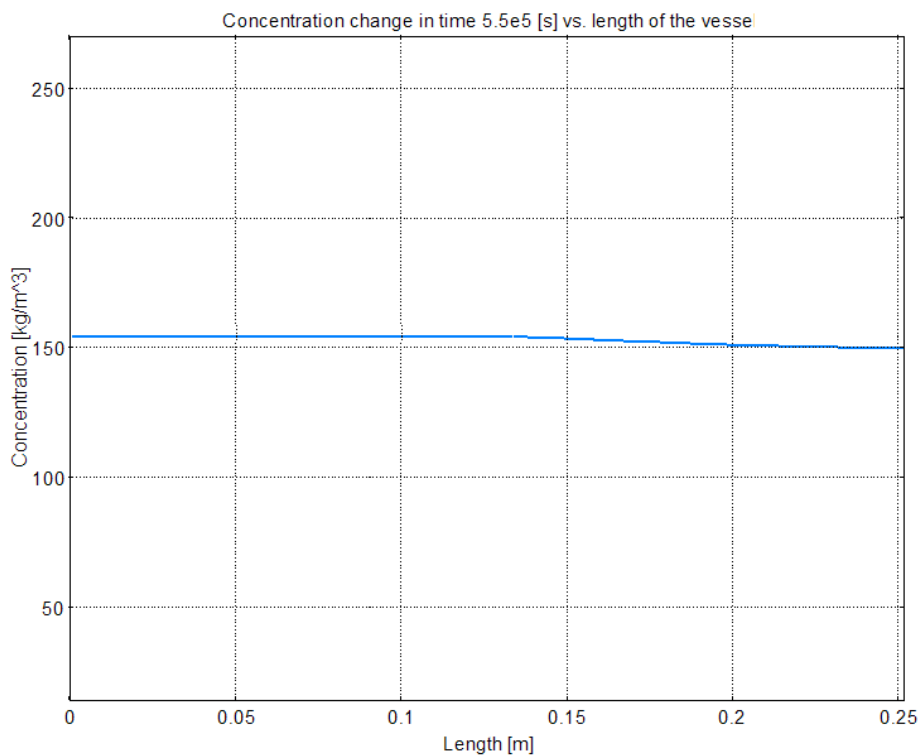


**Figure A4.1 i:** Concentration change in the reference vessel (represented by length 0 – 0.133m) and in the sample vessel (represented by length 0.133 – 0.258m) in time 5.5e5 (T=61°C, p=95bar).

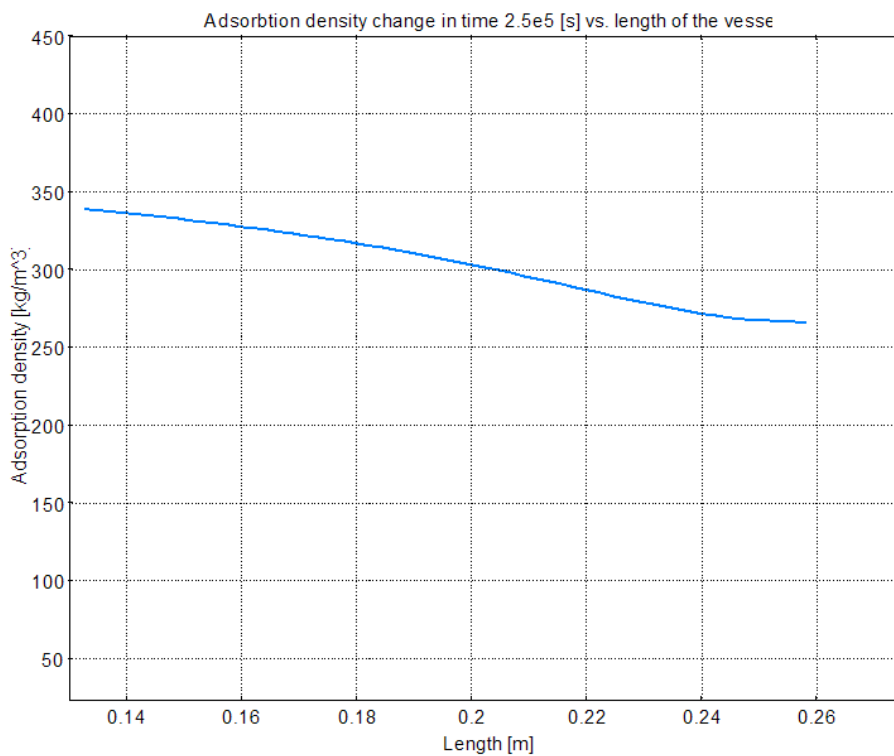


**Figure A4.2 a:** Adsorption density reached after 2.5e5 seconds (T=61°C, p=80bar). Chart corresponds to the sample vessel– length 0.125m.

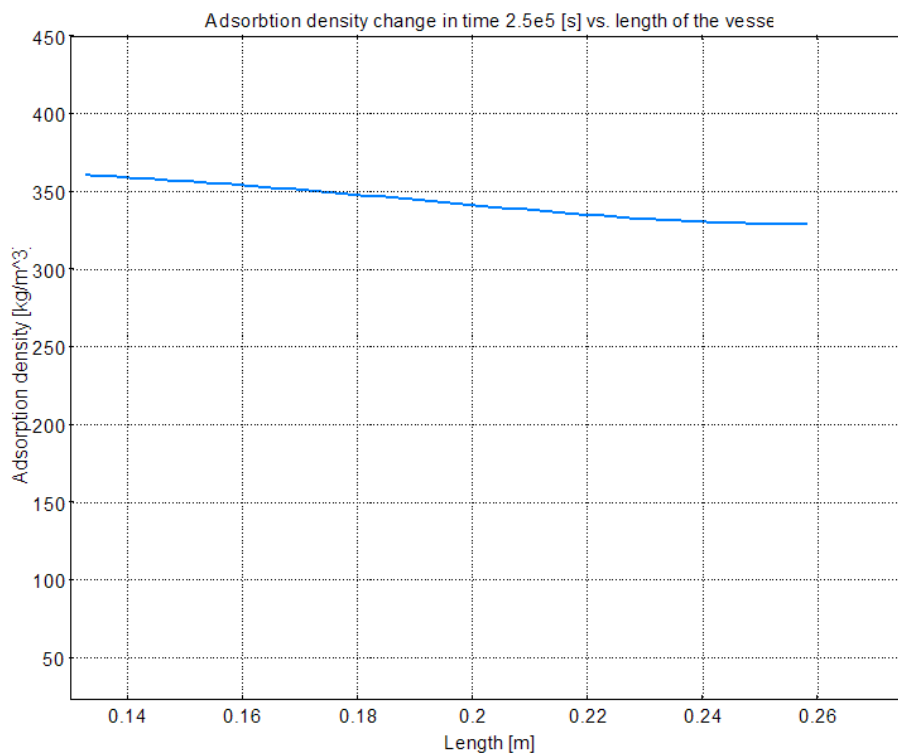


**Figure A4.2 b:** Adsorption density reached after 2.5e5 seconds ( $T=61^{\circ}\text{C}$ ,  $p=95\text{bar}$ ). Chart corresponds to the sample vessel – length 0.125m.

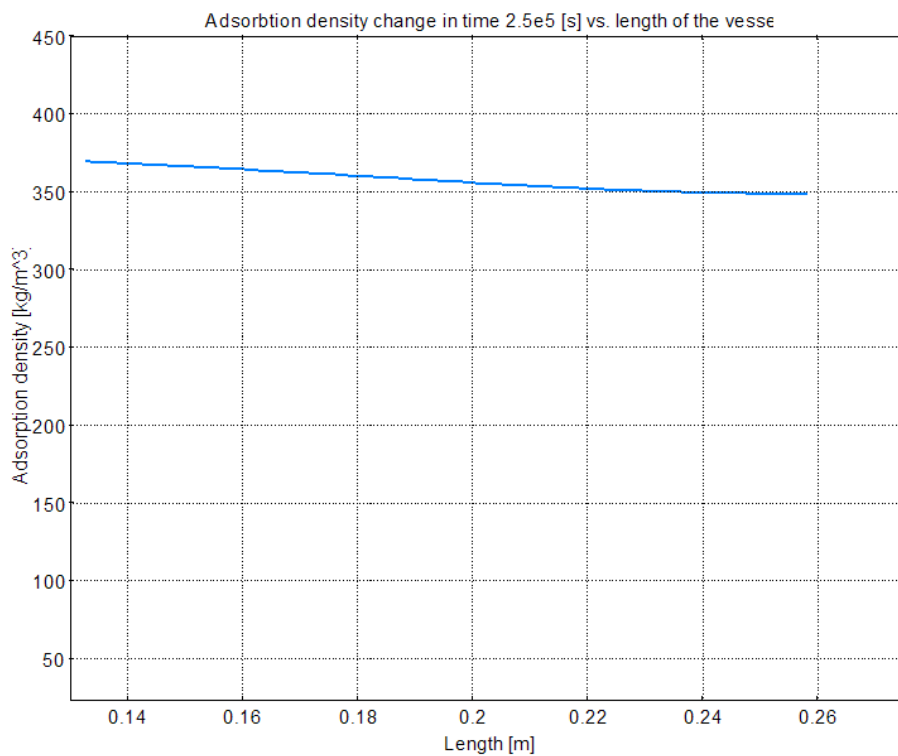


**Figure A4.2 c:** Adsorption density reached after 2.5e5 seconds ( $T=61^{\circ}\text{C}$ ,  $p=100\text{bar}$ ). Chart corresponds to the sample vessel – length 0.125m.

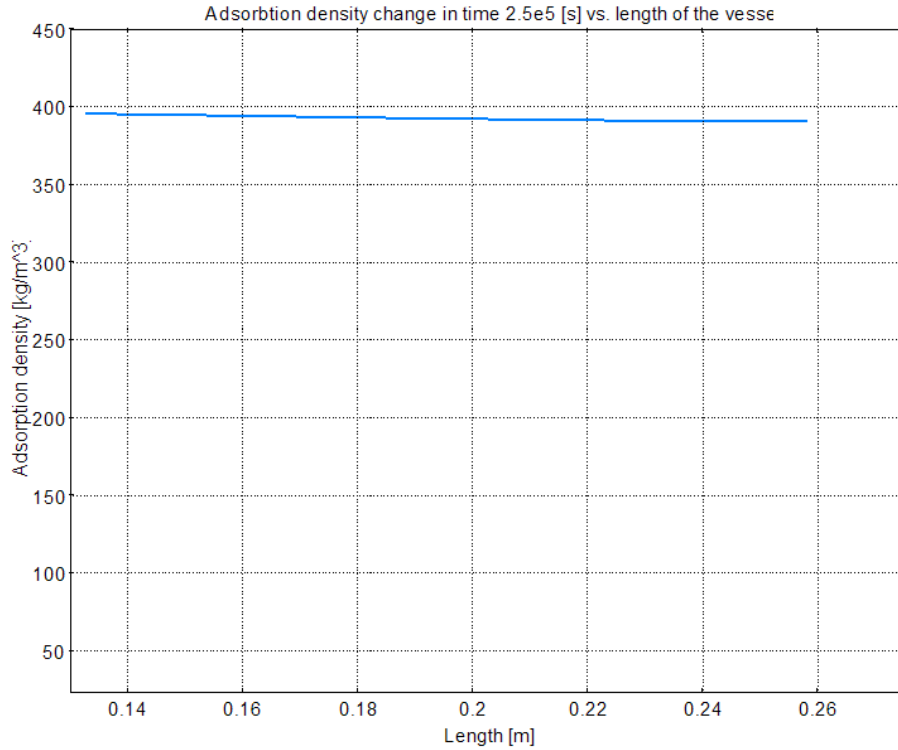


**Figure A4.2 d:** Adsorption density reached after 2.5e5 seconds ( $T=61^{\circ}\text{C}$ ,  $p=120\text{bar}$ ). Chart corresponds to the sample vessel – length 0.125m.

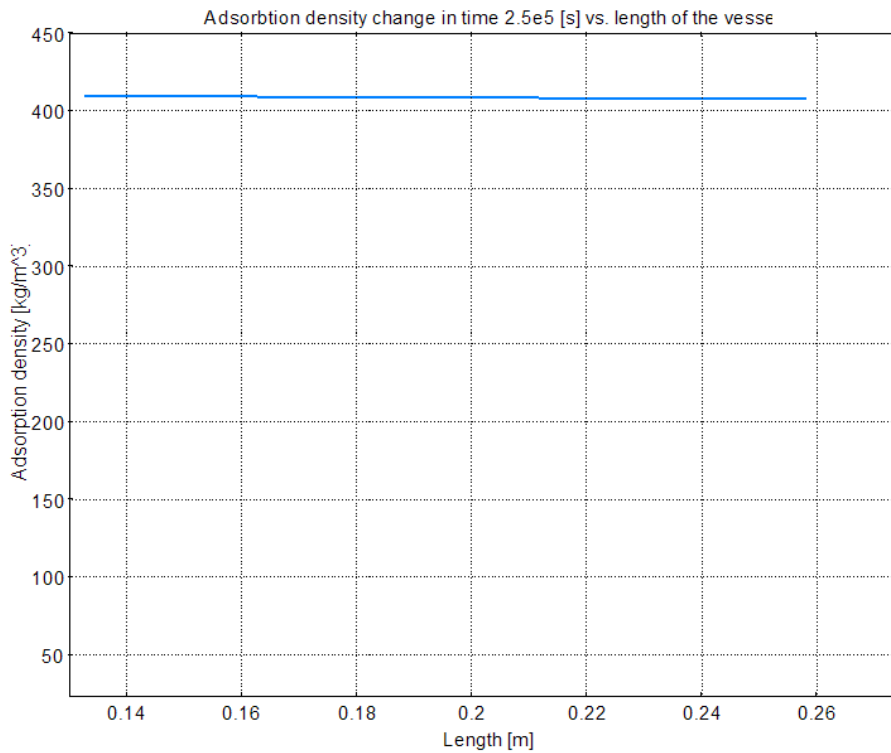


**Figure A4.2 e:** Adsorption density reached after 2.5e5 seconds ( $T=61^{\circ}\text{C}$ ,  $p=140\text{bar}$ ). Chart corresponds to the sample vessel – length 0.125m.

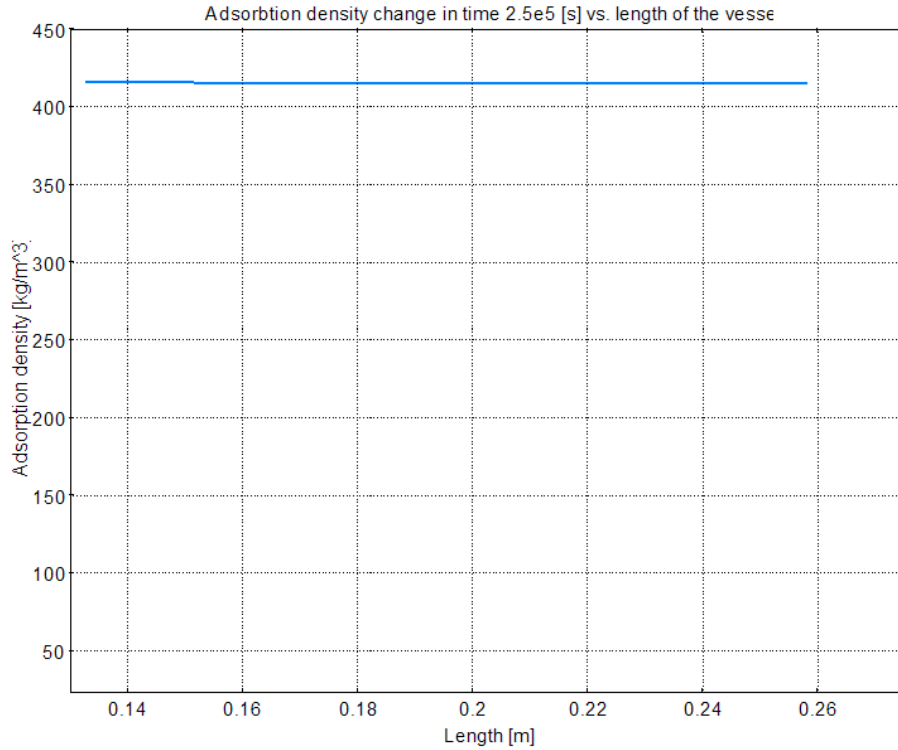


**Figure A4.2 f:** Adsorption density reached after  $2.5 \times 10^5$  seconds ( $T=61^\circ\text{C}$ ,  $p=160\text{bar}$ ). Chart corresponds to the sample vessel – length 0.125m.

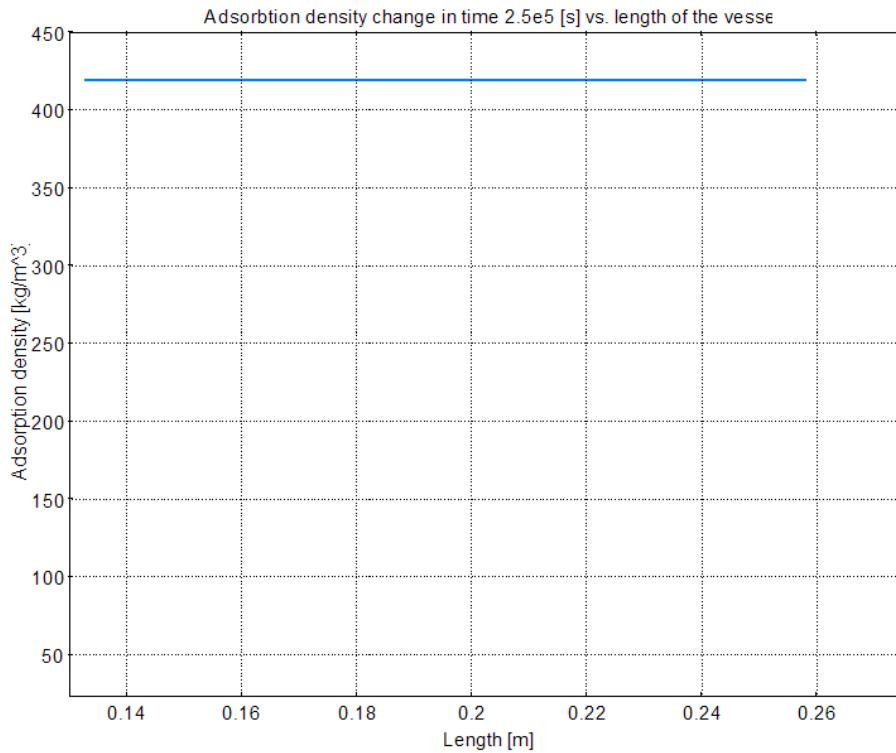


**Figure A4.2 g:** Adsorption density reached after  $2.5 \times 10^5$  seconds ( $T=61^\circ\text{C}$ ,  $p=180\text{bar}$ ). Chart corresponds to the sample vessel – length 0.125m.

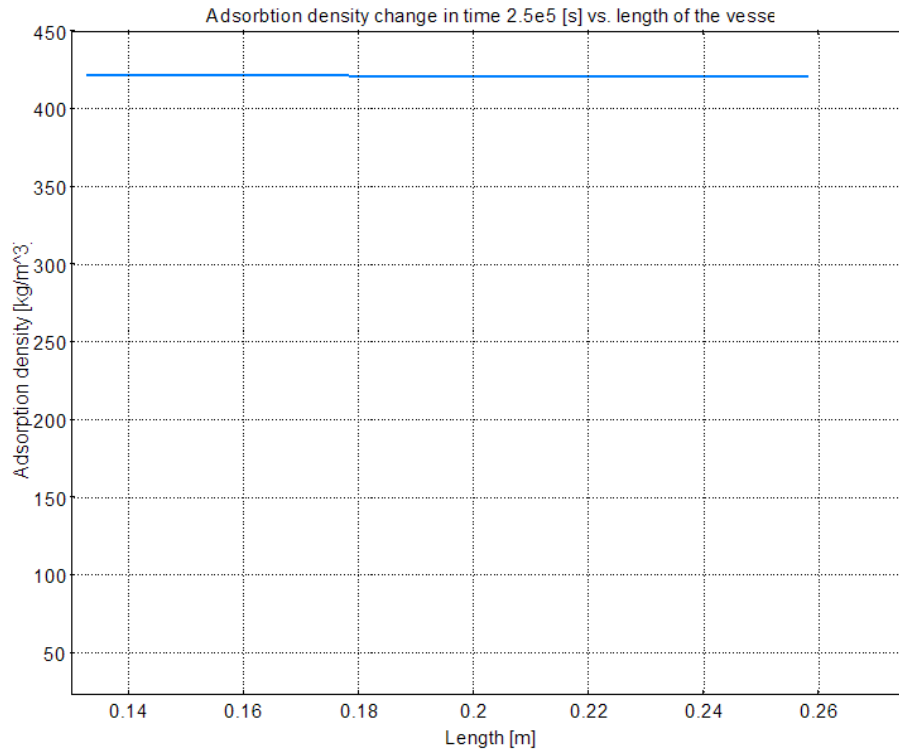


**Figure A4.2 h:** Adsorption density reached after 2.5e5 seconds ( $T=61^{\circ}\text{C}$ ,  $p=200\text{bar}$ ). Chart corresponds to the sample vessel – length 0.125m.

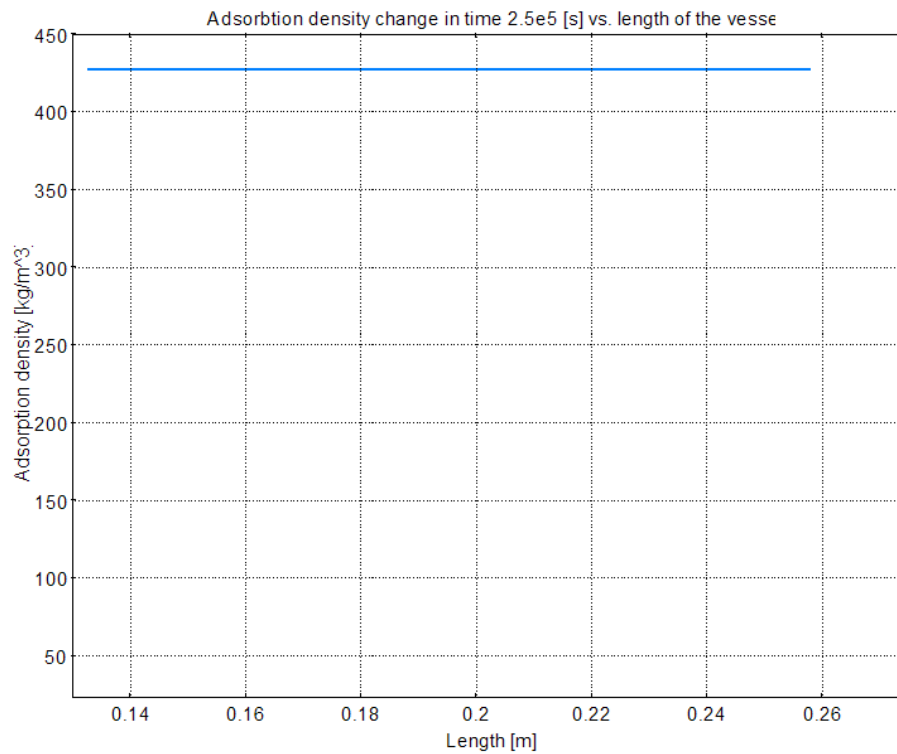


**Figure A4.2 i:** Adsorption density reached after 2.5e5 seconds ( $T=61^{\circ}\text{C}$ ,  $p=300\text{bar}$ ). Chart corresponds to the sample vessel – length 0.125m.